Mu'tah University

Mutah University

ISSN (Online) 2790-7678
ISSN (Print) 2790-766X

Jordan Journal of ENERGY

(JJE)

An International Peer-Reviewed Research Journal

JORDAN JOURNAL OF ENERGY (JJE)

Jordan Journal of Energy (JJE) is an international, multi-disciplinary journal in energy. It is peer-reviewed journal with ISSN (print): 2790-766X and ISSN (online): 2790-7678.

JJE publishes free of charge high quality, original research articles in various fields of energy. The Journal publishes original articles that contribute to promoting knowledge in all disciplines of all energy-related research. The journal covers research on energy analysis, energy modelling and prediction, integrated energy systems, energy planning and energy management. The journal also welcomes papers on related topics such as electrical and mechanical energy, energy conservation, energy efficiency, biomass and bioenergy, renewable energy, electricity supply and demand, energy storage, energy in buildings, and on energy related economic and policy issues. Articles published in JJE provide rigorous and innovative analyses of interest to academics and energy industry professionals. JJE also publishes review articles, short communication as well as technical notes.

JJE's editorial and international advisory boards are very committed to making JJE a leading platform and an authoritative source of information for analyses, reviews and evaluations related to energy.

JJE is published quarterly by the Deanship of Scientific Research at Mutah University. It applies the highest practices and professional standards of publication ethics.

Editorial Team

- **Prof. Abdullah Ibrahim Al-Odienat**
Electrical Engineering Department
Mutah University
Editor-in-Chief
jje@mutah.edu.jo
odienat@mutah.edu.jo

- **Prof. Hussein AL-Majali**
Electrical Engineering Department
Mutah University/Jordan
halmajali@mutah.edu.jo

- **Dr. Talib K. Murtadha**
Mutah University/Jordan
Talib_km@Mutah.Edu.Jo

- **Prof. Ahmed Said Al-Salaymeh**
Jordan University/Jordan
salaymeh@ju.edu.jo

- **Prof. Mohammed Abu-Dayeh Matouq**
Al-Balqa Applied University/Jordan
matouq@bau.edu.jo

- **Dr. Amer Saif Al Hinai**
Sultan Qaboos University/ Sultanate of Oman
hinai@squ.edu.om

- **Prof.Marwan Suleiman Mousa**
Dept. of Physics, Mutah University/Jordan
mmousa@mutah.edu.jo

- **Prof. Adnan Al-Harahsheh**
Chemical Engineering Department
Mutah University/Jordan
Adnan@mutah.edu.jo

- **Prof. Muwaffaq Alomoush**
Yarmouk University/Jordan
ma@yu.edu.jo

- **Prof. Saleh Al Jufout**
California State University, Long Beach/USA
saleh.aljufout@csulb.edu

- **Prof. Abdullah Al-Badi**
Sultan Qaboos University/ Sultanate of Oman
albadi@squ.edu.om

- **Prof. Mohammad Affan Badar,**
PhD, CPEM,Professor, Applied Engr & Tech Mgmt Dept
Indiana State University, USA,
affan.badar@indstate.edu

- **Dr. Salaheddin Malkawi**
Jordan University of science & Technology (JUST)
salahm@just.edu.jo

SUBMISSION ADDRESS
https://dsr.mutah.edu.jo/index.php/jje

"The views expressed in this issue are those of the authors and do not necessarily reflect the views of the editorial board or the policies of mutah University "

JORDAN JOURNAL OF ENERGY (JJE)

Aims and Scope

JJE aims to providing a highly readable and a valuable addition to the literature in the field of energy to reflect the evolving needs of energy sector. All energy-related research is in scope, including interdisciplinary and multidisciplinary studies. The journal will serve as an indispensable reference tool for years to come. The journal's scope includes all new theoretical and experimental findings that cover a wide range of topics in energy. JJE aims to strengthen relations between the energy sector, research laboratories, and universities. All the manuscripts must be prepared in English and are subject to a rigorous and fair peer-review process.

Specific Topics

The Journal might cover the energy & environmental issues; energy analysis; optimization; modelling and prediction; petroleum (upstream & downstream); natural gas; oil shale research; electricity markets; renewable energies (e.g., geothermal, solar, wind, hydro, tidal, wave, biomass); energy policy issues; energy market and power issues; econometric modeling; alternative transportation fuels; energy efficiency; regulatory economics; nuclear power issues; carbon emissions reduction; carbon capturing and storage technologies; energy efficiency; clean coal technologies; energy conversion; energy conservation; CO_2 sequestration and storage; energy management; energy systems; batteries; supercapacitors; hybrid/combined/integrated energy systems for multi-generation; hydrogen energy and fuel cells; hydrogen production technologies; micro- and nano-energy systems and technologies; smart energy system; electrical power systems; smart electric grids; physics of energy; artificial intelligence in complex power and energy systems; organic and inorganic photovoltaics; energy and power forecasting; waste energy management; reliability evaluation and risk analysis of energy systems; energy and environmental data acquisition and remote sensing.

Publishing Rules

After Greetings,

In line with the strategic plan of the University of Mutah and its vision to achieve the standards of international classifications of universities, and based on the strategic plan and the vision of the Deanship of Scientific Research, which states:

"Towards a Deanship that hosts distinguished scientific research that elevates the University's classification locally, regionally and globally."

and, Its Mission that includes:

"Providing an environment capable of producing scientific research that contributes to enhancing the role of the University in research and innovation locally, regionally and globally."

The Deanship of Scientific Research has decided to develop **Jordan journal of Energy (JJE)**

When submitting your research for publication in the Journal, the followings shall be considered:

- Adopting the Modern Language Association (MLA) system, for more information: visit https://www.mla.org
- The research and all the required files should be electronically uploaded online at https://ejournal.mutah.edu.jo.
- The technical specification for printing of the research appeared at the website of the Journal should be strictly followed, keeping in mind that the research is subordinated to precise technical auditing when received, in case these specification is violated, the research will be returned.
- Failure to comply with any of the foregoing points exempts the Journal from proceeding with the arbitration proceedings.

Publication Procedures (Steps)

The Jordan Journal of Energy (JJE) follows the highest standards of publication ethics, and it takes all measures necessary to prevent publication misconduct.

Our editorial board does not accept any type of plagiarism. This means that works replicating another author's work without acknowledging him/her shall be automatically disqualified. All authors submitting their papers to JJE affirm that their papers are their own creations and have not been copied in whole or in part from other works.

1. The author(s) submit the research manuscript to the Deanship of Scientific Research at Mutah University at the Journal's Website http://dsr.mutah.edu.jo/
2. The author(s) signs a publication pledge in an official form available at the Journal's website.
3. The manuscript is registered in the Journal special records.

4. The submitted manuscript is technically checked and initially reviewed by the Editorial Board to determine its eligibility for peer review. The board is entitled to assign peer reviewers or to reject the manuscript without giving reasons.
5. If initially accepted by the Editorial Board, the manuscript will be sent to two reviewers, who should reply within a maximum period of one month. In case of failure to reply within the specified time, the manuscript shall be sent to another reviewer. Once receiving the reports of the reviewers, the Editorial Board decide the following:
6. The manuscript will be accepted for publication if receiving positive reports from the two reviewers, and after the author(s) make(s) the required corrections, if any.
7. If negative reports are received from both reviewers, the manuscript is rejected.
8. If a negative report is received from one reviewer, and a positive one from the other, the manuscript will be sent to a third reviewer to decide its validity for publication.
9. The author must make the suggested corrections of the reviewers within a maximum period of two weeks. Failing to meet this requirement will stop the procedure of publishing the manuscript.
10. If the reviewer rejects the required corrections, the author will be given a period of two weeks to make the necessary corrections, otherwise, the paper will be rejected.
11. Even if the reviewers approve the required corrections, the author(s) must abide by completing the essential technical specifications to be eligible to obtain the letter of acceptance.
12. The accepted manuscripts in the Journal are arranged for publication in accordance with the policy of the Journal.
13. What is published in the journal reflects the point of view of the author(s) and does not necessarily represent the views of Mutah University or the Editorial Board.

Publication Ethics

First: Duties of Editorial Board

- Justice and independence: Editors evaluate the manuscripts submitted for publication on the basis of importance, originality, validity, clarity and relevance of the journal, regardless of the gender of the authors, their nationality or religious belief, so that the editor has full authority over the entire editorial content and timing of publication.
- Confidentiality: Editors and editorial staff are responsible for the confidentiality of any information about the submitted manuscripts and not to disclose this information to anyone other than the author, reviewers, and publishers, as appropriate.
- Disclosure and Conflicts of Interest Editors and editorial members are responsible for the non-use of unpublished information contained in the research submitted for publication without the written consent of the authors. The editors themselves will ***** to consider research with which they have conflicts of interest such as competitive, cooperative or other relationships with any of the authors; instead they will ask another member of the editorial board to deal with the manuscript.
- Publishing Decisions: Editors shall ensure that all manuscripts submitted for publication are subjected for reviewing by at least two reviewers who are experts in the field of manuscript. The editor-in-chief is responsible for determining which of the research papers will be published, after verifying their relevance to researchers and readers, and the comments of the reviewers.

Second: Duties of the reviewers

- Contributing to the decisions of the editorial board.
- Speed and accuracy in time: Any reviewer who is unable to review the submitted manuscripts for any reason should immediately notify the editors and reject the invitation for reviewing so that other reviewers can be contacted.
- Confidentiality: Any manuscript received by the Journal for reviewing and publishing is confidential; it should not appear or discussed with others unless authorized by the Editor. This also applies to the invited reviewers who have rejected the invitation for reviewing.
- Objectivity criteria: The reviewing process of the submitted manuscript should be objective and the reviewer comments should be clearly formulated with the supporting arguments so that the authors can use them to improve the quality of their manuscript away from the personal criticism of the authors.
- Disclosure and Conflict of Interests: Any invited reviewer must immediately notify the editors that he/she has a conflict of interest resulting from competitive, cooperative or other relations with any of the authors so that other reviewers may be contacted.
- The confidentiality of information or ideas that are not published and have been disclosed in the manuscript submitted for reviewing and not use without the express written consent of the authors. This applies also to the invited reviewers who refused the reviewing invitation.

Third: Duties of the Authors

- Criteria for the preparation of the manuscript: Authors must provide an accurate description of the presented work and the achieved results, including a subjective discussion of the importance of work.
- Originality and plagiarism: Authors must ensure that their work are original and that the works of other authors in the same field must be consulted and referenced in their manuscript. In all of its forms, plagiarism behavior is an immoral behavior and takes many forms, such as the adoption of the research of other author, copying or rephrasing large parts of other researches (without referencing) ... etc.
- The authors should not send or publish the manuscript to different journals simultaneously. Also, authors should not submit a manuscript that has already been published in another journal, because submitting the manuscript simultaneously to more than one journal is unethical and unacceptable.
- Authorship of the manuscript: Only persons who meet the following authorship criteria should be listed as one of the authors of a manuscript as they should be responsible for the manuscript content: 1) present significant contributions to the design, implementation, data acquisition, analysis or interpretation of the study; 2) critically contribute to the manuscript writing and revision or 3) have seen and approved the final version of the manuscript and agreed to submit it for publication.
- Disclosure and conflicts of interest: Authors must report any conflict of interest that can have an impact on the manuscript and its reviewing process. Examples of potential conflicts of interest to be disclosed such as personal or professional relationships, affiliations, and knowledge of the subject or material discussed in the manuscript.
- Risks and Human or Animal subjects: If the research involves the use of chemicals, procedures or equipment that may have any unusual risks, the authors must clearly identify them in their work. In addition, if it involves the use or experimentation of humans or animals, the authors must ensure that all actions have been carried out in accordance with the relevant laws and regulations and that the authors have obtained prior approval of these contributions. Moreover, the privacy rights of human must also be considered.
- Authors must fully cooperate and respond promptly to editors' requests for clarifications, proof of ethical approvals, patient approvals, and copyright permissions.
- In the case of making an initial decision on the submitted manuscript of some the necessary amendments and corrections, the authors must respond promptly to the comments of the reviewers and carry out the required corrections and re-submit it to the journal by the deadline.
- When authors find significant errors or inaccuracies in their submitted manuscripts, they must immediately notify editors or publishers of the journal and collaborate with them to either correct or withdraw their work.

Contents

Jordan Journal of Energy
Volume1, Number 1, 2023

ISSN (Online): 2790-7678
ISSN (Print): 2790-766X

Jordan Journal of Energy (JJE)
Journal Homepage:ttp://dsr.mutah.edu.jo/index.php/jje
JJE an official peer review journal of Mutah University,

Adaptive Overcurrent Protection Scheme for Power Systems with High Penetration of Renewable Energy Recourses

Khaled Al-Maitah[1], Batool AL-Khreisat[2]

*[1] Technical Department, Electricity Distribution Company EDCO, Aqaba, Jordan

[2] Electrical Engineering Department, Mutah University, karak, Jordan

Received: 14th May, 2022; Accepted: 2nd August, 2022

*Corresponding Author Email: kmaitah@outlook.com

ABSTRACT. *Due to high penetration of renewable energy recourses in the existing distribution network, the protection system faced a new challenge. This paper presents an adaptive overcurrent protection scheme for active distribution network ADN enhanced by real time measurement gathered from micro phasor measurement unit μPMU. The μPMU measurement is used in this paper to estimate the network topology of the ADN. The proposed scheme has been tested and validated using MATLAB programing environment. The simulation results demonstrate the effectiveness of the proposed adaptive protection scheme.*

Keywords: Power System Protection, Adaptive protection, renewable energy recourses, active distribution network, optimization technique.

1. Introduction.

Nowdays, a high penetration of renewable energy in an electrical distribution network, this penetration lead to convert the passive distribution network to be an active distribution network[1-3]. The conventional distribution networks are a dual structure system that consist of substations and loads, with the power flowing from the grid to consumers. Since there are no distributed generations (DGs) connected into the grid, this kind of network can be called a passive distribution network (PDN) [4].

An active distribution network (ADN) is a ternary structure system, which consists of DGs, substations and loads, where a flexible network topology is employed to manage power flows and achieve the proactive regulation of DGs [5].

The increase in the short circuit level and change in fault current directions in the ADN influence the protection coordination between relays installed in the ADN, and disturb the functionality and the selectivity of those relays. Further, dynamically changing load, generation

and topology cause a significant change in fault currents which sometimes results in a miscoordination of one or more primary - backup relay pairs.
Furthermore, blinding of protective devices and false tripping are the most common protection problems associated with integrating DGs in the DN [6].
Many researches have been presented in literature to deal these problems. Whereas, the non-adaptive protection scheme provides settings of relays, which can coordinate properly in both grid-connected and islanded modes. However, such a scheme cannot provide proper coordination when one or more lines in the system go out-of-service for any reason [7, 8]. On the other hand, adaptive protection scheme provides optimum settings for each operating topology and the circuit breaker status of DERs [9]. The adaptive protection provides much better coordination with relatively low operating times of all the relays [10, 11].
To reduce the possibility of the unwanted power outage, proper coordination among the direction overcurrent relays DOCRs is necessary. That's mean, the minimum coordination time interval (CTI) must be maintained between the operating times of primary and the corresponding backup relay pairs. Proper protection coordination can be achieved through optimum settings of the two parameters of DOCRs, namely, time multiplier setting (TMS) and plug setting (PS).
Normally, optimization-based approaches are used to obtain the optimum settings of the relays. In term of this, the problem is formulated as either a linear programming (LP) or a nonlinear programming (NLP) problem and various optimization techniques are applied to solve these problems. In LP formulation, the operating times of relays are expressed as the linear function of the TMSs of the relays whereas the PSs of the relays are assumed to be already known. A simple approach and its variants have been proposed to determine the TMS of the relays in [12]. In NLP formulation, the operating time of a relay become a nonlinear function of TMS and PS of the relay [13]. Subsequently, application of various metaheuristic optimization methods such as particle swarm optimization (PSO), genetic algorithm (GA), and evolutionary algorithm (EA) have also been proposed in the literature.
The proper adaptive overcurrent protection needs a real time information, this information generally obtained by s supervisory control and data acquisition (SCADA) system or intelligent electronic devices (IEDs). These data face two types of issues. The first one is a high time delay, whereas the second one is considerable measurement errors. From this point in this paper the phasor measurement unit PMU is used to enhanced the adaptive protection scheme. real-time monitoring and protection scheme of AC MGs by employing a synchrophasor at the point of common coupling (PCC) has been discussed [14]. The μPMU provides phasor measurements at very high-resolution, which is one of the most important requirements to use them at distribution level [15].
This paper proposed an adaptive overcurrent protection scheme enhanced with micro phasor measurement unit μPMU. The MATLAB program is used to solve the nonlinear optimization problem. The proposed scheme has been tested in an active distribution network. The micro

phasor measurement unit μPMU is used in the proposed scheme to gathered the real time information from the network to the control center via suitable communication link.
The organization of the rest of this paper is as follows, In Section II, the proposed adaptive overcurrent protection is presented, which include the optimal relay setting calculation. In Section III, Simulation results and discussion is presented. Finally, the conclusion is presented in Section V.

2. The Proposed Adaptive Overcurrent Protection.

The main aim of protection schemes is to limit the damage, by separating the faulted section from the healthy one as quickly as possible. There is a minimum time gap between the operating times of primary and its corresponding backup relay. This time gap is known as the coordination time interval (CTI) of the primary-backup relay pairs. The proper protection coordination is achieved through the optimum settings of the direction over current relays DOCRs. However, the settings need to be changed as the network topology changes.
The operating time of a DOCR is dependent on its two parameters for given fault current. These parameters are time multiplier setting (TMS) and pickup current setting (PCS). The value of TMS and PCS parameters is called settings of the relay. In numerical DOCRs, TMS and PCS parameters are considered as the continuous variable within their range. Also, these parameters can be modified remotely from the control centers through a suitable communication link.
The real-time measurements obtained from μPMUs can be used to estimate the correct topology of the network. On the other hand, the status of various CBs, DGs, and PCCs can be obtained through the μPMUs. All this information will send continuously to the main control center to determine the short circuit current. The time coordination of primary and backup relay also will check in the control center.
Figure.1 present the proposed adaptive protection scheme the data is collected by using μPMUs and send to the main control center. In the control center there are two main function. the first one is calculating the short circuit current in each branch in the system by using the information gathered from the μPMUs.

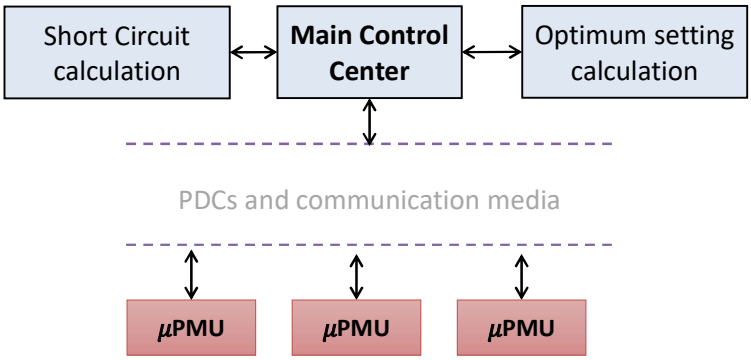

FIGURE.1 The proposed adaptive overcurrent protection

Whereas, the second function that must be done according to the proposed scheme is calculating the time coordination between the primary and the back-up protection relays, if the coordination time within the range the process well repeated. On the other hand, if the coordination time is out of range the optimum relay setting must to calculated and sent to the DOCRs.

The optimum setting of overcurrent relay is usually formulated as a constrained optimization problem. Several objective functions have been discussed in recent literature. The most common objective function used in literature is the minimization of the sum of the operating times of all the Directional Over Current Relays (DOCR) for the maximum fault current, this objective function is expressed as follows:

$$OF = \min \sum_{i=1}^{m} t_{op,i} \qquad (1)$$

Where *m* is the number of relays, $t_{op,i}$ is the operation time for relay R_i . The operation time for relay R_i can be calculated by:

$$t_{op,i} = \frac{\mu \, . TMS_i}{(I_{F,i}/PS_i)^{\beta} - 1} \qquad (2)$$

Where TMS_i is the time multiple setting for Relay R_i , $I_{F,i}$ is the maximum current flow through relay R_i. PS_i is the relay plug setting and μ, β is the relay characteristic constant as shown in table 1.

TABLE 1 . Overcurrent Relay Constant [16]

Relay type	**μ**	**β**
standard inverse relays	0.14	0.02
very inverse relays	13.5	1
extremely inverse relays	80	2

The objective function (1) minimizes the operating time only for primary relay without taking in account the backup relay operating time. To minimize the operating times of the backup relays along with those of the primary relays, the objective function in (3) can be used also:

$$OF_{i,j} = \sum_{i=1}^{m} (t_{op,i})^2 + \sum_{i=1}^{n} (t_{op,j} + MCT)^2 \qquad (3)$$

Where, $OF_{i,j}$ is the summation of operating time for the primary relay R_i and the backup relay R_j. $t_{op,i}$, $t_{op,j}$ are the operating time for the primary relay R_i and backup relay R_j, respectively. MCT is the minimum coordination time between primary and backup relays. The objective function (3) is subjected to the following set of constraints:

1. If a primary relay R_i has a backup relay R_j for a fault at any line k, then the coordination constraint can be expressed as follows:

$$t_{op,j} - t_{op,i} \geq MCT \quad (4)$$

Where $t_{op,i}$, $t_{op,j}$ is the operating time for the primary and backup relays, respectively.

2. The operating time for the relay R_i should be larger than the minimum operating time and less than the maximum operating time, this constraint can be expressed as:

$$t_{i,min} \leq t_{op,i} \leq t_{i,max} \quad (5)$$

Where $t_{i,min}$, $t_{i,max}$ is the minimum and maximum operating time of the relay R_i.

3. The TMS and PS should be within relay rang:

$$TMS_{i,min} \leq TMS_i \leq TMS_{i,max} \quad (6)$$

$$PS_{i,min} \leq PS_i \leq PS_{i,max} \quad (7)$$

Where $TMS_{i,max}$, $TMS_{i,min}$ are the minimum and maximum limits of the time multiple setting, respectively. $PS_{i,min}$, $PS_{i,max}$ are the minimum and maximum limits of plug setting, respectively.

For numerical/digital type of relays, TMS and PS can have any continuous value within their ranges. Whereas, for static or electromechanical relays, TMS can be any continuous value but PS can only have certain fixed discrete value within their respective ranges. Anyway, numerical relay has been used to conduct this paper.

3. Result and Discussion.

To investigate the effectiveness of the proposed protection scheme, an active distribution system has been chosen. The single line diagram of the chosen distribution system is shown in figure.2. It has 4 buses and 4 lines. The distribution system is connected to the grid at bus 1. There are two 5MVA distributed generators DGs connected to the system at bus 2 and bus 4. The short-circuit rating of the grid is 250 MVA, whereas the generators have a short-circuit rating of 25 MVA. In simulation, the base voltage is taken as 11 kV and base MVA is 100. Each transmission line of the network has a resistance and reactance of 0.02 pu and 0.05 pu, respectively.

In order to provide proper protection system, the system has 8 directional numerical over current relay DOCRs, 2 relays at each line.

The current transformer CT for each relay based on the maximum loading current and short circuit current. Table 2 proposes the selected CT ratio for all relays, the load current at peak load, the maximum and the minimum short circuit currents for each relay in the system.

TABLE 2. Load Current, Fault Current And CT Raio

Line No.	Relay No.	I_{load} (A)	$I_{f\,min}$ (A)	$I_{f\,max}$ (A)	CT Ratio
L1	1	597	6543	8261	3000/5
	2	597	1701	2148	3000/5
L2	3	117	3412	4187	1200/5
	4	117	2271	2788	800/5
L3	5	178	3875	4735	1200/5
	6	178	1426	1742	1000/5
L4	7	62	3129	3810	1000/5
	8	62	1827	2225	600/5

Firstly, DG2 which is connected in bus 4 is assumed to be isolated from the network. after all measurements and topology information sent to the main control center, the short circuit current is calculated in each line, in order to determine the coordination time of primary-backup relay pairs.

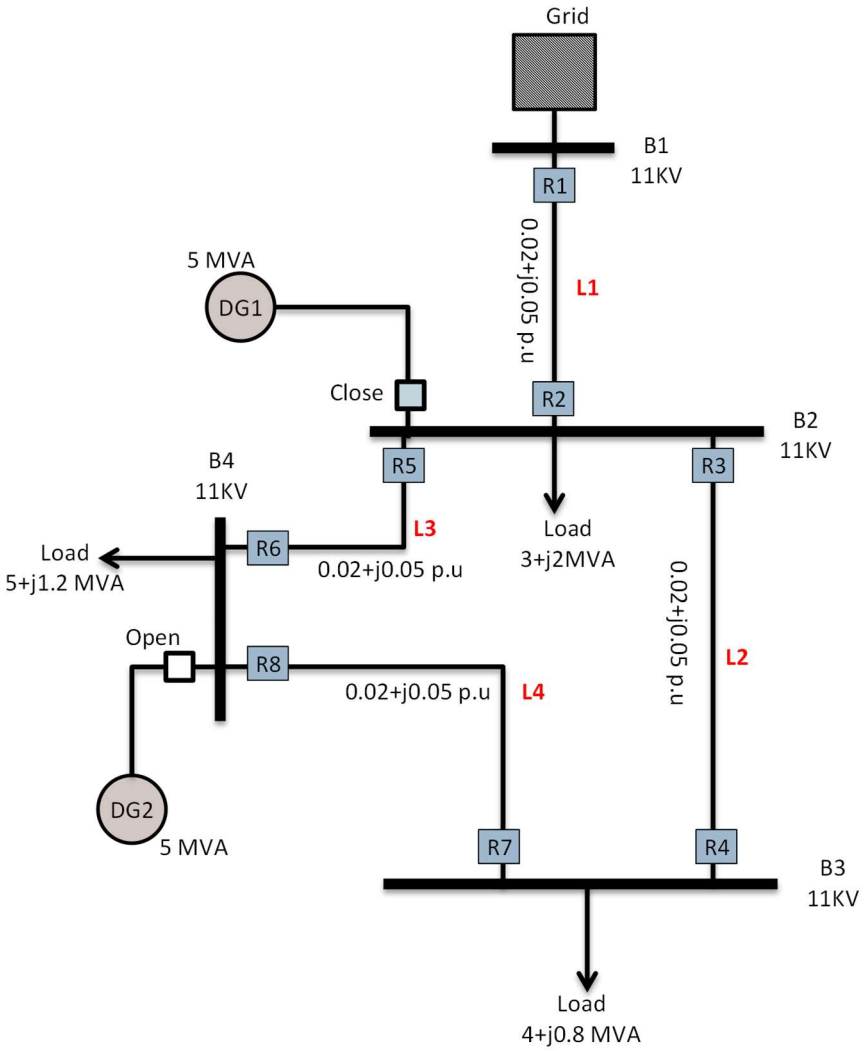

FIGURE. 1. Distribution system under study

Referring to the figure 2, there are 10 pairs of primary-backup protection relays in the system. So, the short circuit current for each pair is shown in table 3.

TABLE 3. Short Circuit Current For Primary And Backup Relays

Fault Location	Pair No.	R_{prim}	R_{Back}	I_{prim} (A)	I_{Back} (A)
L1	1	2	4	2527	1542
	2	2	6	2527	821
L2	3	3	1	4466	4627
	4	3	6	4466	465
	5	4	8	3048	436
L3	6	5	1	4987	4481
	7	5	4	4987	384
	8	6	7	1989	1874
L4	9	7	3	4066	1587
	10	8	5	2491	2369

After obtaining the short circuit current for all relays, the optimal setting is generated from the control center and sent to the relays. Figure.3 shows the PS and TMS setting for all relays. To ensure suitable setting for proper coordination between the primary and back up protection, the operating time for all pairs of primary and backup relays, the coordination time interval CTI for all pairs and the minimum acceptable coordination time MCT have been calculated and presented in figure.4. For example, if a fault is occurred at line L1, the primary protection is R2 and the Backup protection is R4, pair No. 2 in table 6.

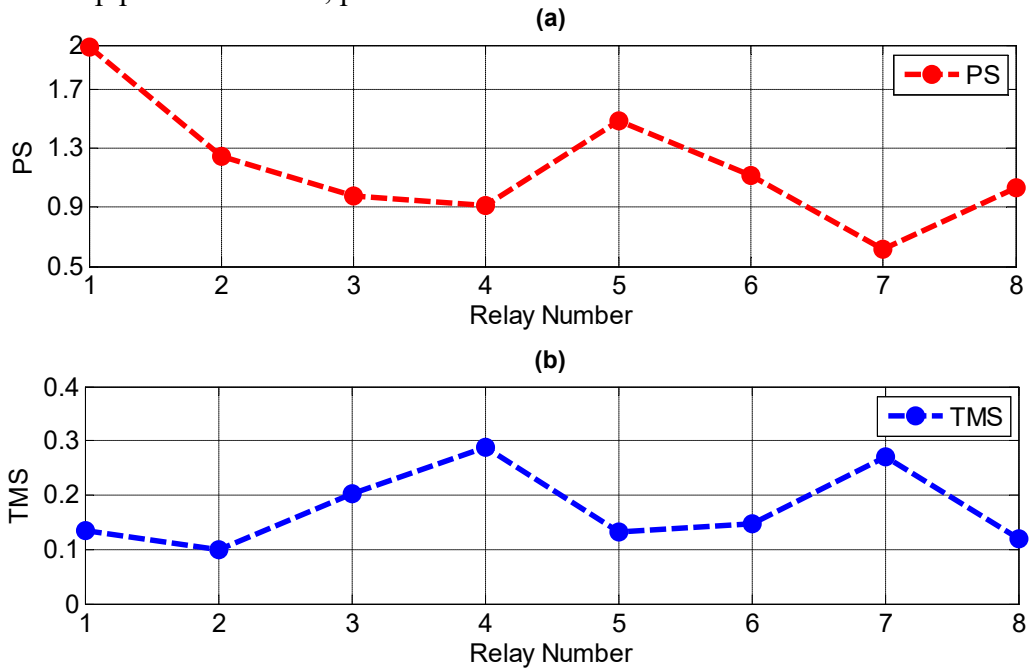

FIGURE. 2 Relay setting from control center for all relays (a) Pluge setting PS (b) Time multiple setting TMS.

Figure.4 (a), shows the operating time of the primary protection (R2) is about 0.5 seconds. The operating time for the backup protection (R4) is about 0.7 seconds. The coordination time exactly equals 0.2 seconds. Similarly, the coordination time for pair No. 3 is about 0.22 seconds, and for pair No. 4 is about 0.9 seconds, and so on. So, there is no pair of primary and backup relay has a coordination interval less than 0.2 sec.

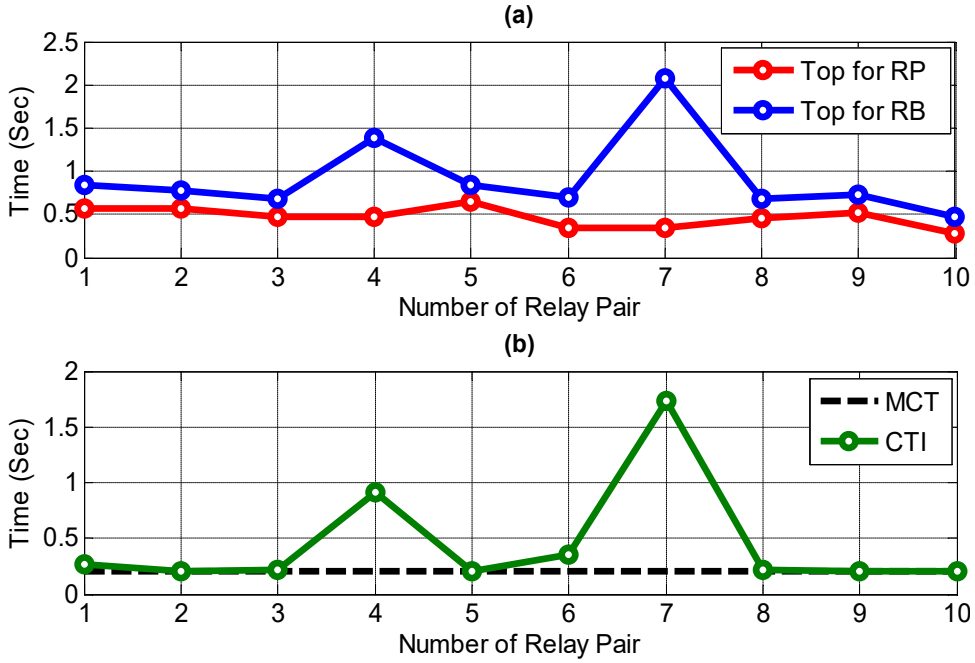

FIGURE. 3 (a) operating time in second for primary and back-up relay (b) Coordination time interval CTI and Minimum coorination time for all pairs of primary and back-up relays

With integration of DG2 at bus 4 the short circuit must be recalculated; this is done in the control center. All measurements and topology information are sent to the control center to calculate the short circuit current for the entire network in order to determine the optimal relay setting to ensure the proper coordination between primary and backup protection. The short circuit calculation is shown in table 4. Must to be noted, the short circuit current increased in some line after DG integration.

By assuming the relays' setting remains without any change. Then, by the short circuit current, which is presented in table 4, and relays setting presented in figure3, the operating time for primary and backup protection pairs and the coordination time interval CTI are shown in figure 5.

TABLE 4. Short Circuit Current After Dg2 Is Integrated

Fault Location	Pair No.	R_{prim}	R_{Back}	I_{prim} (A)	I_{Back} (A)
L1	1	2	4	3207	1693
	2	2	6	3207	1373
L2	3	3	1	4840	4523
	4	3	6	4840	465
	5	4	8	3382	919
L3	6	5	1	5074	4457
	7	5	4	5074	505
	8	6	7	2866	1595
L4	9	7	3	4091	1741
	10	8	5	3342	2111

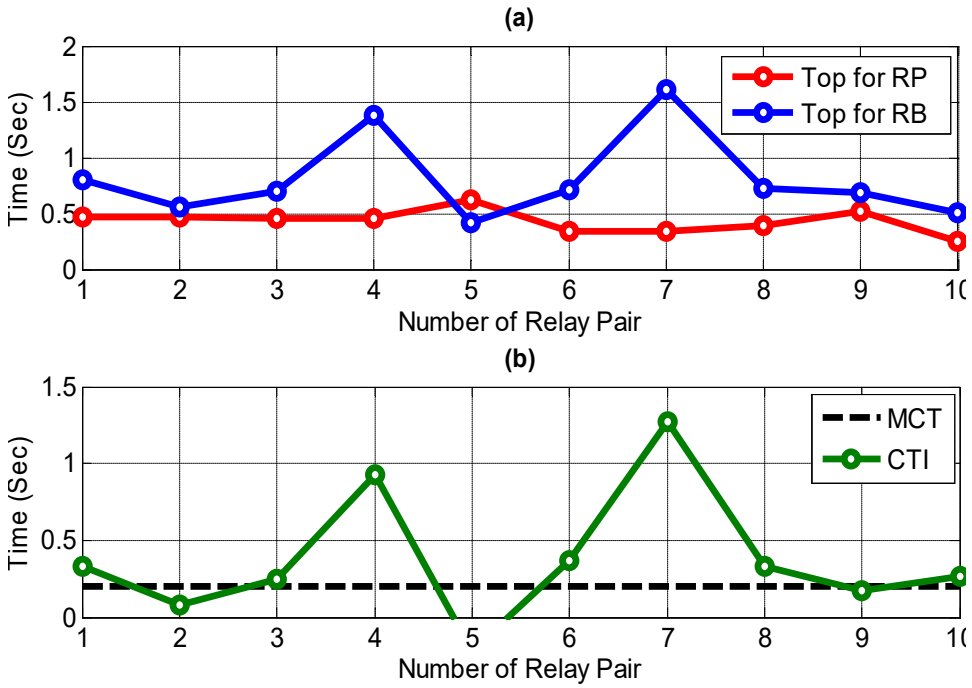

FIGURE. 4 (a) The operating time for all relay pairs after DG2 is integrated without change the relay setting (b) The coordination between primary and backup protection without change the relay setting.

Figure.5 (b) clearly shows the coordination time is failed in pairs 2, 5, and 9, i.e. the coordination time between primary and backup protection relay less than 0.2 seconds. Based on the proposed scheme when the coordination time out of range the optimum setting should be calculated and sent to the relays.

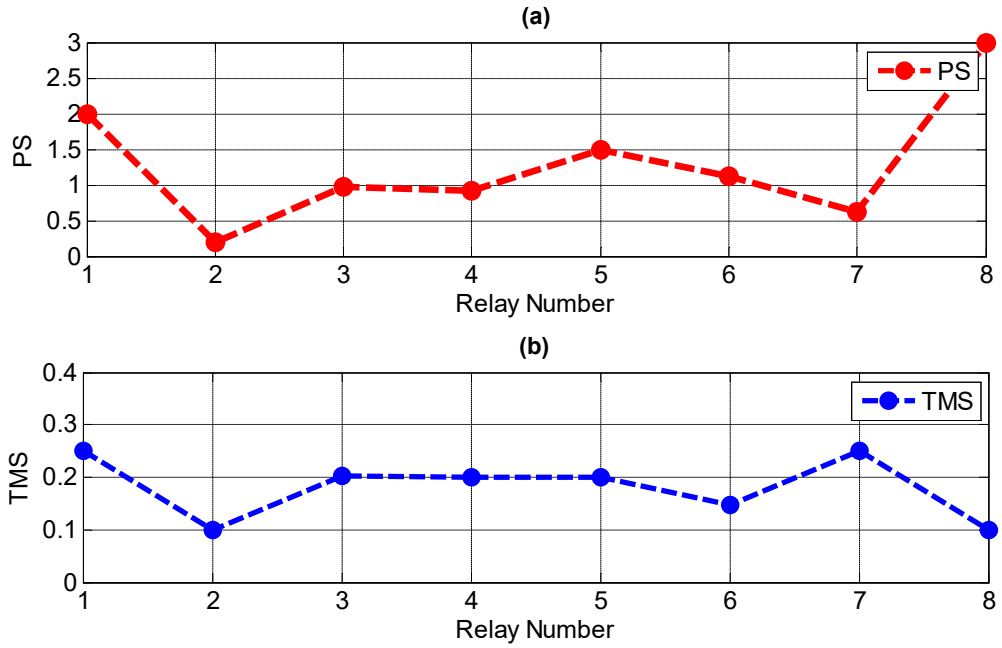

FIGURE. 5 (a) Plug Setting PS, (b) TMS for all relays, by proposed scheme after the communication link return to the service.

Figure. 6 shows the new setting od relays generated by control center after the DG2 is integrated. It is clear that all relays have been properly optimized. By applying the short circuit current given in table IV for the new relays setting, the operating time for each relay can be obtained. Figure. 7 shows the operating time of the relay pairs after applying the new relay setting. Figure 7 (b) clearly shows that there is no coordination time interval CTI less than MCT (0.2 sec.). Where, the coordination time between the primary relay R6 and the backup relay R7 in pair No. 8 is about 0.27seconds, and similarly between R2 and R6 is about 0.34 seconds.

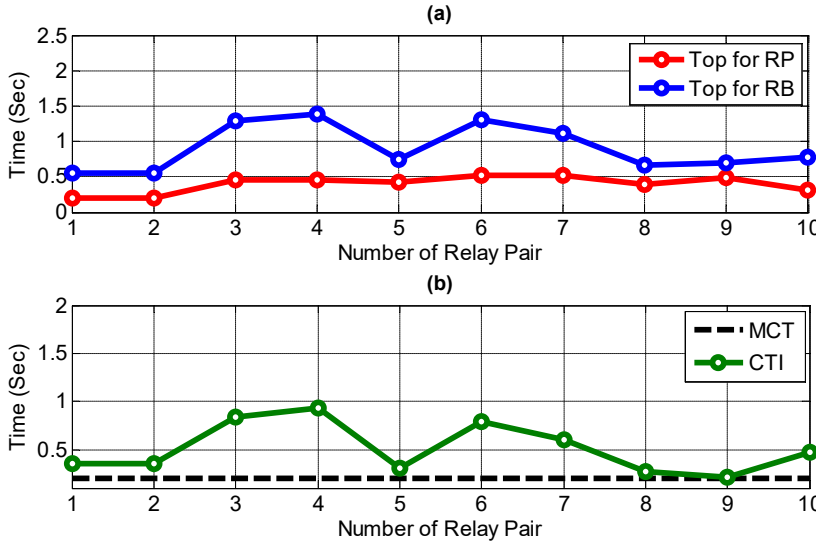

FIGURE. 6 (a) Operating time relay pairs (b) CTI and MCT for all for all relay pairs, by using optimal setting form the proposed scheme

4. Conclusion.

In this paper an adaptive protection scheme based on a micro phasor measurement unit μPMUs is proposed. The proposed scheme used the μPMUs to obtain the accurate measurement form the network to the control center. The coordination time between the primary and back-up protection relay is calculated continuously in the proposed scheme. The settings of all relays have been optimized to maintain the coordination time between the primary and the back-up relay. The simulation result shows that the proposed scheme is effective and sufficient to overcome the negative impact of distributed generation DGs in the distribution network.

REFERENCES

[1] K. Al-Maitah and A. Al-Odienat, "Wide Area Protection Scheme for Active Distribution Network Aided μPMU", 2020 IEEE PES/IAS PowerAfrica, 2020, pp. 1-5.

[2] Abdullah I. Al-Odienat, Khaled Al-Maitah, "A New Wide Area Protection Scheme Based on the Phase Angles of the Sequence Components", Electric Power Components and Systems, 2021, pp. 1-13.

[3] Khaled Al-Maitah and Abdullah Al-Odienat, "Local Decision Module for A More Reliable Wide Area Protection Scheme", International Journal of Innovative Computing, Information and Control. Volume 17 (2), April 2021.pp. 671–685.

[4] J. H. He, Y. H. Cheng, J. Hu and H. T. Yip, "An accelerated adaptive overcurrent protection for distribution networks with high DG penetration," *13th International Conference on Development in Power System Protection 2016 (DPSP)*, Edinburgh, 2016, pp. 1-5.

[5] F. T. Dai, "Impacts of distributed generation on protection and autoreclosing of distribution networks," *10th IET International Conference on Developments in Power System Protection (DPSP 2010)*. Managing the Change, Manchester, 2010, pp. 1-5.

[6] Z. Bo, Q. Wang, Y. Zhao, L. Wang, L. Chen and F. Wei, "A new concept intelligent integrated protection system for distribution network,"*5th International Conference on Electric Utility Deregulation and Restructuring and Power Technologies (DRPT)*, Manchester, 2015.

[7] W. K. A. Najy, H. H. Zeineldin, and W. L. Woon, "Optimal protection coordination for microgrids with grid-connected and islanded capability," *IEEE Trans. Ind. Electron*., vol. 60, no. 4, pp. 1668–1677, Apr. 2013.

[8] H. M. Sharaf, H. H. Zeineldin, and E. El-Saadany, "Protection coordination for microgrids with grid-connected and islanded capabilities using communication assisted dual setting directional overcurrent relays," *IEEE Trans. Smart Grid*, vol. 9, no. 1, pp. 143-151, Jan. 2018.

[9] M. Y. Shih, A. Conde, Z. Leonowicz, and L. Martirano, "An adaptive overcurrent coordination scheme to improve relay sensitivity and overcome drawbacks due to distributed generation in smart grids*," IEEE Trans. Industry Appl*., vol. 53, no. 6, pp. 5217–522.

[10] M. Y. Shih, A. Conde, Z. Leonowicz, and L. Martirano, "An adaptive overcurrent coordination scheme to improve relay sensitivity and overcome drawbacks due to distributed generation in smart grids," *IEEE Trans. Industry Appl.*, vol. 53, no. 6, pp. 5217–522.

[11] L. Che, M. E. Khodayar, and M. Shahidehpour, "Adaptive protection system for microgrids: Protection practices of a functional microgrid system." *IEEE Electrification Magazine*, vol. 2, no. 1, pp. 66–80, Mar. 2014.

[12] B. Chattopadhyay, M. S. Sachdev and T. S. Sidhu, "An on-line relay coordination algorithm for adaptive protection using linear programming technique," in *IEEE Transactions on Power Delivery*, vol. 11, no. 1, pp. 165-173, Jan. 1996.

[13] M. N. Alam, B. Das, and V. Pant, "An interior point method based protection coordination scheme for directional overcurrent relays in meshed networks," *Electric Power Energy Syst*., vol. 81, pp. 153–164, Oct. 2016.

[14] S. Choi and A. P. S. Meliopoulos, "Effective real-time operation and protection scheme of microgrids using distributed dynamic state estimation," *IEEE Trans. Power Del.*, vol. 32, no. 1, pp. 504–514, Feb. 2017.

[15] A. von Meier, E. Stewart, A. McEachern, M. Andersen, and L. Mehrmanesh, "Precision micro-synchrophasors for distribution systems: A summary of applications," *IEEE Trans. Smart Grid*, vol. 8, no. 6, pp. 2926–2936, Nov. 2017.

[16] E. J. Holmes, Protection of Electricity Distribution Networks, 3rd Edition, 2011.

Jordan Journal of Energy
Volume1, Number1, 2023

ISSN (Online): 2790-7678
ISSN (Print): 2790-766X

Jordan Journal of Energy (JJE)
Journal Homepage:ttp://dsr.mutah.edu.jo/index.php/jje
JJE an official peer review journal of Mutah University,

Islanding Detection Method Based Artificial Neural Network

Mohammad M. Al-Momani[1*], Seba F. Al-Gharaibeh[2] , Ali S. Al-Dmour[3], Allaham Ahmed J.[4]

[*1]Electrical Engineering department, Mutah University, Al Karak, Jordan

[1]monqedmohammad@gmail.com

[2]Electrical Engineering department, Mutah University, Al Karak, Jordan

[2]620180441015@mutah.edu.jo

[3]Electrical Engineering department, Mutah University, Al Karak, Jordan

[3]aldmourali2016@gmail.com

[4]Sustainable Energy Technologies Department, University of Oldenburg, Oldenburg, Lower Saxony, Germany

[4]Ahmed.allahham@uni-oldenburg.de

Received: 25th May, 2022; Accepted: 29th July, 2022

*Corresponding Author Email: monqedmohammad@gmail.com (M. M. Al-Momani)

ABSTRACT. *This paper presents a new islanding detection technique based on an artificial neural network (ANN) for a doubly fed induction wind turbine (DFIG). This technique takes advantage of ANN as pattern classifiers. Five different ANN systems are presented in this paper based on various inputs: three phase power, phase voltage, phase current, neutral voltage, and neutral current. An ANN structure is trained for each input, and the comparison between the different structures is presented. Feedforward ANN structures are used for the five systems. Three different learning algorithms are used: backpropagation and two artificial optimization techniques: Genetic Algorithm (GA) and Cuckoo optimization algorithm. For each method in each training technique, the results and the cost function are presented. The comparison of different inputs different algorithms is conducted. MATLAB 2020a is used to simulate the ANN structure and code the training algorithms. A detailed discussion of the input sample rate has also been manipulated to make the computational burden a factor in assessing the performance.*

Keywords: Islanding Detection Method (IDM), Artificial neural network (ANN), Genetic Algorithm, Cuckoo algorithm, optimization, backpropagation, feedforward, distributed energy resources (DER), double fed induction wind turbine (DFIG), micro-grid.

1. Introduction.

Islanding detection is one of the most critical issues considered in any distributed energy resource (DER). Islanding occurs when a part of the distribution system becomes isolated from the main supply. If islanding is detected, the DER should be tripped out. Typically, a DER should be disconnected within 0.1-2 seconds after the loss of the main supply [1-3]. If the islanding is failed to detect, the islanding may lead to power inequality issues and safety issues for machines and humans. Different techniques are presented in the literature for these purposes. These techniques can be broadly divided into remote and local techniques. Remote techniques are associated with islanding detection on the supply side and the local on the DER side. In remote techniques, communication is needed to send a trip signal to the DER when the islanding is detected. Furthermore, Local algorithms divide into passive, active, and hybrid methods.

The main philosophy of the local techniques is based on monitoring the output of the DER and detecting the status of the main supply. This monitoring may base on output power, voltage, frequency, current, etc. If the external source (auxiliary) injects current, power, harmonic…. to the system, in parallel with the monitoring, the technique is called active techniques, otherwise it is called passive technique.

Some of the remote detection techniques presented in the literate are based on the transfer scheme trip and power line signaling scheme. The concept of the transfer trip scheme is based on monitoring all breaker status and sent a trip signal to the DER if the islanding is detected. Supervisory control and data acquisition (SCADA) [4], or wide-area monitoring system (WAMS) [5-6] are used as remote IDM. The signal is continuously generated at the transmission side in the signaling technique, and the DER has a receiver to detect this signal. In these techniques, the islanding status is proved if the DER does not receive any signal [7-9]. A high-frequency impedance estimation-based technique is an example of active detection techniques [10]. In [10], the potential failure mechanism of the f-Q (frequency-reactive power) drifting is analyzed. Then, the researchers proposed a high-frequency transient injection-based islanding detection method. From the results of this paper, the high-frequency temporary injection method is better than the traditional injection method. Another researcher presents a detection method as an example of passive techniques in [11]. In [11], researchers using the Forced Helmholtz Oscillator to the signal at the point of common coupling. The dynamic characteristics of the synchronous generator and signal processing technique are presented in [12]. This paper proposes a hybrid islanding detection method for distribution systems containing synchronous distributed generation (SDG) based on two active and reactive power control loops and a signal processing technique.

Other techniques based on artificial neural network are presented in [13-15]. In [13], the proposed artificial neural network (ANN) employs minimal features of the power system. The performance comparison between stand-alone ANN, ANN- evolutionary programming, and ANN- particle swarm optimization in the form of regression value is performed. In [14], a new composite approach based on wavelet-transform and ANN for islanding detection of distributed

generation is presented. The wavelet transform is used to detect events, and then the artificial neural network (ANN) is used to classify islanding and non-islanding events. In [15], the S-transform is used to obtain the frequency spectrum at the terminals of the DER; then, the ANN is used to identify whether the event is islanding. Like other protection functions [16-18], WAMS and machine learning can be used to detect the islanding in the system and send a protection signal to the remote protective relays to prevent any mis operation. Still, it is expensive to apply and need a good communication infrastructure.

This paper is organized as follows: Section II presents the ANN structures and the used learning techniques. Section III offers the proposed ANN structure for the three systems. The simulation results and comparisons are shown in section IV. Then the conclusion is presented in Section V.

2. ANN and Learning Techniques

2.1 Feed-Forward ANN structure ANN is a learning technique used in different areas for different purposes. The very widely used applications of ANN are classification applications. The main structure of the ANN is shown in Figure 1.

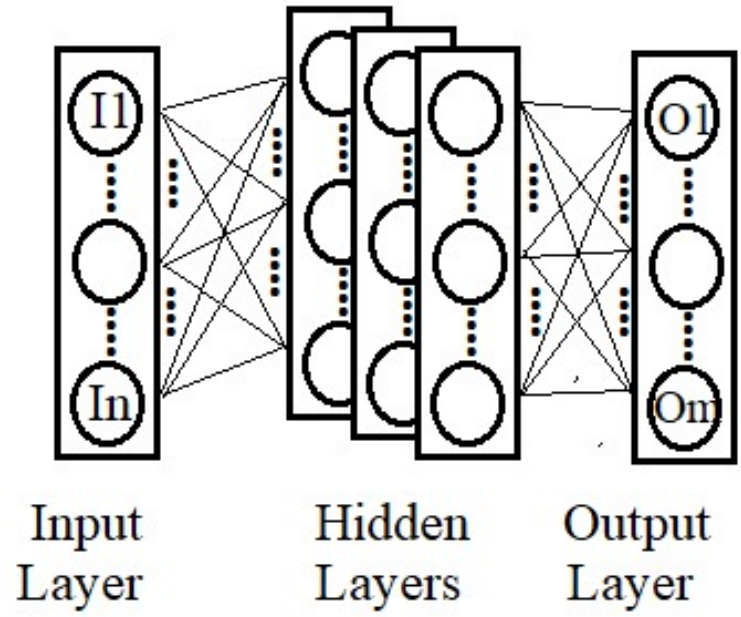

FIGURE 1. General feedforward ANN structure

In general, ANN has three types of layers: an input layer has n neurons, hidden layer(s), and the output layer has m neurons. Where n and m are the number of inputs and outputs, respectively. The number of hidden layers and the neurons in each hidden layer is adjustable. The optimal number of layers needs more information about the problem to identify. For this study, the number of layers and neurons are selected based on experience; then, general formula to determine the number of neurons in each layer is proposed. Each neuron has an activation function, so the neurons' output is a function of the sum of the inputs (net). Different activation

functions are available to use. These activation functions may be divided into step, linear, and nonlinear functions in general. Other nonlinear functions are presented in the literature include sigmoid function, hyperbolic tangent function, rectified linear unit function, leaky rectified linear unit function, soft-max function, and switch function. Each of these functions has advantages and disadvantages. The selection of the activation function is based on the application. The sigmoid function is the most common. Each neuron in layer (i) connects with each neuron in layer (i+1) via a weight. The arrows in Figure 1 refer to the weights.
The weights in the structure are defined by the learning technique based on the inputs/outputs samples. The training samples should represent the overall behavior. The output samples are called targets, where the outputs of the neural network are called outputs. The learning techniques are mainly optimization techniques. The cost function of the methods is to minimize the sum of the absolute (square) error between the output and the target. Once the outputs and the targets are very close together, the learning is done. The backpropagation learning technique is very commonly used in this context. The main disadvantage of this algorithm is the highest probability of sticking to a local solution. Based on this concept, any optimization algorithm (hard or soft computational techniques) can be used to solve this optimization problem. In this paper, two soft computational methods: Genetic algorithm (GA) and cuckoo algorithm (CA) and one hard computational technique (backpropagation), are used and then compared.

2.2 Genetic Algorithm.

Genetic algorithm (GA) is one of the very widely used techniques in optimization problems. This algorithm is based on the concept of human gene behavior. Firstly, a considerable population generated randomly has a specific number of randomly proposed solutions. Each solution is called a gene. The behavior of these genes is getting from the cost function (the value of the cost function at a specific solution 'chromosome'). If the problem is to maximize, the chromosomes with the highest values have the best performance and vice versa. From the first iteration, the chromosome which has better performance is selected, then these chromosomes will be mated to get a new population. The mating is similar to human mating, but for variable cross-over, so the latest population performs better than the old one. This procedure will repeat more and more to get the specific cost function. The mutation idea is created to prevent any predicted local solution. In the mutation process, the genes in the chromosomes are changed randomly. This simple step is used to add noise to the signal, which will help the algorithm to go over any local solution.

2.3 Cuckoo Algorithm

This algorithm is inspired by the eggs laying feature of a family of birds called Cuckoo. Like other evolution approaches, Cuckoo start by generation random population. There are two types of population: cuckoo bird and eggs, each Cuckoo has a nest with an arbitrary number of eggs, and each egg refers to a proposed solution. The position of eggs in the nest is organized based on the egg-laying radius (ELR). Cuckoos search for the best area to maximize their eggs' life

lengths. After hatching and turning into adult cuckoos, they form societies and communities. Each community has its habitat to live in. The best habitat of all communities will be the next destination for cuckoos in other groups. All groups immigrate to the best current existing area. Each group will be the resident in an area near the best current existing site. An egg-laying radius (ELR) will be calculated regarding the number of eggs each Cuckoo lays and its distance from the current optimized area.

2.4 Backpropagation algorithm

For the first iteration, the weights are selected randomly. Then the output of each neuron is calculated for each input sample. A weight will be modified to decrease the error. So, the weights' effect on the total error is calculated (a partial derivative of the error to the weight i). For all weights, the derivative is added in the first iteration. Then the new weights are used for the next iteration and so on.

3. Proposed ANN Structure.

In this paper, three different systems are designed: Power-based system, voltage-based system, and current-based system. Five different sampling rates are tested: 400 Hz, 800 Hz, 1600 Hz, 3200 Hz, and 6400 Hz (8, 16, 32, and 64 per cycle). A complete cycle is considered as a data window. So, in a 400 Hz sampling, the system has eight inputs and a single output. The number of layers in each system (400, 800, 1600, 3200, 6400) is selected due to Equation (1). The number of neurons in each hidden layer is defined by Equation (2). These equations are based on experience in the classification application. These equations may be used in other classification applications to identify the optimal number of the layers and neurons.

$$N_{Hidden\ layer} = \log_2 \frac{N_{input}}{N_{output}} - 1 \qquad (1)$$

$$N_i = \frac{N_{input}}{N_{output} 2^i} \qquad (2)$$

Where, N_i: number of neurons in hidden layer number i. Two biases are added to the structure: input and output biases (independent neurons have constant output '1'). Figure 2 shows the design of the 800 Hz system. Based on previous equations, the number of hidden layers for 16 inputs and one output equals 3. The numbers of neurons are (8, 4, 2) per each layer, respectively. In this example, the number of weights (size of the optimization techniques) = 51. Generally, the number of weights (N_w) is given by Equation (3), where N_h is the number of the hidden layer.

$$N_w = \left(\frac{N_{input}}{N_{output}}\right)^2 * \sum_{i=1}^{i=N_h} \left(\frac{1}{2 * 4^i}\right) + \frac{N_{input}}{2} + N_{output} \qquad (3)$$

The sigmoid function is selected as an activation function of all neurons in this paper. In Figure 2, the green cycles refer to inputs, grey cycles refer to the neurons in hidden layers, red cycles refer to the output neuron, and white cycles refer to biases. Each simulation cycle is used as a sample in the training phase, either with the islanding status or non-islanding status. For each data rate, there is a specific number of inputs. In the simulation phase, the algorithm uses several cycles to decide either the system is islanding or not. The number of cycles depends on the sample rates used. The higher the sample rate, the better the accuracy.

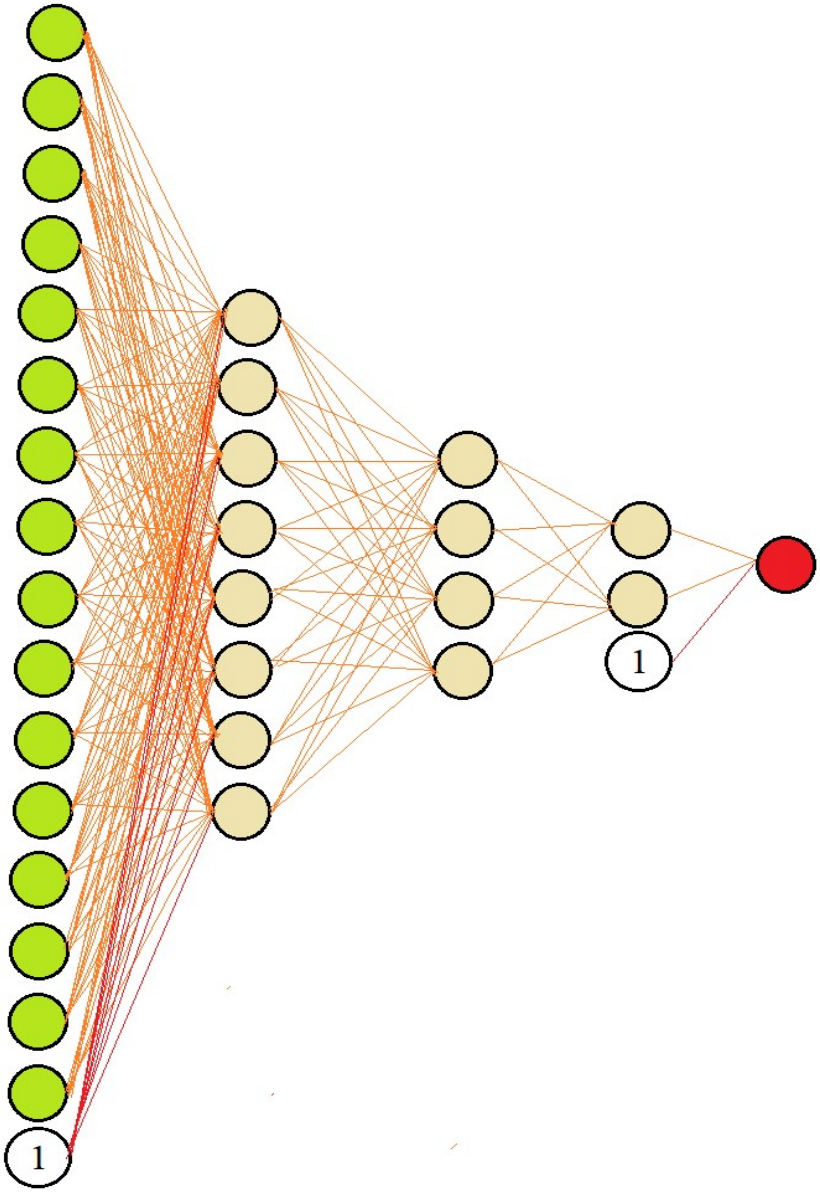

FIGURE 2. ANN structure, for an example of sample rate equal to 800 Hz

4. System Understudy.

Different sample rates are considered in this section: 0.4, 0.8, 1.6, and 3.2 KHz. Figure 3 shows the simulation system. Three scenarios are covered here: increase the load to its double value, decrease load to its half value, and trip main supply. Ten cycles are covered for each scenario (five cycles before the event and five cycles after the event). So for each load level, 30 samples are generated (10 samples for load up event, 10 samples for load down event and 10 for the islanding event). Two data sets are generated at different load levels: test data used in training systems and validation data used in simulation systems. Different load levels are covered from 0.2 Pu to 2 Pu stepped by 0.1 Pu for the training data set and from 0.25 to 1.95 stepped by 0.1 for the validation data set. The size of the test data for the 0.8 kHz system is 600×16. Figure 4 shows the sampling technique. Then these inputs are normalized. Figure 5 shows the Simulink model for the system.

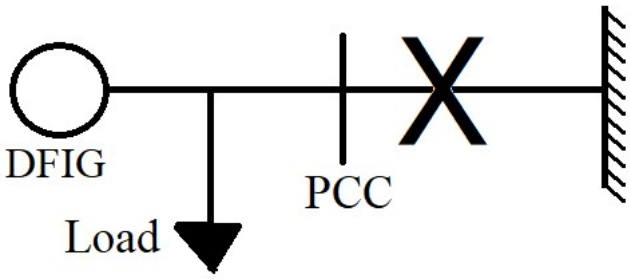

FIGURE 3. System understudy

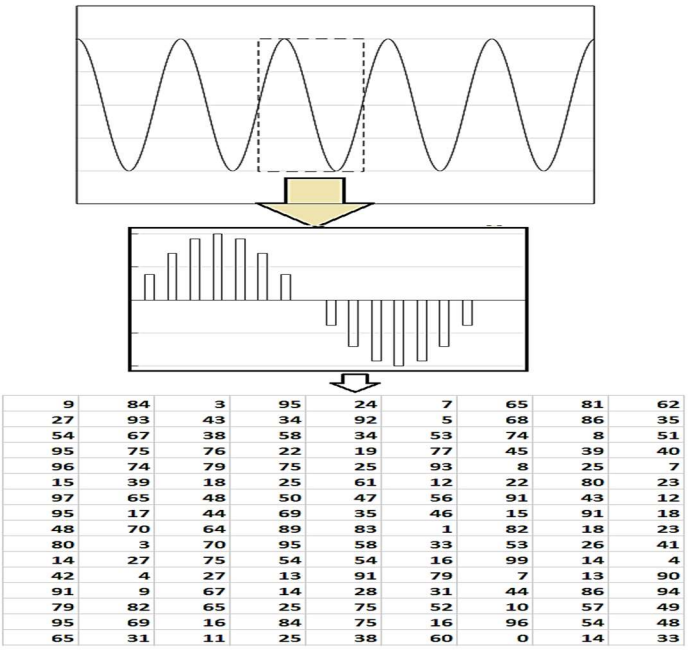

9	84	3	95	24	7	65	81	62
27	93	43	34	92	5	68	86	35
54	67	38	58	34	53	74	8	51
95	75	76	22	19	77	45	39	40
96	74	79	75	25	93	8	25	7
15	39	18	25	61	12	22	80	23
97	65	48	50	47	56	91	43	12
95	17	44	69	35	46	15	91	18
48	70	64	89	83	1	82	18	23
80	3	70	95	58	33	53	26	41
14	27	75	54	54	16	99	14	4
42	4	27	13	91	79	7	13	90
91	9	67	14	28	31	44	86	94
79	82	65	25	75	52	10	57	49
95	69	16	84	75	16	96	54	48
65	31	11	25	38	60	0	14	33

FIGURE 4. Sampling technique

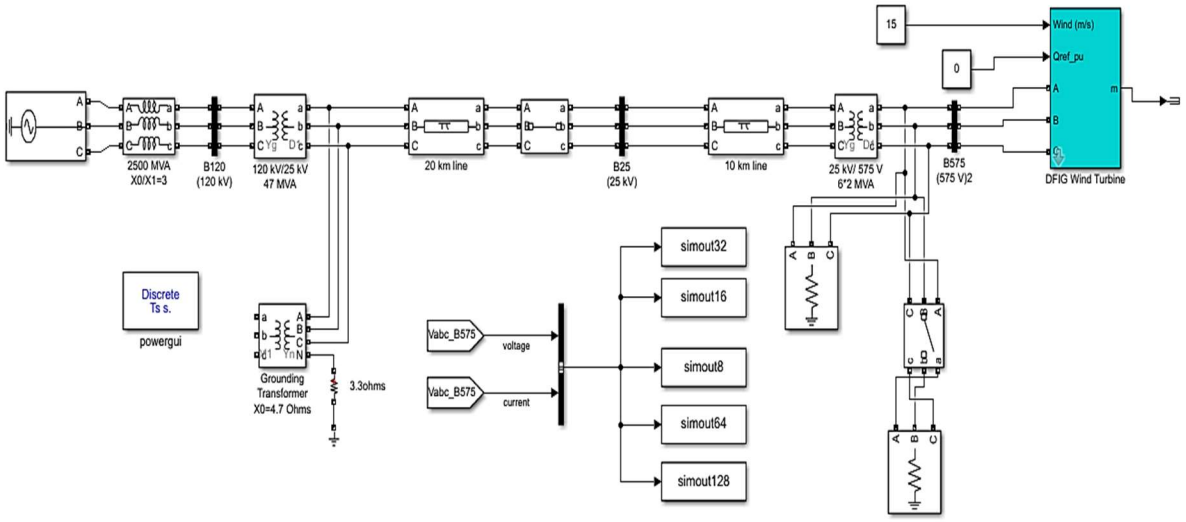

FIGURE 5. Simulink blocks of the system under study

5.Training and Simulation.

The five systems are presented in this section in three different algorithms: backpropagation, Cuckoo, and genetic algorithm. In this section, the test sample is used to train the systems. For each specific load, three scenarios are considered: increase the load, decrease load, trip main supply.

5.1. Backpropagation learning technique.

5.1.1. Phase Voltage-Based ANN classification. The voltage-Based techniques are used to the ANN inputs in this section. The results for the different rates are shown in table 1. In this table, the mean absolute error (AE), maximum absolute error (MAE), computational time (Tc), number of iterations (N), the best performance (BP), the best test performance (BTP), and the best validation performance (BVP) where the performance function is the mean square error. The performance diagram of the tanning data, validation, and test data are shown in figure 6.

TABLE 1: performance of phase voltage-based ANN classification

Parameter/system	400 Hz	800 Hz	1600 Hz	3200 Hz
AE (%)	0.0077	3.2771e-05	0.0036	3.5348e-05
MAE (%)	0.4154	0.0032	0.2371	0.0025
Tc (sec)	7.8993	13.1665	80.7673	2.9896e+03
N	32	42	42	67
BP	6.5521e-08	1.8647e-15	4.0507e-10	1.9343e-13
BVP	4.7966e-07	3.0771e-11	5.5616e-09	1.7872e-11
BTP	4.4202e-10	1.8448e-11	1.9192e-07	1.1457e-13

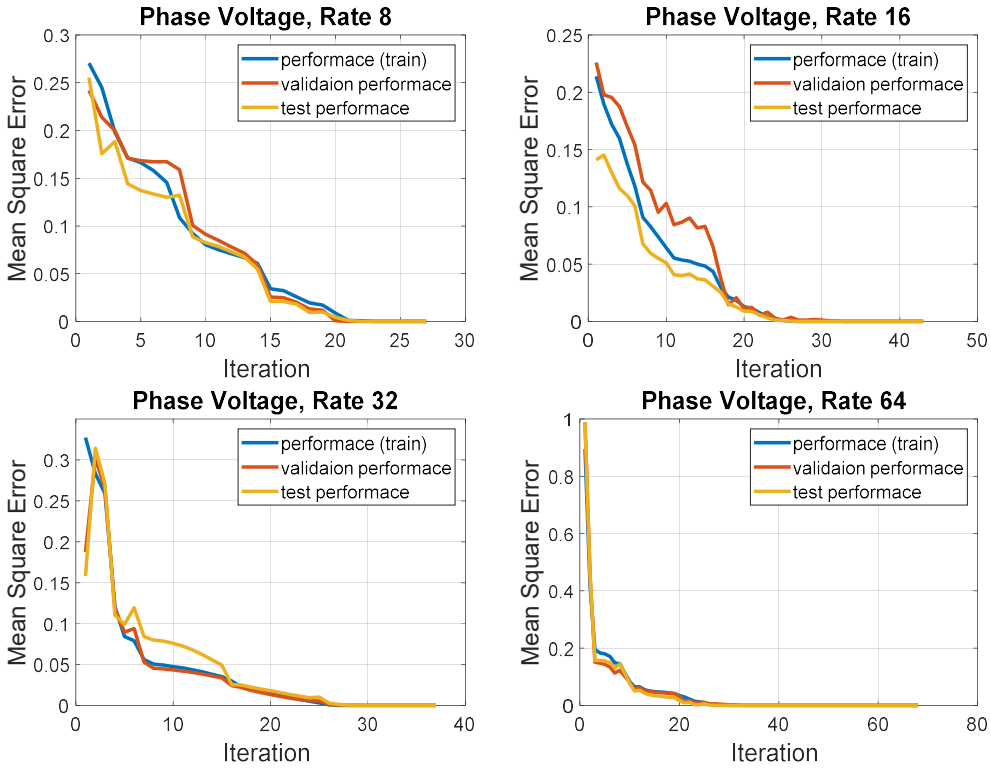

FIGURE 6. Performance values at different sample rates: 8, 16, 32, 64 sample/cycle for phase voltage classification technique.

5.1.2 Neutral voltage-based ANN classification technique. The results of neutral voltage-based techniques are shown in table 2. All training parameters are presented. Figure 7 shows the performance diagrams (mean square error).

TABLE 2: Neutral Voltage-Based ANN Classification

parameter	Rate 8	Rate 16	Rate 32	Rate 64
AE (%)	4.4626	5.8859	3.1438	0.5304
MAE (%)	97.9332	100.1624	99.9997	99.9851
Tc (sec)	8.2904	8.7641	53.5698	985.7196
N	36	18	28	26
BP	0.0175	0.0063	1.0173e-09	2.9969e-10
BVP	0.0605	0.0412	0.0285	0.0298
BTP	0.0276	0.1378	0.1685	4.0495e-10

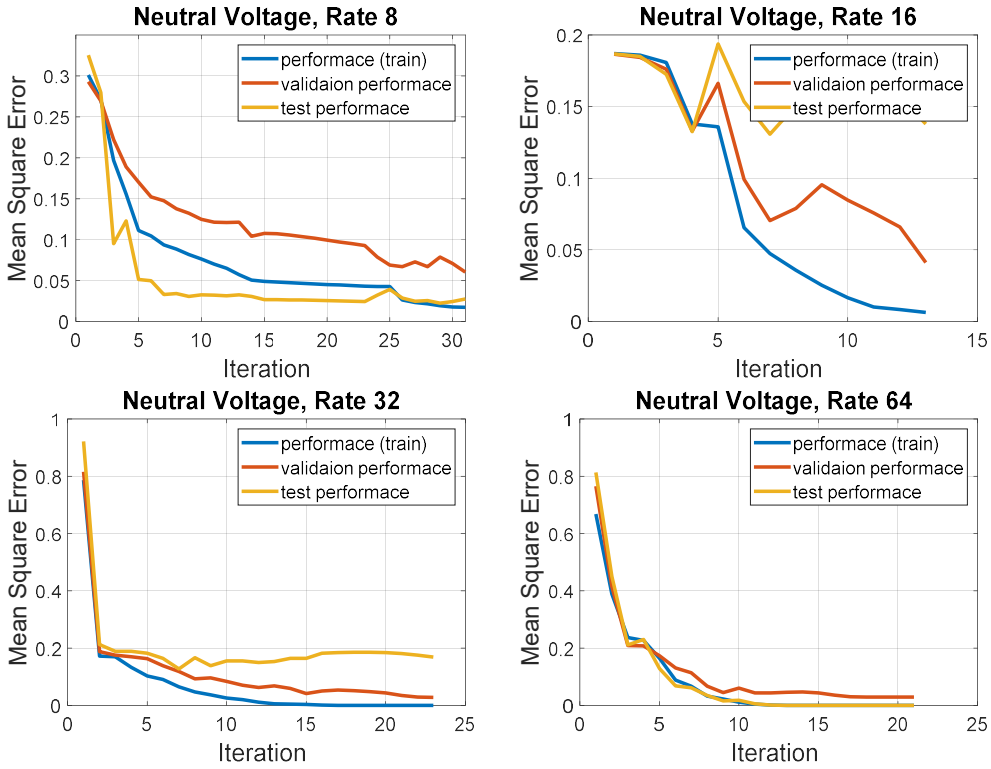

FIGURE 7. Performance values at different sample rates: 8, 16, 32, 64 sample/cycle for neutral voltage-based classification technique.

5.1.3 Phase Current-based ANN classification technique. The results of phase current based techniques are shown in Table 3. All training parameters are presented. Figure 8 shows the performance diagrams (mean square error).

TABLE 3: performance of phase current-based ANN classification technique

Parameter	Rate 8	Rate 16	Rate 32	Rate 64
AE (%)	0.0516	0.0144	0.4164	1.2158e-04
MAE (%)	12.3667	1.8671	100	0.0260
Tc (sec)	13.0758	12.1063	105.2228	1.7868e+03
N	35	36	54	43
BP	7.2882e-14	1.0687e-14	1.5602e-14	1.5435e-14
BVP	7.6036e-11	1.1724e-05	3.1091e-11	1.0475e-11
BTP	4.2482e-04	4.9432e-16	0.0278	4.0495e-10

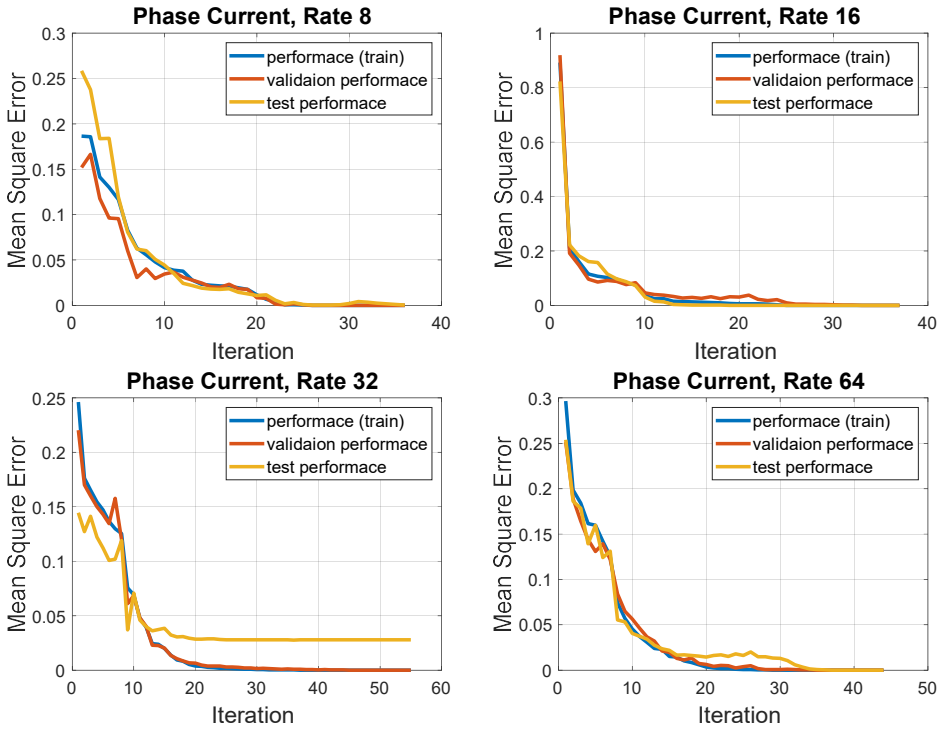

FIGURE 8. Performance values at different sample rates: 8, 16, 32, 64 sample/cycle for phase current-based classification technique.

5.1.4 Neutral Current-based ANN classification technique. The results of neutral current based techniques are shown in Table 4. All training parameters are presented. Figure 9 shows the performance diagrams (mean square error).

TABLE 4: performance of neutral current-based classification technique

parameter	Rate 8	Rate 16	Rate 32	Rate 64
AE (%)	5.7508	3.6738	7.4295	1.6682
MAE (%)	99.9508	100	100	99.9998
Tc (sec)	8.1301	11.7517	26.3722	1.0442e+03
N	25	33	12	27
BP	0.0117	6.9086e-09	0.0059	4.0477e-10
BVP	0.0350	0.0253	0.0853	0.0278
BTP	0.1771	0.1895	0.1533	0.0829

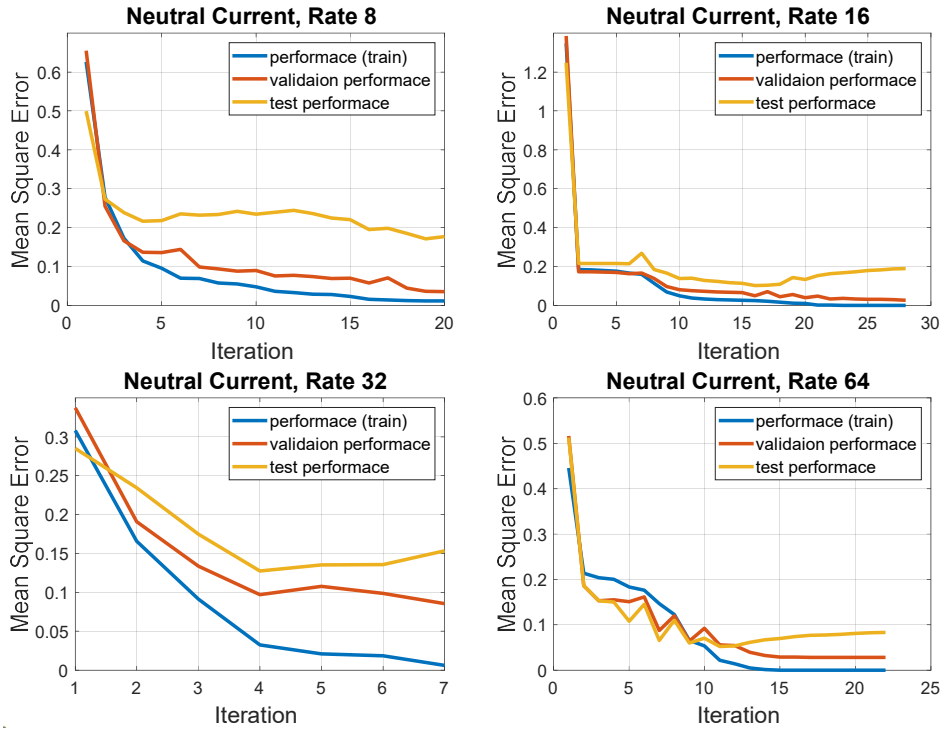

FIGURE 9. Performance diagram at different sample rates: 8, 16, 32, 64 sample/cycle for neutral current-based classification technique.

5.1.5 Power-Based ANN classification technique. The results of the power-based technique are shown in table 5. All training parameters are presented. Figure 10 shows the performance diagrams (mean square error).

TABLE 5: performance of power-based classification technique

Parameter	Rate 8	Rate 16	Rate 32	Rate 64
AE (%)	3.9743e-05	0.0014	0.6151	0.7150
MAE (%)	0.0078	0.3098	99.9563	33.2028
Tc (sec)	8.9601	16.2225	92.0121	2.7580e+03
N	46	58	48	58
BP	7.7913e-14	1.2236e-14	7.9597e-09	5.7312e-05
BVP	7.6225e-17	1.3894e-14	0.0022	0.0038
BTP	1.6947e-10	2.6772e-07	0.0278	6.9807e-04

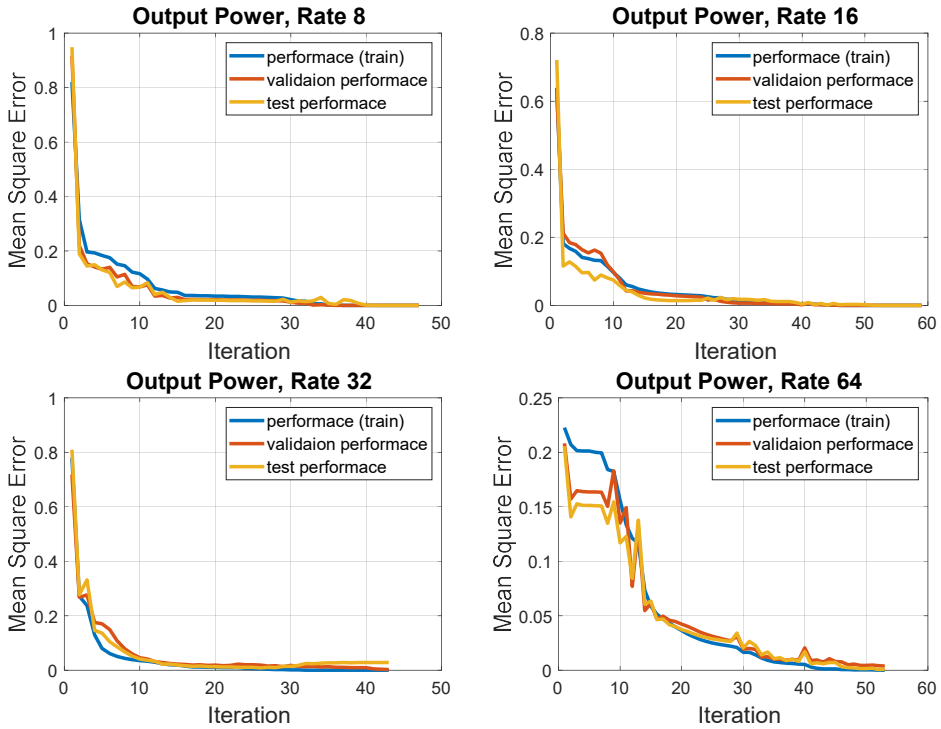

FIGURE 10. Performance diagram at different sample rates: 8, 16, 32, 64 sample/cycle power-based classification technique

5.2 Cuckoo optimization algorithm.

The tables below (Tables 6-9) show the results of rates 8, 16, and 32 sample/ cycle system using Cuckoo Algorithm. Where Va is a phase (A) voltage and Vn is a neutral voltage, Ia: phase (A) current, In: neutral current, and P is the three phase power. From these tables, the better results are shown in three-phase power sampling. The better sampling rate is 32 samples/ cycle.

TABLE 6: results of rate eight samples/cycle

parameter	Va	Vn	Ia	In	p
AE (%)	5.55	21.5145	7.7674	19.9547	1.2625
MAE (%)	5.401	11.8281	3.908	10.5221	1.2502
Tc (sec)	53.05	50.0236	48.21	49.586	48.1732
N	600	600	600	600	600

TABLE 7: results of rate 16 samples/cycle

parameter	Va	Vn	Ia	In	p
AE (%)	3.50335	11.2507	4.3074	22.2548	2.9179
MAE (%)	3.3181	11.2500	2.9891	11.74	2.9151
Tc (sec)	92.36	89.93	90.36	90	90.17
N	600	600	600	600	600

TABLE 8: results of rate 32 samples/cycle

parameter	Va	Vn	Ia	In	p
AE (%)	1.6667	19.066	2.1753	12.0833	0.8333
MAE (%)	1.6667	11.1769	2.0924	12.0833	0.8333
Tc (sec)	268	250	251	250	249
N	600	600	600	600	600

TABLE 9: results of rate 64 samples/cycle

parameter	Va	Vn	Ia	In	p
AE (%)	4.032	14.7198	1.25	22.955	2.0681
MAE (%)	3.7427	13.107	1.25	12.0912	1.6553
Tc (sec)	3053.4	1066.2	1084.6	1078	1142.4
N	2000	800	800	800	800

The figure below (Figure 11) show the cost function (mean square error) using the Cuckoo algorithm for each system.

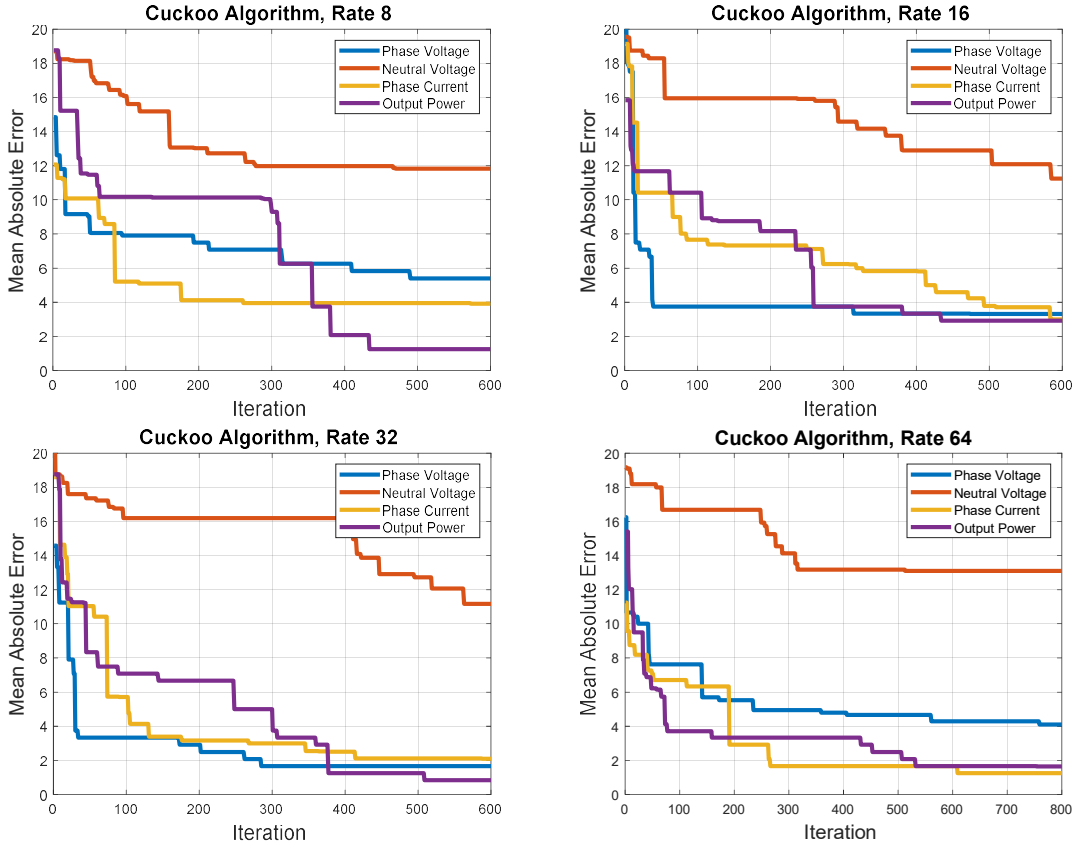

FIGURE 11. The cost function of different systems: phase current, three-phase power, phase voltage, and neutral voltage for 400Hz, 800Hz, 1600Hz, and 3200 Hz system.

5.3 GA Algorithm

The tables below (Tables 10-11) show the results of rates 8, and 16 samples/cycle systems using the GA Algorithm.

Where Va is a phase (A) voltage and Vn is a neutral voltage, Ia phase (A) current, In neutral current, and P is power. From these tables, the better results are shown in three-phase power sampling. The better sampling rate is 16 samples/ cycle.

TABLE 10: results of rate eight samples/cycle system

parameter	Va	Vn	Ia	In	p
AE (%)	5.4310	37.5047	13.4394	28.9243	12.01
MAE (%)	4.94	18.75	6.4282	14.98	8.6894
Tc (sec)	1404	1396	1392	1389	1390
N	1000	1000	1000	1000	1000

TABLE 11: results of rate 16 samples/cycle system

parameter	Va	Vn	Ia	In	p
AE (%)	7.1271	34.5123	1.25	37.5002	2.92
MAE (%)	2.49	17.19	1.25	18.75	2.92
Tc (sec)	2655	2663	2661	2645	2709
N	1000	1000	1000	1000	1000

The figure below (Figure 12) shows the cost function (mean square error) using the GA algorithm for each system.

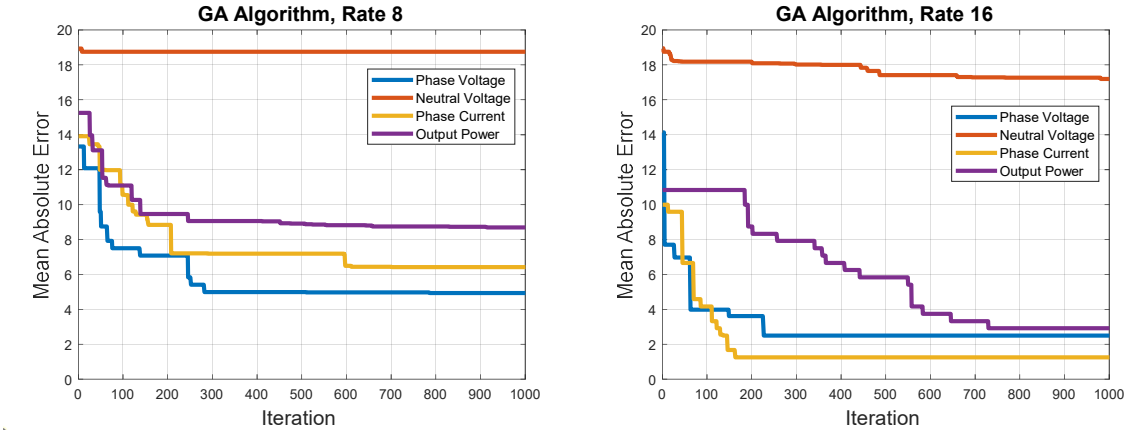

FIGURE 12. The cost function of different systems: phase current, three-phase power, phase voltage, and neutral voltage for 400Hz and 800Hz systems.

6. COMPARISON

In the previous section, five ANN systems are simulated using MATLAB 2020a: phase voltage-based ANN, phase current-based ANN, neutral voltage-based ANN, neutral current-

based ANN, three phase power-based ANN system. Three different learning techniques are used to optimize the ANN: backpropagation and two soft computation optimization techniques: Cuckoo and Genetic algorithms. The objective function of these optimization techniques (cost function) minimizes the sum square error between the target and system output.
This section presents a complete comparison between the learning techniques for the five systems at different sample rates.

Based on section 5, the best system which gives the best performance in learning testing validation is the power-based system using backpropagation technique. The phase voltage-based approach is better than the phase current, phase quantities (voltage and current) are better than neutral quantities, and the results of the phase voltage are very acceptable at different sample rates.

The optimal sample rate in voltage is 64 samples/cycle. More than one cycle may be needed to increase the algorithm accuracy. In table 12, the optimal sample rate and the minimum number of cycles may make a good decision for different systems.

TABLE 12: optimal selection

System	Sample/cycle	Number of cycles
Power	8	4
Phase Voltage	64	6
Phase current	64	8
Neutral voltage	64	13
Neutral current	64	14

The number of cycles in table 12 is based on validation data collected at different load levels. The cuckoo algorithm is better than GA in this context. The computational time of the cuckoo algorithm (or the number of iterations) is lower than GA to get the same accuracy.

Backpropagation techniques are the best in this application. Power-based at rate 16 sample/cycle is the best for the islanding detection. At least four cycles are needed (80 ms for 50 Hz) to make a 100% correct decision. Finally, the cuckoo algorithm solves this problem better than GA.

7. CONCLUSION

In this paper, the ANN-based technique in the islanding detection application is studied. Doubly fed induction generator wind turbine is selected as distributed generators. Different ANN systems are simulated based on various inputs: Phase voltage/current, neutral voltage/current, and three-phase power, different sample rates are considered: 8, 16, 32, and 64 sample/cycle for each system, and three learning algorithms are simulated using MATLAB 2020a: Backpropagation, Genetic Algorithm, and Cuckoo optimization technique.

From the results, the ANN is a very effective method to detect the islanding in the micro-grid. Different inputs may be used to feed the trained ANN system: Power, phase voltage, and

phase current, where the neutral quantities (voltage, current) are not able to use in this application. The accuracy of the system depends on the sample rate. The higher the sampling, the better the performance. 16 sample/cycle is enough to detect the islanding within four cycles in the case of power-based input data.

REFERENCES

[1] Dash PK, Padhee Malhar, Barik SK. Estimation of power quality indices in distributed generation systems during power islanding conditions. Int J Electr ower Energy Syst 2012;36(1):18–30.

[2] A. Odienat, M. M. Al Momani, K. Alawasa and S. F. Gharaibeh, "Low Frequency Oscillation Analysis for Dynamic Performance of Power Systems," 2021 12th International Renewable Engineering Conference (IREC), 2021, pp. 1-6, doi: 10.1109/IREC51415.2021.9427818.

[3] M. M. Almomani, A. Odienat, S. F. Al-Gharaibeh and K. Alawasa, "The Impact of Wind Generation on Low Frequency Oscillation in Power Systems," 2021 IEEE PES/IAS PowerAfrica, 2021, pp. 1-5, doi: 10.1109/PowerAfrica52236.2021.9543283.

[4] M. A. Refern, O. Usta, and G. Fielding, “Protection against loss of utility grid supply for a dispersed storage and generation unit,” IEEE Transaction on Power Delivery, vol. 8, no. 3, pp. 948-954, July 1993.

[5] A. I. Al-Odienat, K. Al-Awasa, M. Al-Momani and S. Al-Gharaibah, "Connectivity Matrix Algorithm: A New Optimal Phasor Measurement Unit Placement Algorithm", IOP Conference Series: Earth and Environmental Science, vol. 551, no. 1, pp. 012008, August 2020. Doi. 10.1088/1755-1315/551/1/012008

[6] M. M. Al-Momani, A. Odienat, S. F. Algharaibeh, K. Awasa and O. Radaideh, "Modified Connectivity Matrix Algorithm," 2022 Advances in Science and Engineering Technology International Conferences (ASET), 2022, pp. 1-6, doi: 10.1109/ASET53988.2022.9735116.

[7] Al-Momani, Mohammad M., and Seba F. Al-Gharaibeh. "Prediction of Transient Stability Using Wide Area Measurements Based on ANN." International Journal of Emerging Trends in Engineering Research 9.11 (2021).doi:10.30534/ijeter/2021/029112021

[8] M. M. Al-Momani, A. Odienate, S. F. Algharaibeh, K. Awasa and I. Reda, "Ringdown analysis for Low-Frequency Oscillation Identification," 2022 Advances in Science and Engineering Technology International Conferences (ASET), 2022, pp. 1-6, doi: 10.1109/ASET53988.2022.9735122.

[9] G. Wang, J. Kliber, G. Zhang, W. Xu, B. Howell, and T. Palladino, “A power line signalling based technique for anti-islanding protection of distributed generators—part ii: field test results,” IEEE Tran. Power Delivery, vol. 22, no. 3, pp. 1767-1772, July 2007.

[10] K. Jia, H. Wei, T. Bi, D. W. P. Thomas and M. Sumner, “An Islanding Detection Method for Multi-DG Systems Based on High-Frequency Impedance Estimation,” in IEEE Transactions on Sustainable Energy, vol. 8, no. 1, pp. 74-83, Jan. 2017, DOI: 10.1109/TSTE.2016.2582846.

[11] M. Bakhshi, R. Noroozian and G. B. Gharehpetian, “Novel Islanding Detection Method for Multiple DGs Based on Forced Helmholtz Oscillator,” in IEEE Transactions on Smart Grid, vol. 9, no. 6, pp. 6448-6460, Nov. 2018, DOI: 10.1109/TSG.2017.2712768.

[12] Zamani, Reza, et al. “A novel hybrid islanding detection method using dynamic characteristics of synchronous generator and signal processing technique.” Electric Power Systems Research 175 (2019): 105911.

[13] Raza, Safdar, et al. “Minimum-features-based ANN-PSO approach for islanding detection in the distribution system.” IET Renewable power generation 10.9 (2016): 1255-1263.

[14] Guan, Zhengyuan, and Yuan Liao. “A New Islanding Detection Method Based on Wavelet-transform and ANN for Micro-grid Including Inverter Assisted Distributed Generator.” International Journal of Emerging Electric Power Systems 20.5 (2019).

[15] Menezes, Thiago S., et al. “Islanding Detection for Distributed Generators Based on Artificial Neural Network and S-transform.” 2019 IEEE PES Innovative Smart Grid

Jordan Journal of Energy
Volume1, Number 1, 2023

ISSN (Online): 2790-7678
ISSN (Print): 2790-766X

Jordan Journal of Energy (JJE)
Journal Homepage:ttp://dsr.mutah.edu.jo/index.php/jje
JJE an official peer review journal of Mutah University,

Distributed Energy Resources Electrical Systems: Future prospective

Khaled Alawasa
Department of Electrical and Computer Engineering, Sultan Qaboos University, Muscat, Oman
k.alawasa@squ.edu.om

Received: 29th May, 2022; Accepted: 7th August 2022

ABSTRACT. *Distributed generation (DG) is an approach that utilizes small scale technologies to generate electricity close to the consumer side. Generally, DG can provide high reliability, high security, low-cost electricity, and less environment impact. This paper gives an overview of some of the most significant issues related to the distributed generation (DG). It discusses different aspects of DG, such as definitions, technologies, motivation for moving to DG, some drawbacks associated with the centralized systems which have led to DG. DGs challenges, standards and polices are also presented. In addition, the economic impact, and a price comparison between central power plants and DGs are discussed. Also, a case study was conducted in order to study the impact of using distributed generations in Edmonton downtown. Three distributed generations, combustion turbine types with 25 MW capacities each have been implemented in Edmonton power system. The total cost estimations have been studied in this case, and the results have revealed that this type of distributed generation is inexpensive and more economic compared with price from the utility. It was estimated from the calculation that the price for the energy is about ¢6.27/kWh while the current electricity price from the utility is ¢8.561/kWh, for long term estimation it is found that the proposed CTs in this project has 11 years for a payback period, after that the project start earning money which is relatively good and wroth investment. The second part of the study analyses the impact of DGs on the system losses using Power-World software, and the result have proven that the loss is significantly decreases when the DG systems are in operation, hence DGs help reducing the costs that associated with the system's losses.*

Keywords: Distributed generation, Centralized generation, Environmental Concerns, Economic Impact.

1. Introduction.

Distributed generation (DG) generally refers to small scale electric power generators (typically 1 kW – 50 MW) that produce electricity at a site close to customers or that are interconnected at the substation, distribution feeder or customer load levels [1]. It is expected that DG will play an important role in the electric power system in the near future. Distributed generation is not a new concept. The earliest power utilities were using DG to generate and transmit electricity. Then the centralized power systems have been introduced to make large interconnected systems to ensure more reliable and more economic power systems.

Recently, DG has gained a lot of interest in the power industry, the reasons behind this recent restoration for this concept is due to market deregulation, as in the current deregulation, it is hard to stimulate market players and stakeholders to invest multi-billion dollar in power generation and transmission projects where the payback time may be very long. Additionally, the liberalization of the electricity markets, along with the massive increase in demand for electricity, the environmental concerns, the development of new DG technologies, and the limitations in the ability to site new transmission lines, all these factors and others have made DG an attractive option for utilities and industries [2] .

DG technologies include renewable sources of energy, such as photovoltaic and wind. Conventional sources, such as fossil fuel fired reciprocating engines or gas turbines could be used in DG for reliability and power quality consecration. Recent developments in DG technologies have created a substantial role for DG in the future energy due to its improved performance, reliability, and flexibility to achieve higher energy efficiency, fewer environmental problems and reduce emission.

This paper will provide an overview of the DG technology including economic, environmental, technological impacts of this technology. Also, policies, challenges, recent development, and future of DG will be addressed. Moreover, a comparison between the central power system and DG concerning of the cost of the electricity, the capital cost, operation cost and the power transmission cost will be discussed in this report.

Additionally, Edmonton downtown power system has been studied as a study case. Three combustion turbines with 25 MW capacities each were implemented in Edmonton power system. Estimations of the total cost including: the capital, maintenance and fuel costs were studied, and the results have shown that this type of distributed generation is more economic. Then the impact of distributed generations on the system losses have been analyzed, and the results have showed that the loss is drastically declined during the operation of DGs, in such a case the costs that related to the system' losses is decreased.

2. DG Definition

Many definitions are used in the literature to define the distributed generation (DG). For instance, the term 'embedded generation' is used in Anglo-American countries, the term 'dispersed generation' is used in North America, and in Europe and parts of Asia, the term 'decentralized generation' is applied as a DG [3]. The definition of DG varies between countries. Some countries define DG based on the capacity of the units; others based on the location of the system. There is no universal definition for the capacity of DGs. The following are the most common use definition in the literature:

- IEEE defines the DG as a facility with power capacity that less than the centralized grid, usually less than 10 MW [4]
- The US Department of Energy (DOE) defines DG as follows [5]: "Distributed power is modular electric generation or storage located near the point of use. Distributed systems include biomass-based generators, combustion turbines, thermal solar power and photovoltaic systems, fuel cells, wind turbines, micro turbines, engines/generator sets, and storage and control technologies. Distributed resources can either be grid connected or independent of the grid. Those connected to the grid are typically interfaced at the distribution system". The DOE considers a system DG with capacity range from less than kW to tens of MW [5].
- The Electric Power Research Institute (EPRI) considers DG as storage devices that are located close to the customer side with capacity from a few kW up to 50 MW [6].
- According to the Gas Research Institute, the system's capacity between 25 kW to 25 MW is considered as DG [7][3].
- Swedish legislation defines that DG capacity in Sweden is defined under 1500 kW [3] [8].
- The International Council on Large Electricity Systems (CIGRE) considers DG capacity is smaller than 100 MW and is not centrally planned, and not centrally dispatched [9].
- In the English and Welsh power markets, DG is referred to any generating unit under 100 MW in this market [8].
- In New Zealand, usually DG units are having capacity less than 5 MW [3].
- In Australia, generating units less than 30 MW are considered as DG [8]

3. DG Growth worldwide

In 2003, the installed capacity of DG in the US was about 168 GW, at most containing reciprocating engines for backup power [10]. In Canada, in 2000, there were about 7.7 GW industrial cogeneration capacities and less than 500 MW of renewable energy technology capacities including PV, wind power and tidal [11]. In Europe, the installed capacity of DG is evaluated to be about 50 GW, including wind turbines and small hydro systems [12].

In Europe, distributed generations are growing in demand, as they are seen to meet the energy challenges of the 21st century. For example, In Denmark, roughly 57% of electrical capacity produces from combined heat and power (CHP) and 31% from renewable sources of energy this has an important role to enhance CHP and renewable energy technologies [2].

The capacity of electricity generation in the world was around 3365 GW in 2001, utilizing thermal units, hydro plants and nuclear plants, these units roughly accounted for 67%, 21.2%, and 10.7% respectively. About 1.1% was generated from other sources of generation [10]. This capacity is predicted to increase to be about 4000 GW by 2010 and 5000 GW by 2020 [2].

In 2001, the US had 813 GW of electricity generation capacity which was estimated to grow to about 1070 GW in 2010, while Canada, in the same year (2001) possessed 111 GW and this capacity was expected to increase up to 130 GW by 2010 [2][14][15]. Additionally, by 2020, it is expected that 3000 GW new generation capacity would be required worldwide to meet the demand for electricity. It is also predicted that DG would contribute by about 1500 GW [20].

According to the Distributed Power Coalition of America (DPCA), over the next two decades DG would participate in about 20% of all the new generating capacity in the US [16]. It was projected that in 2010, DG market would be in the range of $10 to $30 billion in the US and $75 billion worldwide [15].

4. DG Motivations

The major driving forces behind the recent revival of distributed generation are: the liberalization of the electricity markets, environmental concerns (GHG emissions) and the drawbacks in the conventional generation systems.

4.1 Liberalization of Electricity Markets

Liberalization of electricity market has allowed DG systems to enter the open markets in which they have the chance to sell power to a larger range of customers. Recently, DG has gained a lot of interest by electricity suppliers in the power industry, because they realize that DG can be the best solution to help covering the increased demand for electricity and take the advantages of the centralized power system generations deficiencies. Moreover, the smaller size of DGs, their quick installation and their lower cost compared with central power system, make them more flexible to respond to any change in the market conditions. In some areas it is uneconomical to build a centralized generation plant, geographical and operational flexibility of DGs make them more practical in such a case. One of the main derivers for moving toward DG technology in the US is the ability of DG to serve against the price fluctuations. Another factor is the reliability concerns which is represented by the power outages [1].

The liberalization of energy markets has an important role to enhance power reliability awareness among customers. The poor reliability of the centralized system has motivated companies to invest in DG units to achieve the required reliability for power grid. Figure 1

below shows how DG can obtain the cost reliability spectrum, that for a particular application high reliability and high cost or low reliability and low cost, DG can be obtained at both ends [17]. DG can support power quality in the system by prohibiting and mitigating system problems before they are detected by customer side. DG is used as back up generation with a space capacity to provide electricity to critical location, such as hospitals to prevent operational failures in cases of network problems.

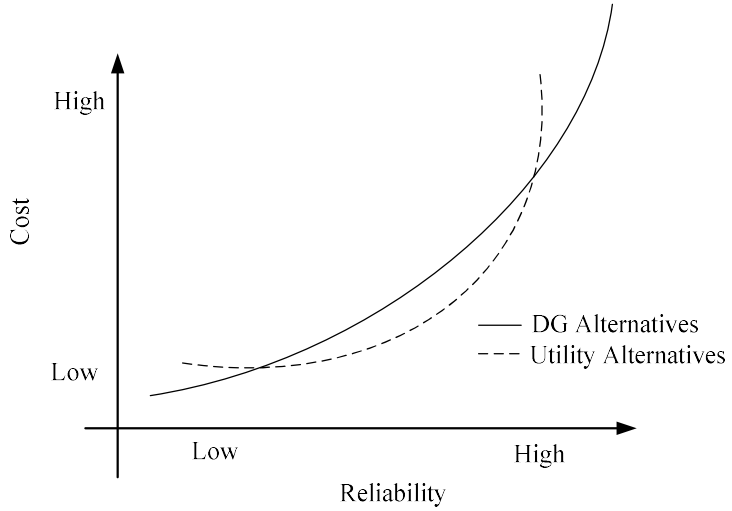

FIGURE. 1. Flexibility of cost and reliability for DG applications [17].

4.2 Environmental Concerns

The second motivator behind the revival of distributed generation is related to environmental policies. Environmental regulations force players in the electricity market to find suitable solutions for more efficient and cleaner energy. In addition, the target of most of the government policies is boosting the use of renewable sources of energy in many countries. Distributed generation has been able to achieve these targets through: Combined heat and power generation (CHP): Considering CHP instead of producing the heat in a separate boiler and generating electricity from the grid has a substantial role to reduce emissions and increase the energy efficiency. These units called cogeneration units which heavily depend on the distributed generation. Use of alternative fuel: distributed generation has been used to diversify away from coal, fuel, natural gas and nuclear fuel. Also, DG technologies allows taking the opportunities of using cheap fuel including burning landfills and collect their gases to generate electricity and biomass resources can also be used to produce local energy.

Furthermore, DG that uses renewable energy that is inherently produces no emissions. While DG technologies which based on using conventional fossil fuels can reduce the emissions through energy conversion processes, such as fuel cell, CO reservation, and production of gas [17].

4.3 Drawbacks of Central Generation (CG) Technology

Typically, Central Generations are located in remote areas, they required long transmission lines to deliver power to the load centers and customers, and this causes line losses in the transmitted electricity. Also, conversion losses resulted when the characteristics of the power flow is changed to meet the characteristics of the network [18] . These losses lead to high cost for transmission and distribution of electricity, which account for about 30% of average cost of the delivered electricity. Table 1 shows the total amount of losses in the US between 2002 and 2008 [19].

TABLE 1 Transmission and distribution losses for electricity in the U.S [19].

Date	Net Generation Billion kWh/ year	Transmission and distribution losses	Percentage %
2002	3858	248	6.4%
2003	3883	228	5.9%
2004	3971	266	6.7%
2005	4055	269	6.6%
2006	4065	266	6.5%
2007	4157	264	6.4%
2008	4115	241	5.9%

5. DG Technologies

Generally, DG technologies can be classified as renewable or non-renewable technologies. Renewable technologies include wind, solar (thermal or PV), geothermal or ocean. The non-renewable DG technologies are including internal combustion engines (ICE), combined cycles, combustion turbines, micro-turbines, and fuel cells. Energy storage uses combustion engines and turbines, micro-turbines, fuel cells and photovoltaic play an important role in DG applications compared with other available technologies [1].

5.1 Internal Combustion Engines (ICE):

This type of technology is widely spread and the most mature of the DG technologies worldwide. The most common available types of ICE are natural gas, and diesel fuel. This

technology uses compressed air and fuel to produce mechanical power then this mechanical power is converted to electrical energy. The most attractive feature related to this type are: low capital costs, high efficiency (36-43% diesel fuel, 28-42% gas fuel), high reliability, quick start-up, high energy efficiency when combined with heat recovery systems (CHP) that increases the total electric and thermal efficiency up to 90%, and easy maintenance [1]. The capacity of ICE generation ranges from a few kilowatts to more than 30 MW. In the US, about 70% of engine has a range between 10 kW to 200 kW and the majorities are with capacity less than 1 MW. The total installed capacity in the US was accounted for around 52 GW in 2000 which represented about 7% of the total installed capacity in the country. Based on the size of the ICE DG units, the cost for diesel-fired units is almost 350-500 $/kW and for gas-fired ICE DG units is about 600-1000 $/kW [5]. Maintenance cost for diesel-fired ICE DG units ranges between 0.005-0.01 $/kWh and between 0.007-0.015 $/kWh for gas-fired ICE DG units [22] . In the US, the main applications of the ICE DG units are gas, electric and water utilities, manufacturing facilities, hospitals, educational and office buildings. However, as ICE DG units have large number of moving parts, this leads to high maintenance cost the highest among the DG technologies, poorly in terms of noise, as noise is low frequency and more difficult to control, and high emissions, which makes other technologies competitive with them.

5.2 Combustion Turbines (CT)

Gas turbines are vastly used for electricity generation in the globe. Typical applications for CT are in CHP with capacity between 500 kW to 25 MW. The typical efficiency is around 35% in the 5 MW ranges [2]. The efficiency of these turbines increases as the capacity increases. For example, for the units with 100kW the efficiency around to 16%, while the efficiency for units with 30 MW capacities about 45%. The efficiency may reach up to 55%, and these units mainly used in the central power system. The availability of the natural gas in most countries and its fixed price, make this type of units more attractive. Moreover, CT has low installation time and low capital cost, high efficiency, and significantly low NOx emissions (0.3-0.5 kg/MWh) [5]. However, the amount of CO2 emissions is very high about 580-680 kg/MWh. For installing a typical gas turbine, this needs initial cost around 650- 900 $/kW, and with a heat recovery unit the cost increases to1000-1200 $/kW. Average maintenance costs for combustion turbines are approximately 0.004-0.005 US$/kWh [22]. In the US a research

program is conducting in order to obtain good efficiency for these units, reduce their sizes, lower their operational cost and improve their emission performance [5][21].

5.3 Microturbines (MC)

Microturbines can use air, natural gas and diesel to produce power. Their capacity varies between 25 kW to 500 kW, have an electrical efficiency of about 15% for unrecuperated type and between 20% and 30% for recuperated types. The efficiency of MC units becomes very high when they combined with CHP (85%). The main features of microturbines are the availability of the natural gas in many countries, small size, lightweight, less maintenance, easy to control their noise and low NOx emissions (0.1 kg/MWh). However, they have high CO2 emissions (720 kg/MWh) [5]. MC units can cover the base load of electricity, they are suitable for commercial building, and they also can be used as a standby generation unit and in hybrid electric vehicles [1]. The capital costs of installing MC is higher than installing IEC, it is evaluated between (700 and1100 $/kW) and the maintenance costs is between (0.005 and 0.016 $/kW) [21] [22] .

5.4 Fuel cells (FC)

Fuel cells can convert chemical energy of a fuel (natural gas or hydrogen) to electricity without combustion. The first applications for Fuel cell technologies were initially developed for space program applications, and then the transportation sector. Today, fuel cells are projected to have an important role in distributed generation applications. The main fuel used in fuel cells is hydrogen which is usually derived from natural gas, diesel, and landfill gas [5]. There are four main fuel cell technologies based on the type of the electrolyte material used. These include phosphoric acid fuel cells (PAFC), molten carbonate fuel cells (MCFC), solid oxide fuel cells (SOFC), and proton exchange membrane fuel cells (PEMFC). The most commercialized technology among these types in power generating application is PAFC [21]. PAFC achieved about 80% of installed fuel cells capacity in the period between 1970 and 2003. PAFC generation units are now available in small sizes (3-5 kW) for residential applications and large size (100-250 kW) for commercial application. Various units with about 200 kW capacity which is good for distributed generation applications has been installed in the US, Europe, and Japan [23]. The main advantages for this technology are high electrical efficiencies (36 - 42%), very low noise and vibration, negligible emissions, compact size, and high reliability. While high capital cost and low energy density are the drawbacks for this technology. The capital cost of fuel cells plants reaches about $1.1 million, which very expensive compared with other types of DG technologies, units with 25 kW capacity cost about 4000 $/kW and 5500 $/kW for a 200-kW unit. Maintenance costs of fuel cells is objected to be

0.005-0.01 US$/kW [22][5]. In 2003, many countries, such as the US, Japan, the European Union, and Canada have supported fuel cells research programs to make this technology more applicable for commercial and residential applications in the current future.

5.5 Photovoltaic (PV)

Photovoltaic (PV) cells or solar cells technology can directly convert sunlight into electricity. So, the fuel for PV is the sunlight, this leads to no emission resulted from this technology. PV can be the best DG technology for residential and commercial applications. This technology available in small size (less than 10 kW), medium size (10-100 kW) and large size the utility scale (more than 100 kW) [22], PVs generate electricity with no noise, and quite operation since there is no moving parts are used. Additionally, PVs need low operation cost and maintenance cost which is around 1% of the capital cost annually. The main disadvantages face wider deployment of this technology is the high capital cost, the cost is estimated to be 6000-10000 $/kW, need large area to be installed, intermittency, as the power from the sun vary based on the weather conditions, and the need for storage devices. The price of electricity generated by PV systems could be as high as 0.30 $/kWh [22], and this price justified when transmission facilities are required to connect PV systems with remote areas. The efficiency of the commercially available PV modules ranges from about 5 to 15%, many efforts is exerting to improve PV efficiencies [22].

5.6 Wind Energy Technology

Wind turbines use the wind to produce electrical power. When wind blows it rotates the blades of the turbine to convert the kinetic energy of wind to mechanical energy, and then this mechanical energy rotates the rotor of the generator to generate electricity. Then the electricity is transmitted through underground cables to the load. The range of wind turbines size varies from less than 100kW to multi-MW [24]. Usually, several wind turbines are grouped together to form a wind farm. The capacity of wind farm ranging from a few MW to tens of MW. The large wind farms are often connected to the power grid. Small wind farms can be directly connected to the distribution units. The small-scale wind farms and individual wind turbines are typically known as distributed generation. Wind power is commercially available, produces no emissions; preserve land (no mining process). Moreover, the areas around wind turbine can be used for other purposes, such as farming and animal grazing. The main disadvantages for this technology are high capital cost, variable nature for wind, and bird mortality. The cost of wind turbines depends on the location and the type of the turbine. For example, the capital cost for 10 kW home wind turbine system costs about $25,000 - $35,000 [22] .Table 2 summarizes the main points for the above DG technologies.

TABLE 2 Summary for the DGs technologies

Technology	Capital cost $/kW	O&M Cost $/MWh	Capacity	NOx Kg/MWh	CO2 Kg/MWh	Main features
ICE diesel	350-500	5-10	a few kW -30 MW	10	650	-Low cost -High efficiency -High emission
ICE gas	600-1000	7-15	a few kW -30 MW	0.2-1	500-620	-Low cost -High efficiency -High emission
CT	650-900 (Depend on the size)	4-5	500 kW - 265 MW	0.3-0.5	580-680	-Low cost -Good efficiency -Readily available
MT	700-1100	5-16	25 kW - 500 kW	0.1	720	-Low noise -Small size -Long maintenance time
FC (PAFC)	4000-5500	5-10	5 kW - 250 kW	0.005-0.01	430-490	-Very low noise -Good efficiency -Compact size -No emission
PV	600-1000	1% of first investment	a few kW-10MW	0	0	-Clean -No noise -No emission -Expensive
Wind	2500-3500	--	100kW-multi-MW	0	0	-No emission -Clean -Expensive - Birds mortality

6. Economic Impact

6.1 Benefits

DG technologies have introduced many economic advantages to the systems and customers. Interconnecting DG to the system has contributed to increase the reliability of electricity, reduce losses that related to transmission and distribution systems. Additionally, DG has a big potential to cover the demand for higher power quality compared with the central grid. Due to the lack

investment in the central power transmission systems which has led to many blackouts in many regions, DG is playing a significant part in generating power [25].

In rural areas where central grids are considered uneconomical, DG can be the most effective solution to supply power and creates more new jobs in these areas.
The sites of DG units eliminate the need for systems' transmission and distribution upgrading. As DG is located close to the load, this helps avoiding the cost related to building new lines or upgrading the system, moreover, reduces the losses and overloading in the system [25].
DG has a substantial role to stimulate competition in electricity supply, allowing customers without DG greater choice in suppliers [25] .
In the case of combined heat and power CHP where the efficiency is high and the capital cost is low, the total energy cost is cheaper than central systems.
DG utilities are small, which make them easy to build and more flexible in operation compared with conventional power plants.

6.2 Drawbacks

Although DGs have many economic advantages and cost reduction, there are some economic drawbacks compared with central power grids. Due to the economy of scale, DGs cost more per kilowatt to build than central power systems. The prices of fuel delivery (retail-market) are more expensive compared to the price for central generation (whole-sale). DGs have low fuel-conversion efficiencies compared with central plants unless they used with CHP. Moreover, subsidies are needed to make DG market competitive for system applications.
Renewable DG technologies, such as wind and PV are variable sources of energy, non-dispatchable as their energy share cannot be predicted, therefore back up generations are required to cover the power that not supplied by DG units. This increases total costs and may weaken the power system.

In the case of DGs connection, the local grid may need reinforcement. Based on the principle of economic the cost for upgrading the distribution system should be covered by the DG producers [25]. This increases the total investment cost of DGs.

Table 3 below gives cost comparison between the distributed generations and central generations

TABLE 3 CG and DG Cost Implication [2]

Component Cost	Centralized Generation (CG)	Distributed Generation (DG)
Cost of Capital	Lower Cost per unit	Higher cost per unit. Saved cost of system design due to reduced capacity. Saved cost of system design due to use of waste heat in cogeneration.
Fixed Operation and Maintenance Cost	Higher	Lower
Variable Operation and Maintenance Cost	Lower	Higher
Transmission	High voltage transmission is mandatory. High losses and transmission failure.	Only distribution line required. Reduced capital cost.

7. Technical impacts

Distribution systems in the conventional power grid are considered as passive elements, as they transfer the power in only one direction from the transmission system to the consumers, also their stability is associated with the stability of the transmission systems; they are stable if the transmission systems are stable. With the introducing of DGs, distribution systems have become active elements in the power system since they can generate and consume energy at load sides. From other side, the integration of DG has some technical impact in the power system in different aspects. It may affect the power flow, voltage stability, protection, and the power quality for both the electricity providers and end users. Below some of the technical impacts related to integrating DGs in the power system.

Power quality: The variable nature for wind and PV energies has direct effects on the quality of the energy. They may cause fluctuation, and flicker in the output voltages and powers [26], [27] resulting in violations of the power quality standards. Moreover, using power electronics converters (AC-DC, DC-AC) for the interconnection purposes produces harmonic distortion.

These harmonics have severe impact on the output power unless they are filtered. Also, the integration of DGs at some level may cause voltage drop in the system [28], [29] .

Power flow: Installation DGs influences the power flow in the network. It may change the power flow direction, decrease, or increase power losses and change the operation of other devices such as, voltage and reactive power compensation.

Protection system: The flow of power in the electrical system is unidirectional from the grid through the transmission system to the distribution systems then to the loads. High penetration of DGs may interface with the protection of the system. This interfacing may lead to over-current protection, instantaneous reclosure, ferro resonance, and ground faults [30][31].

8. Public Policy and Regulatory Impact

Public policies and regulations are different from place to place. Public policies and regulations also represent a main obstacle to the increased penetration for DG market and do not allow a smooth integration of new generation technologies. Difficulties in finding affordable connections to the power system, difficulties, and high cost for getting a declaration for a site, deficiency of national standards for interconnection additional costs for transaction, are some of the DG's regulatory barriers. Additionally, environmental standards have been intensified in some countries, with the same standards applied irrespective of the generator size.

It is important not to neglect the tax incentive impact on the development of DG technologies. In clean energy technologies, such as wind and PV, the facilities of construction and operation of DG are almost completely driven by tax incentives, which often significantly vary from one region another and from one year to another. These tax incentives mainly are provided at two levels: the first incentive is construction tax incentives, whether in the form of an upfront grant or accelerated depreciation schedules. The second one is operational tax incentives, generally in the form of revenue tax abatements [32].

9. Standards and Policies

9.1 Standards

Standards play an important role in addressing many of the needs for safety, power quality, lower cost, regulation, and education utilizing DG units. Standards have a key role in the prosperous future for DG deployment. IEEE Standards 1547 has developed into a series of

documents that cover several DG technologies issues, most of which are also of interest to Canada. This series includes:

IEEE 1547 – Standard for Interconnecting Distributed Resources with Electric Power Systems [36] . This standard has been issued in 2003; it gives the basic information for interconnection of distributed resources up to 10MVA.

IEEE P1547.1- Conformance Test Procedures for Equipment Interconnecting Distributed Resources with Electric Power Systems [36]. This standard was released in 2005, gives a common set of test procedures to confirm the proportionality of interconnection system or component intended for use in the interconnection of distributed resources technologies with the power systems.

IEEE P1547.2 – Draft Application Guide for IEEE 1547 Standard for Interconnecting Distributed Resources with Electric Power Systems [38] . This document includes technical depictions, applications instruction, and interconnection examples to promote the use of IEEE Standard 1547.

IEEE 1547.3 – Guide for Monitoring, Information Exchange, and Control of Distributed Resources Interconnected with Electric Power Systems [39] . This standard was published in 2007.

IEEE P1547.4 – Draft Guide for Design, Operation, and Integration of Distributed Resource Island Systems with Electric Power Systems [40] [68]. It gives alternative processes and practices for the design, operation, and integration of DG with power systems.

IEEE P1547.5 – Draft Technical Guidelines for Interconnection of Electric Power Sources Greater than 10MVA to the Power Transmission Grid, this guide will provide information regarding to design, construction, commissioning approval testing and maintenance demands with utilities more than 10MVA capacity to a power transmission grid [41].

IEEE P1547.6 – Draft Recommended Practice for Interconnecting Distributed Resources with Electric Power Systems Distribution Secondary Networks. This standard provides information about interconnection distribution secondary system with distributed resources [41].

9.2 DG policies

The current regulatory framework supports DG through subsidies, incentives, and recognition of DG in procurement and planning processes. The main drivers for DG policies are support competition and economic efficiency, protect consumers from cost-shifting,

preserve a viable utility privilege, protect the environment, and ensure safety and grid reliability. Table 4 summarizes the current regularity framework for DG [42].

TABLE 4 Summary of Current Regulatory Framework [42].

Regulatory Characteristics	Current Situation
Planning and Procurement Policy	State energy policy aims to incorporate DG into utility procurement and DG into distribution planning processes. Cogeneration has little consideration in utility procurement and planning processes.
Rate Structures	Energy prices are not transparent; inhibits customer response to actual costs. Current rate structure is based on controlled averaged pricing that does not include location and environmental externalities. It is difficult for DG to participate in wholesale power markets.
Incentives	Incentives (subsidies, tax credits, low interest loans) are in place to promote clean DG. Incentives are limited for cogeneration.
Rules and Regulations	Rules and regulations (e.g. interconnection rules, net metering, and exemptions from standby charges) have been changed to benefit some or all DG.

10. Case Study

Edmonton system has been adopted in this project to study the effectiveness of installed DG in the distribution system. The downtown Edmonton main area is being supplied by three substations, namely: Rossdale, Victoria and Garneau substations where the former is supplied from Bellamy substation [33]. Figure 2 shows the schematic diagram for the main substations of Edmonton downtown. In this study three combustion turbines (CTs) as distributed generations have been installed in Edmonton downtown system with total capacity 75MW (25 MW each). The main reasons behind using this type of DGs are that combustion turbines are very mature technology, gas combustion turbines are relatively inexpensive and readily available in most countries, their efficiencies in the range of 20 to 55%, and relatively have low environmental impact if control used. This case study will be divided into two parts; in the first part the price of generation electricity per kilowatt hour will be calculated and compared with

the current price of the electricity generated from the utility. In the second one, the impact of combustion turbines on the transmission system losses will be studied.

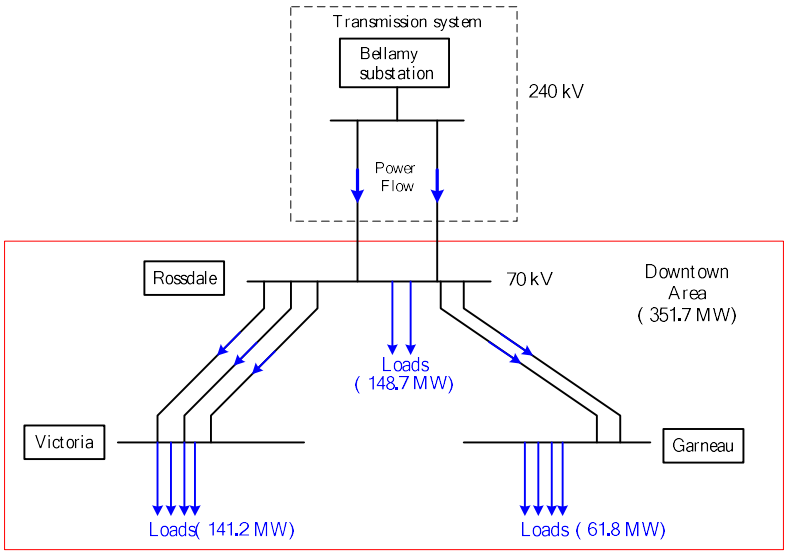

FIGURE. 2. Schematic diagram for the main substations in Downtown – Edmonton/Canada

The combustion turbine parameters that have been used in this study are shown in table 5 and the schematic diagram for the main substations in Downtown – Edmonton with the installation of DGs are shown in figure 3.

TABLE 5. The main parameters for the combustion turbine generation

DG Size	**25 MW**
Capital and installation costs	$1200/kW
O&M Cost Average Maintenance Costs	0.005 $/kWh
Efficiency	50%
Gas price	$6/MMBtu
Lifetime	20 years

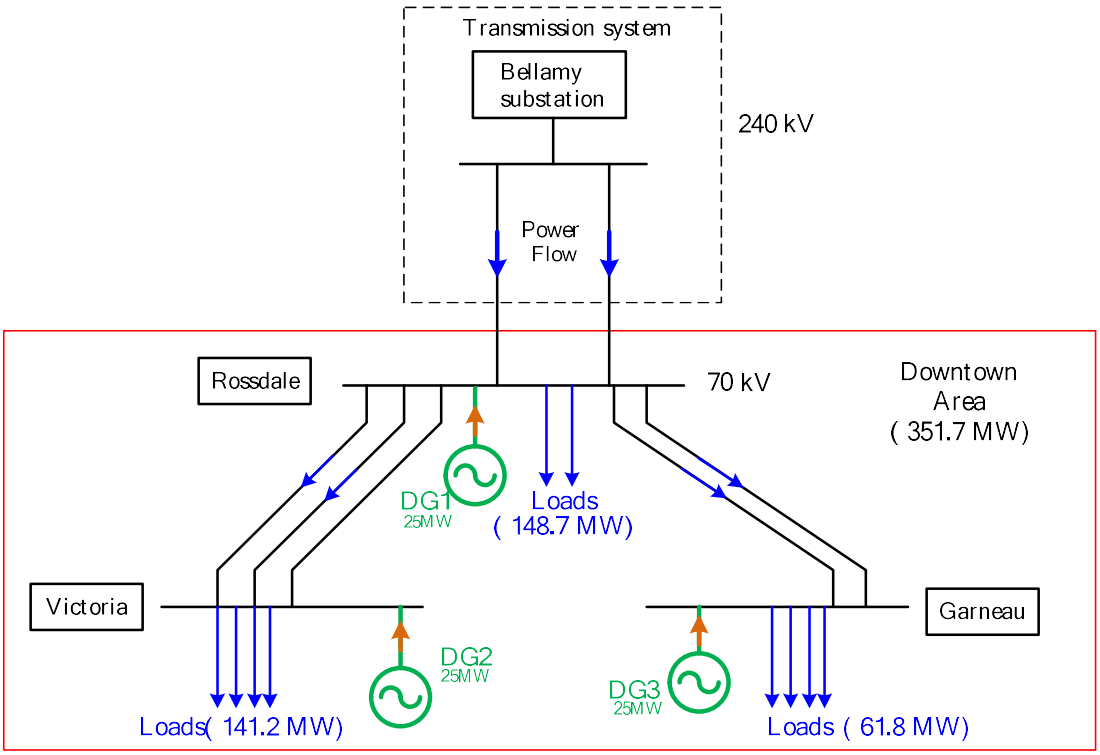

FIGURE. 3. Schematic diagram with the installed of DGs.

Calculations of Generating Electrical Energy

The cost of electricity (COE) is consisted as the sum of three components, capital and installation cost, operation and maintenance cost and fuel cost. The latter is the most significant part, it accounts for around 75% of the total cost.

$$COE(\$/kWh) = C\,\&\,I + O\,\&\,M + F \qquad (1)$$

Where, C&I: Capital and installation cost, and O&M: Operation and maintenance cost, and F: Fuel cost.

Calculations of Capital cost

Capital and installation cost can be calculated by Equation (2)

$$C\,\&\,I(\$/kWh) = \frac{TICperkW \times FCR}{CF \times 8760\ hrs\ per\ year} \qquad (2)$$

Where, CF: the capacity factor and TIC: the total installed cost, and FCR: the fixed charge rate

CF is the capacity factor which is equal to the number of hours per year that the CTs will operate divided by the total number of hours per year it can be calculated as:

$$CF = \frac{Operating\ hrs\ per\ \ year}{8760\ hrs\ per\ year}$$

With 200 days per year → CF=0.55

Assuming FCR is equal to the annual amortized installed cost ($/yr) divided by the total installed cost ($):

$$FCR = \frac{TIC\ per\ kW\ /\ life\ time\ of\ \ unit}{TIC\ per\ kW} \equiv \frac{1}{life\ time\ of\ \ unit}$$

With 20 years lifetime → FCR =0.05

The total installed cost (TIC) for 25MW is $1200/kW (with heat recovery):

$$C\ \&\ I(\$ / kWh) = \frac{\$1200\ /kW \times 0.05}{0.55 \times 8760\ hrs\ per\ year} = \$0.0124 / kW$$

Calculations of Fuel cost

$$F(\$ / kWh) = \frac{Fuel\ \mathrm{Pr}\,ice}{1000000\ Btu\ per\ MMBtu} \times HR$$

$$HR = \frac{3413\left(Btu/kWh\right)}{Efficiency} = \frac{3413}{0.904 \times .5} = 7550.8\,Btu/kWh$$

$$F(\$ / kWh) = 0.0453\ kWh$$

Calculations of O&M cost

The average operation and maintenance cost is 0.005 $/kWh

The cost of electricity (COE)

By substituting the capital and installation cost, operation and maintenance cost and the fuel cost which we obtained from the above calculation in equation (1) we got:

$$COE(\$ / kWh) = \$0.0124 / kWh + 0.005\ kWh + 0.0453\ kWh = 0.0627 / kWh$$

According to electricity company, EPCOR, that responsible for the power system in Edmonton, the current electricity price is ¢8.561/kWh [34]. From the above results, it has been concluded that the price of the electricity generated from the CTs is less expensive than from the utility, therefore installation of CTs would be a cost-effective solution to meet the demand for electricity [35]. Also, it seems that CTs has a good motivation for the private and business owners to have their own generators [36-39].

Estimation of annual energy cost for the proposed Project

This part shows the annual energy cost for the proposed project and evaluates the financial investment in utilization CTs as a DG [40-42]. Using the previous equations, an excel sheet has been generated and the results are shown in table 5. The calculations are made based of the following assumptions:

All capital costs incurred in first year (which is reasonable for DG).

Discount rate is 7.5 %.

Labor cost is 2% of the revenue.

Capital cost allowance (CCA) is not considered (due to lack of information). Tax is not considered (due to lack of information) (i.e., gross revenue ($) is same as net revenue after tax ($)).

From the table we can answer the common questions in any project investment which is how long we would have to wait before we have earned more than we invested at the beginning, this value is obtained when the total cumulative net present value (NPV become positive [43] which is after 11 year (i.e. on the year 12 the project start earning money).

Loss Calculations. In this part of the study, Powerworld simulator [35] has been used to study the impact of distributed generation on the power losses in Edmonton downtown transmission system. Figure 4 shows the circuit that has been implemented by the Power World software for Edmonton-downtown with DGs implementation.

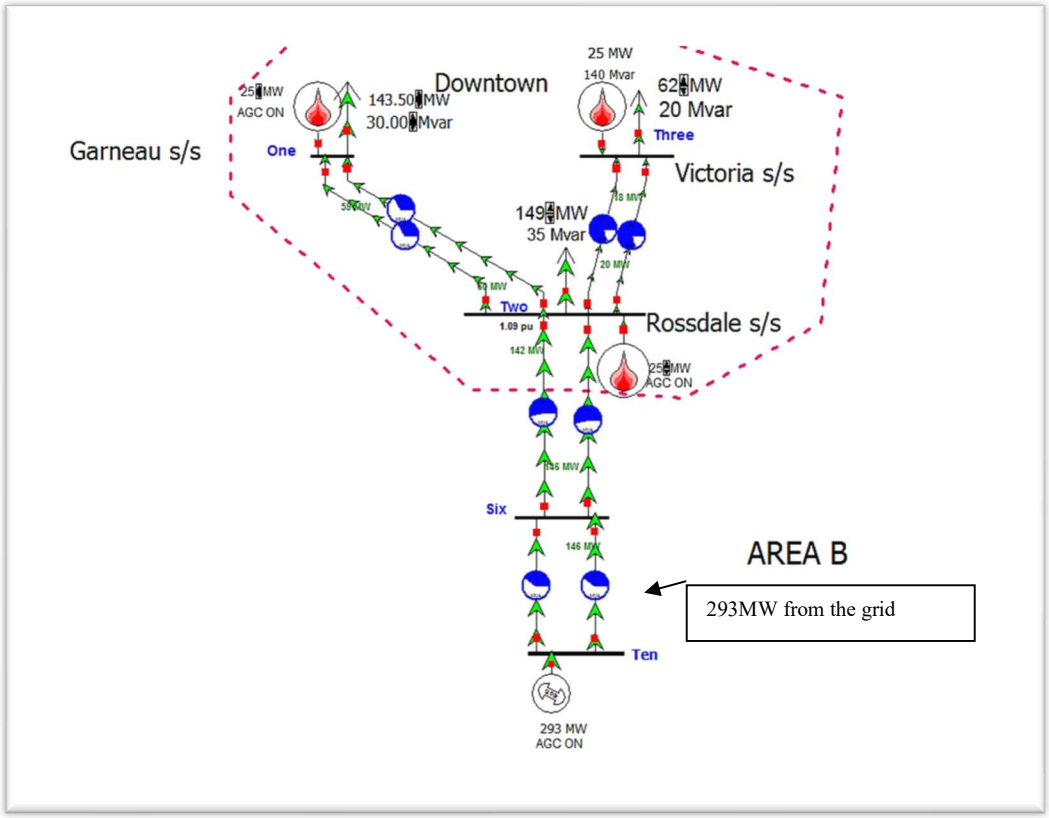

FIGURE. 4. Edmonton-downtown with DGs using the Power World software.

The amount of losses without DGs can be calculated as:

$$Power_{loss} = Power_{\sup ply} - Power_{load}$$

$$\begin{aligned} Power_{loss} &= 369.5MW - 351.7MW \\ &= 17.58MW \end{aligned}$$

While the losses with DGs:

$$\begin{aligned} Power_{loss} &= 293MW - 351.7MW + 75MW \\ &= 16.3MW \end{aligned}$$

The cost of the power losses without using DGs and when DGs are in operation can be obtained as:

$$withoutDG \rightarrow Cost_{loss} = 17.\ 58MW \times 8760hrs \times \$85.61 / kMh = \$13.184M$$

$$with\ DG \rightarrow Cost_{loss} = 16.3MW \times 8760hrs \times \$85.61 / kMh = \$12.224M$$

The results revealed that using combustion turbines has reduced the amount of power losses resulted in the system. The result shows that when there is no distributed generation in operation the amount of power losses is about 17. 58 MW which corresponding to losses cost 10.16 ($M/year), while when the three (CTs) distributed generations are in operation this amount of losses is significantly decreased to become around 13.58 MW which corresponding to losses cost 10.16 ($M/year). Additionally, about M$ 0.96 can be saved in Edmonton downtown power system when these DGs are used.

11. Conclusion.

In this paper an overview about distributed generation (DG) systems has been provided. Distributed generation is generally perceived to be the technology that can help to achieve the environmental targets in some countries worldwide. It also can provide greater flexibility and energy efficiency to the end-users. Different definition based on the DG locations and capacities and the development of DG in the world were discussed in this work. Liberalization of electricity markets, environmental concerns, and the drawbacks of central power generation (CG) are the main drivers for using DG technologies, they were discussed in detail. A wide range of DG technologies, renewable (e.g., photovoltaic and wind) and non-renewable (e.g., internal combustion engines, combustion turbines, microturbines, and fuel cells) technologies were discussed in detail with their advantages, disadvantages, and capital and maintenance costs. Renewable energy resources are used to produce clean energy, while fossil fuels are used to obtain high efficiency using cogenerations or (CHP). Technical and economic impacts for DG also discussed. Additionally, the integration of DG in the grid introduces some technical, economic, environmental, and regulatory problems. Therefore, research is required to increase the benefits, decrease the drawbacks, and educate the public and network operators. Moreover, a case study was conducted to estimate the total costs of using combustion turbines in Edmonton downtown and to study the impact of DGs on the power losses. The results have proven that the total cost for CTs implementation is cheap, the project needs about 11 years to get revenue, and the losses in the power system decreases when DGs are in operations (which save money). The main challenges face distributed generations in Edmonton are lack of the national interconnection standards addressing safety, power quality and reliability for small DG systems

and contractual barriers, such as liability insurance requirements, fees and charges, and extensive paperwork

REFERENCES

[1] A. M. Borbely and J. F. Kreider, Distributed Generation The Power Paradigm for the New Millennium. CRC Press, 2001.

[2] H. B. Putegen, P. R. Macgregor, and F. C. Lambert, "Distributed generation: Semantic hype or the dawn of a new era?" IEEE Power & Energy Magazine, pp. 22–29, January/February 2003.

[3] Thomas Ackermann, Göran Andersson, Lennart Söder, Distributed generation: a definition, Electric Power Systems Research, Volume 57, Issue 3, 20 April 2001, Pages 195-204, ISSN 0378-7796.

[4] IEEE Standard for interconnecting Distributed Resources with Electric Power Systems, IEEE Std 1547.2-2008 , vol., no., pp.1-207, April 15 2009

[5] The US Department of Energy, Office of Distributed Energy Resources, online publications available at: http://www.eere.energy.gov/der/, 2003. Assessed on October 2012

[6] The Electric Power Research Institute, online publications available at: http://www.epri.com/, 2002.

[7] Gas Research Institute, Distributed Power Generation: A Strategy for a Competitive Energy Industry, Gas Research Institute, Chicago, USA 1998.

[8] B. M. Balmat and A. M. Dicaprio, "Electricity market regulations and their impact on distributed generation," in Proc. Conf. on Electric Utility Deregulation and Restructuring and Power Technologies (DRPT 2000), London, 2000, pp. 608–613.

[9] CIGRE, Impact of increasing contribution of dispersed generation on the power system; CIGRE Study Committee no 37, Final Report, September 1998.

[10] The US Energy Information Administration, online publications available at: http://www.eia.doe.gov/fuelelectric.html, 2003.

[11] "Renewable energy in canada, status report," Stelios Pneumaticos Orthologic Consulting, Tech. Rep., 2002.

[12] P. Dondi, D. Bayoumi, C. Haederli, D. Julian, and M. Suter, "Network integration of distributed power generation," Journal of Power Sources, vol. 106, pp. 1–9, 2002.

[13] UK DTI Ofgem Study on Decentralized Generation. 2007 (Ontario)

[14] The North America Energy Working Group, online publications available at: http://www.eia.doe.gov/emeu/northamerica/, 2002.

[15] A. Baueu, D. Hart, and A. Chase, "Fuel cells for distributed generation in developing countries- an analysis," International Journal of Hydrogen Energy, vol. 28, pp. 695–701, 2003.

[16] Distributed Generation in Liberalised Electricity Markets. International Energy Agency, 2002.

[17] H. L. Willis and W. G. Scott, Distributed Power Generation: Planning and Evaluation, Marcel Dekker, New York, 2000.

[18] US EPA, Inventory of US Greenhouse Gas Emissions and Sinks: 1990–2001. EPA 430-R-03-004. US Environmental Protection Agency, Washington, DC, 2003

[19] Power Systems Engineering Research Center, Centralized and Distributed Generated Power Systems - A Comparison Approach, PSERC Publication 12-08, April 16, 2012

[20] K. Huhn, "Market opportunities for distributed generation systems," in Proc. of the Seminar on Distributed Energy Systems, vol. 1. Frost & Sullivan Inc., Jan. 2003.

[21] H. Zareipour, K .Bhattacharya and C. A. Canizares, "Distributed Generation: Current Status and Challenges" IEE Proceeding of NAPS 2004, Feb 2004.

[22] The California Energy Commission, Distributed Energy Resources Guide, Available at: http://www.energy.ca.gov/, 2003. Assessed on October 2012.

[23] UTC Fuel Cells, A United Technologies Company, online publications available at: http://www.utcfuelcells.com, 2004. Assessed on November 2012
[24] Tim Weis, Alex Doukas, Kristi Anderson, (Micro-generation appendix by Gordon Howell) Landowners' Guide to Wind Energy in Alberta, September 2010
[25] Dismbllied General oil ill Liberalised Electricity Markets. Paris. France: International Energy Agency (lEA). 2002.
[26] A. Neris, N. Vovos and G. Giannakopoulos, "A variable speed wind energy conversion scheme lor connection to weak ae systems," IEEE Transactions on Energy Conversion, vol. 14. no. I, pp. 122-127, March 1999.
[27] A. Woyte, T. Vu Van, R. Belmans, and J. Nijs, "Voltage fluctuations on distribution level introduced by photovoltaic systems," IEEE Transaction on Energy Conversion, Vo1.21, Issue 1, March, 2006; pp. 202-209.
[28] M. H. 1. Bollen and M. Hager, "Impact of increasing penetration of distributed generation on the number of voltage dips experienced by end-customers," in Proc. 18/1t International Conference and Exhibition on Electricity Distribution - CIIIED,June 2005, 5 pages)
[29] G. Paap, F. Jansen, and F. Wiercx, "The influence of voltage sags on the stability of 10 kV distribution networks with large scale dispersed co-generation and wind generators," Electricity *Distribution, 2001. Part 1: Contributions. CIRED. 16th International Conference and Exhibition on (IEE Conf. Publ No. 482)* , vol.4
[30] R. C Dugan and T. E. McDermott, "Operating conllicts for distributed generation interconnected with utility distribution systems," IEEE Industry Applications Magazine, pp. 19-25, "2002.
[31] T. Vu Van, J. Driesen, and R. l3elmans, "Interconnection of distributed generators and their influences on power system," International Energy journal, vol. 6. no. **I,** pp. 127-140, June 2005.
[32] Vu Van T., Belmans R., Distributed generation overview: current status and challenges. International Review of Electrical Engineering (IREE), vol. 1, no. 1, pp. 178–189, 2006.
[33] Alberta Electric System Operato**r**, online publications available at: http://www.aeso.ca/downloads/rad148C3.pdf, Assessed on November 2012.
[34] EPCOR, online publications available at: http://www.epcor.com/power/rates-tariffs/Pages/rro.aspx, Assessed on November 2012.
[35] Power World Simulator, http://www.powerworld.com/, Assessed on November 2012.
[36] IEEE, IEEE Standard for Interconnecting Distributed Resources with Electric Power Systems, IEEE Std. 1547, 2003.
[37] IEEE, IEEE Standard for Conformance Tests Procedures for Equipment Interconnecting Distributed Resources with Electric Power Systems, IEEE Std. 1547.1, 2005.
[38] IEEE, Draft Application Guide for IEEE Standard for Interconnecting Distributed Resources with Electric Power Systems, IEEE Std. 1547.2, Rev. D6, 2007.
[39] IEEE, Guide for monitoring, Information Exchange and Control of Distributed Resources Interconnected with Electric Power Systems, IEEE Std. 1547.3, 2007.
[40] IEEE, Guide for Design, Operation and Integration of Distributed Resources Island Systems with Electric Power Systems, IEEE Std. 1547.4, Rev. D2.1, 2007.
[41] Martel, Sylvain; Turcotte, Dave; "Review of Distributed Generation Product and Interconnection Standards for Canada," Electrical Power Conference, 2007. EPC 2007. IEEE Canada, vol., no., pp.242-247, 25-26 Oct. 2007
[42] Carley, S., "Distributed generation: an empirical analysis of primary motivators". Energy Policy, 37, pp. 1648 – 1659, 2009
[43] Kirschen, Daniel; Strbac, Goran (2004). Fundamentals of Power System Economics. John Wiley & Sons.

Jordan Journal of Energy
Volume1, Number 1, 2023

ISSN (Online): 2790-7678
ISSN (Print): 2790-766X

Jordan Journal of Energy (JJE)
Journal Homepage:ttp://dsr.mutah.edu.jo/index.php/jje
JJE an official peer review journal of Mutah University,

Experimental investigation of the effect of using different refrigerant gases on refrigerator performance

Saad S. Alrwashdeh[1], Handri Ammari[2] , Mahmoud Hammad[3], Heening Markotter[4]

[*1]Mechanical engineering department, Mutah University, Al-karak, Jordan
[1]saad.alrwashdeh@mutah.edu.jo
[2] Mechanical engineering department, Mutah University, Al-karak, Jordan
[2]hanamm@mutah.edu.jo
[3] Mechanical engineering department, Jordan University, Amman, Jordan
[3]mah_hamm@yahoo.com
[4] Mechanical engineering department, TU-Berlin, Berlin, Germany
[4]h.markotter@yahoo.com

Received: 2nd April, 2022 ; Accepted: 1st September, 2022
*Corresponding Author Email: saad.alrwashdeh@mutah.edu.jo (Saad S. Alrwashdeh)

ABSTRACT. An experimental study of the performance of a refrigerator using two refrigerants R-134a and R-410A has been conducted. The R-134a was the original design refrigerant, while the R-410A was the drop-in refrigerant. The study was performed on a small refrigerator charged with each refrigerant alone at nearly the same ambient conditions. Temperatures at various locations in the refrigeration system were measured using thermocouples during the running of the experiments, and the data collected were processed into performance refrigeration parameters. The results have indicated that both the refrigeration capacity and coefficient of performance were remarkably higher for the refrigerant R-410a by about 23 and 24%, respectively.

Keywords: Drop in- refrigerants, Office refrigerators, Performance comparison of refrigerants

1. Introduction.

Refrigerants are the working fluids in refrigeration systems that transfer heat from a lower temperature level to a higher temperature level. For several decades' chlorofluorocarbons (CFCs) were considered harmless refrigerants. The most widely used refrigerants were the R-12 and R-22, with R-12 being more common in automotive air conditioning and small refrigerators, and R-22 being used for residential and commercial air conditioning, refrigerators, and freezers. However, in the late twentieth century, ozone depletion and global warming have become dominant environmental issues. The 1987 Montreal Protocol and its amendments

(UNEP, 1987) and Kyoto 1997 Protocols gave a deadline to the use of chlorofluorocarbon (CFC) and hydrochlorofluorocarbon (HCFC) refrigerants, for they destroy the ozone layer. The chlorine atoms contained in CFC and HCFC refrigerants repeatedly combine with and break apart stratospheric ozone molecules, resulting in ozone depletion. The Protocols signed states that CFCs and HCFCs must be reduced and totally banned in the end of 2030.

The Ozone Depletion Potential (ODP) and Global Warming Potential (GWP) issues forced refrigeration engineers to develop alternative refrigerants as substitutes to CFCs and HCFCs. Environmentally benign, 'natural' refrigerants have attracted a considerable attention. The natural refrigerants are the naturally occurring substances, namely, ammonia, hydrocarbons (such as Propane and Butane), carbon dioxide, water, air, etc. These natural refrigerants have zero ODP, and the majority of them have zero GWP, and among them Carbon dioxide has many advantages [1], however some of them can be flammable and/or toxic [2].

Since the early 1996 HFCs (such as refrigerant R-134a) have obtained vital post as the most potential long-term alternatives to replace CFCs and/or HCFCs, and ever since they are widely applied to air-conditioning and heat pumping systems. However, in recent years, the international understanding on the global warming due to alternative refrigerants identifies the HFCs being among those which have considerable impact on the global warming. In accord with such understanding, developing new generation of promising alternative refrigerants that meet the criteria of low global warming besides zero ozone depletion potential is undertaken by researchers [3-9].

A promising alternative refrigerant to replace R134a is the zeotropic refrigerant R-410A as it may enhance the refrigeration cycle performance due to its promising thermophysical properties. However, although R-410A is of zero ODP, it has a high GWP, even higher than that of R-134a.
The goal of this work concentrates on investigating the performance of a small refrigerator with a drop-in refrigerant R-410A in place of the original refrigerant R-134a to examine the possibility of replacement [7, 10-13].

2. Components and Properties of R-410A and R-134a.

Refrigerant R-410A, known in the market as Puron, EcoFluor R-410A, and Genetron R-410A, is a zeotropic, mixture of R-32 (50%) and R-125 (50%) by weight. The blend R-410A is usually used as a refrigerant in air conditioning applications as a substitute to R-22. Whereas, refrigerant R-134a, also known as 1,1,1,2-Tetrafluoroethane Genetron 134a, Suva 134a, is an HFC refrigerant, widely used in household refrigerators and automobile air conditioners as a substitute to R-12 and R-22.

Upon comparison of the thermodynamic properties given in Table 1, it is apparent that R-410A has better qualified properties at the level at which the refrigerant can be used than R-134a.

As for the physical properties of thermal conductivity, viscosity, specific heat, and vapor specific volume, R-410A has better physical properties than R-134a regarding heat transfer during the processes of the refrigeration cycle [14]. That is smaller size of components equipment can be used with R-410.

TABLE 1. Refrigerant Thermodynamic properties

Refrigerant No.	Name	Molecular Mass	Boiling point at pressure$_{atm}$, 1 bar abs	Freezing point at pressure$_{atm}$, 1 bar abs	Critical point		
					Temp (°C)	Pressure (kPa)	Specific volume (m^3/kg)
R-134a	Tetra -fluoroethane	102.03	-26.1	-96.67	101.1	4067.9	552
R-410A	R-32 Difluoromethane (50% weight), + R-125 Pentafluoroethane (50% weight)	72.6	-48.56	(-125) – (-103)	72.2	4757.38	–

As for the chemical properties, both refrigerants in concern are inflammable at normal the operating conditions. In general, R-410A should not be allowed to exist with air above atmospheric pressure or at high temperatures, or in an oxygen enriched environment.

Both of refrigerants; R-134a and R-410A are environment friendly as they don't contribute to ozone depletion (zero ODP). However, they both have a high global warming potential (1890 times the effect of carbon dioxide for R-410A, and 1300 for R-134a).

3. Experimental work and Procedure.

A small refrigerator of 250 W refrigeration capacity located at an engineering laboratory of the University of Jordan, the specifications of which are presented in Table 2, was used for carrying out the experiments. The refrigerator was originally charged with R-134a refrigerant, and then it was charged with drop-in refrigerant R-410A. The temperatures were taken using Copper-Constantan K-type thermocouples connected to the refrigerator components directly. They were placed along the refrigerator cycle. Time intervals were measured using a stopwatch. The refrigeration load was a mass of water. The experiments for both refrigerants were run at nearly the same weather conditions.

TABLE 2. Refrigerator specifications.

Total volume	155
Weight	38-35 kg
Rated voltage	220-240 V
Frequency	50 Hz
Rated input	110 watts
Rated Amperes	0.8 A
Net storage volume	130
Refrigerant used	R-134a
Compressor used	Panasonic 1 hp

The experimental procedure consisted of two parts; the first part was testing the influence of each refrigerant on the refrigerator performance by changing the evaporator temperature while holding the condenser temperature constant, and the second part on variable condenser temperature at constant evaporator temperature.

Variable evaporator readings were taken at normal working conditions of the refrigerator with nearly constant temperatures for the condenser. On the other hand, variable condenser readings were taken with maintaining the evaporator temperature nearly constant. The condenser temperature was changed using a water spray and a fan. The experiments were started with the original refrigerant, R-134a, and finished with the drop-in refrigerant, R-410A.

The temperatures measurements of refrigerator components during the experiments were collected and processed into a data processor concerning the performance of the refrigerator.

There were two sets of experiments. The first set of experiments were for a variable evaporator temperature at constant condenser temperature. The conditions when R-134a was used were; the evaporator temperature was varied from – 14.6 to –25.5°C (saturation pressures range between 100 to 170 kPa), whereas the condenser temperature was kept around 35°C (900 kPa pressure), the load was introduced to the evaporator space at 72.0°C, when the ambient temperature was about 11.6°C. The conditions when R-410a was used were; the evaporator temperature was varied from – 18.8 to –25.2°C, whereas the condenser temperature was kept around 38°C, the load was introduced to the evaporator space at 72.4°C, when the ambient temperature was about 13.0°C. The second set of experiments were for a variable condenser temperature at constant evaporator temperature. The conditions when R-134a was used were; the condenser temperature was varied from 41.4 to 46.5°C (saturation pressures range between 1000 to 1200 kPa), whereas the evaporator temperature was kept around – 19.2°C (135 kPa pressure), the load was introduced to the evaporator space at 12.0°C, when the ambient temperature was about 14.0°C. The conditions when R-410A was used were; the condenser temperature was varied from 40.5 to 47.2°C, whereas the evaporator temperature was kept around – 20.2°C, the load was introduced to the evaporator space at 7.0°C, when the ambient temperature was about 16.0°C.

Theoretical Analysis. The significant quantities of a standard vapor-compression cycle are; the work of compression, the heat rejection rate, the refrigeration effect and capacity, the mass rate of flow, and the coefficient of performance [15].

The work of compression, w, in kJ/kg, is the work required by the compressor, i.e.,

$$W = h_2 - h_1 \qquad (1)$$

where h_1 and h_2 are the enthalpies at inlet and exit of the compressor, respectively. The power consumed by the compressor, W, in kW, is given by,

$$W = \dot{m}\,(h_2 - h_1) \qquad (2)$$

where $\dot{m}$ is the mass rate of flow of the refrigerant.

The compressor isentropic efficiency, η_{is}, was calculated using the following equation,

$$\eta_{is} = (h_{2s} - h_1) / (h_2 - h_1) \quad (3)$$

where h_{2s} is the enthalpy at the exit of the compressor after isentropic compression process. The heat rejection rate, Q_{out}, in kW, is the rate of heat rejected by the refrigerant, i.e.,

$$Q_{out} = \dot{m} (h_3 - h_2) \quad (4)$$

where h_3 is the enthalpy at the exit of the condenser.

The refrigeration effect, q_{in}, in kJ/kg, is the heat absorbed by the refrigerant, i.e.,

$$q_{in} = h_1 - h_4 \quad (5)$$

where h_4 is the enthalpy at the exit of the evaporator.

The refrigeration capacity, Q_{in}, in kW, is the rate of heat absorbed by the refrigerant, i.e.,

$$Q_{in} = \dot{m} (h_1 - h_4) \quad (6)$$

The mass rate of flow of the refrigerant in kg/s is calculated from the following expression,

$$\dot{m} = [(mC\ \Delta T)_{water} + (mC\ \Delta T)_{container}] / [(\Delta h_1 - \Delta h_2) \times time] \quad (7)$$

where m is the mass in kg, C is the specific heat in kJ/(kg.K), ΔT is the temperature difference in °C, and Δh_1 and Δh_2 are the enthalpy difference for the evaporator at exit and inlet during a given period of time, respectively. The mass of water and carton container were 0.5 and 0.2 kg, respectively. The C values for water and carton used were 4.186 and 2.5 kJ/(kg.K), respectively.

The coefficient of performance, COP, is given by,

$$COP = \text{Refrigeration capacity} / \text{Compressor power} = Q_{in}/W \quad (8)$$

These quantities are controlled largely by the cycle suction and discharge pressures. For this work, these pressures were found by taking the temperatures of the middle condenser and evaporator inlet.

For R-134a, ASHRAE code was used, and the saturation pressures were found by interpolation within the data in the table of saturated pressures and temperatures, based on the thermocouples temperature readings that were placed at the middle of the condenser and the evaporator inlet. For R-410A, SUVA code was used, the saturation pressures were also found by interpolation as in the case of the original refrigerant. However, R-410A is a mixture of refrigerant fluids, and thus it has different pressures at each saturation temperature. But, for

simplicity, the average pressure was taken for each state as the difference in pressure between the constituent refrigerants is small. That is,

$$Pavg = (P_l + P_g) / 2 \quad (9)$$

where P_l and P_g are the pressures at the saturated liquid and vapor lines in kPa, respectively. As for the enthalpies at every state of both refrigerants, they were found using the EES (Engineering Equation Solver, commercial version 6.883-3D [09/01/03] software).

Results and Discussion. Comparison between the experimental results of the thermal performance tests performed on the refrigerator using the two refrigerants, R-134a and R-410A, under approximately similar conditions, was carried out and analyzed. The comparison was made for the two sets of experiments (variable evaporator temperature and variable condenser temperature) based on; power of the compressor, refrigeration capacity, heat rejection, coefficient of performance, and compressor isentropic efficiency.

Considering the variable evaporator temperature set of experiments first, Figs. 1 through 5 display the results for the two refrigerants. Figure 1 shows the effect of evaporating temperature on compressor's power. Although the results are scattered, the power consumption is a little lower for the refrigerant R-134a, taking into account that the compressor used was for R-134a.

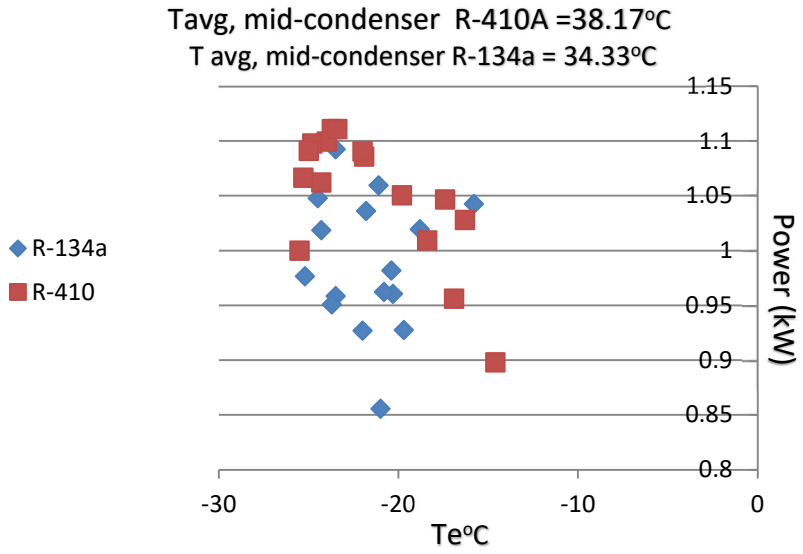

FIGURE.1. Effect of evaporator temperature on compressor power.

Figure. 2, and 3 gives the relation between the refrigeration capacity and the evaporating temperature. For both refrigerants, as the evaporating temperature increases, the refrigeration capacity increases. However, the increase in refrigeration capacity for R-410A is greater than that for R-134a by about 23%. As a result, the heat rejection rate is larger for R-410A as illustrated in Figure. 5.

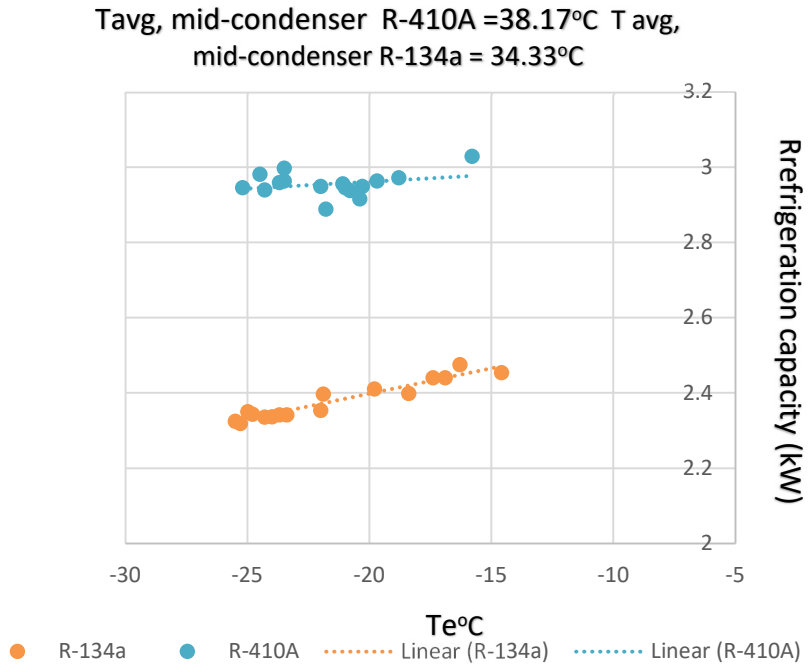

FIGURE. 2. Effect of evaporator temperature on refrigeration capacity.

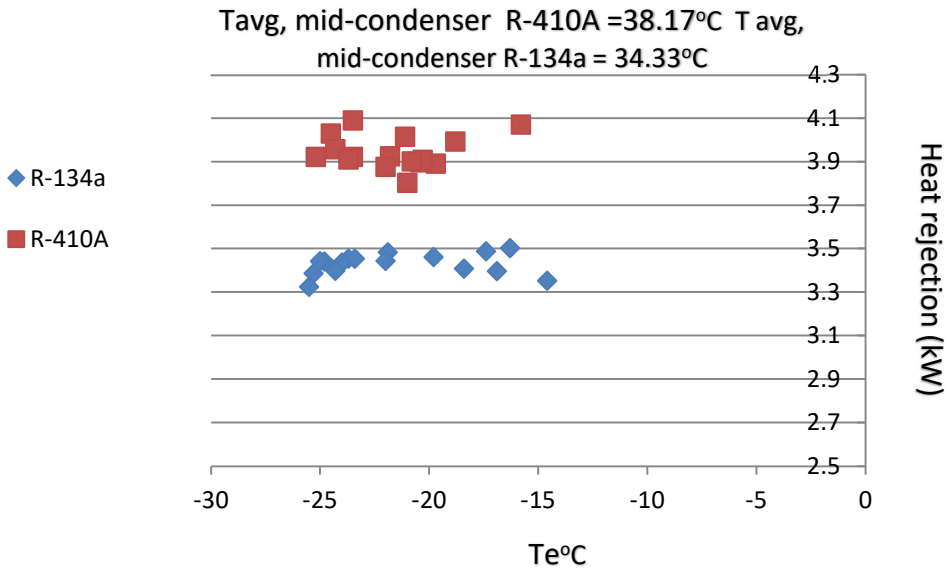

FIGURE. 3. Effect of evaporator temperature on heat rejection rate.

Figure 4 presents the relation between the coefficient of performance, COP, and the evaporating temperature. The figure indicates that as the evaporator temperature increases, the COP increases for both refrigerants, although the COP values are higher for R-410A by about 24% than for R-134a.

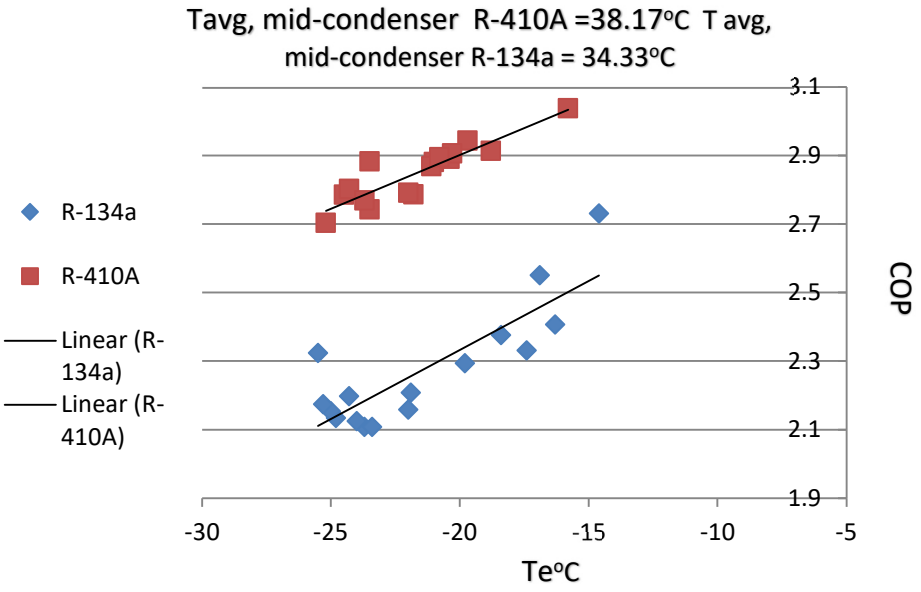

FIGURE. 4. Variation of coefficient of performance with evaporator temperature.

As for the isentropic efficiency of the compressor, it can be noticed from Fig. 5 that it is almost similar for both refrigerant, being around 85% ± 3%.

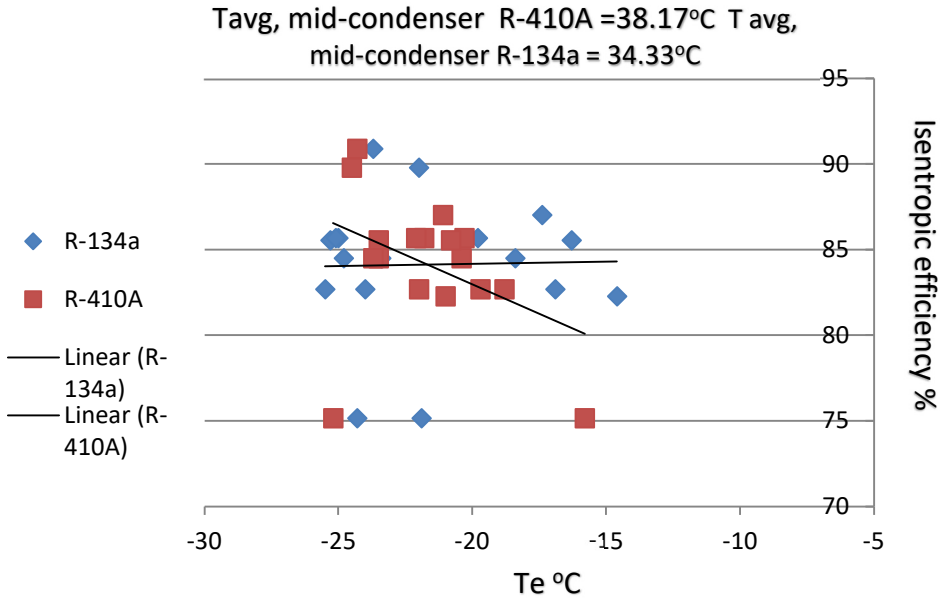

FIGURE. 5. Effect of evaporator temperature on compressor isentropic efficiency.

Figures 6 to 10 present the results of the second set of experiments where the condenser temperature is varied. Figure 6 display the effect of changing the condenser temperature on the compressor's power. The results indicate that the power consumption increases with the

increase of the condensing temperature for both refrigerants, but it is lower for the refrigerant R-410A by about 3.5% than that of R-134a.

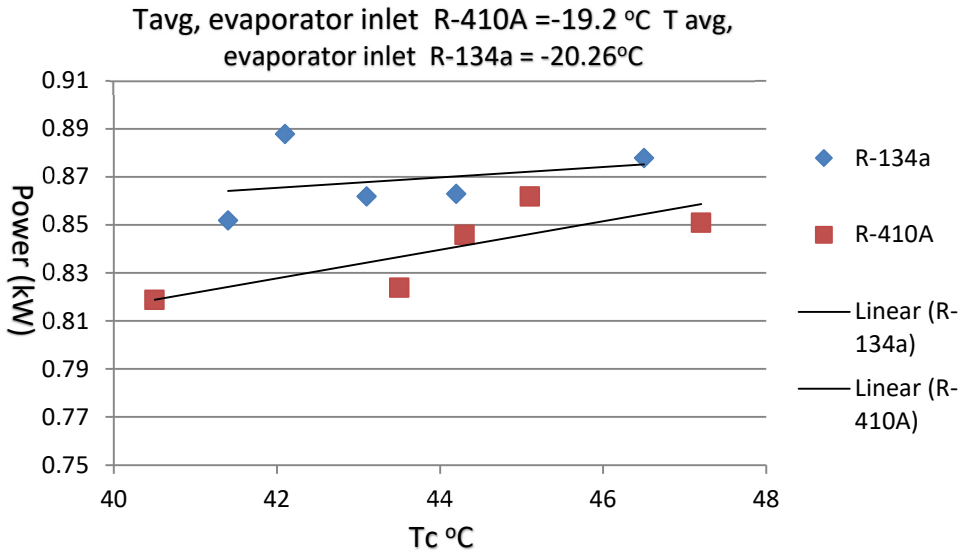

FIGURE. 6. Effect of condenser temperature on compressor power.

Figure 7 shows the influence of varying the condenser temperature on the refrigeration capacity. As one expects for both refrigerants, as the condensing temperature increases, the refrigeration capacity progressively decreases. The trend decrease in the refrigeration capacity for R-134a is lower than that for R-410A by about 3%. The power and refrigeration capacity variation with the condensing temperature results in a heat rejection rate slightly lower and steeper for R-134a than for R-410A as shown in Figure. 8.

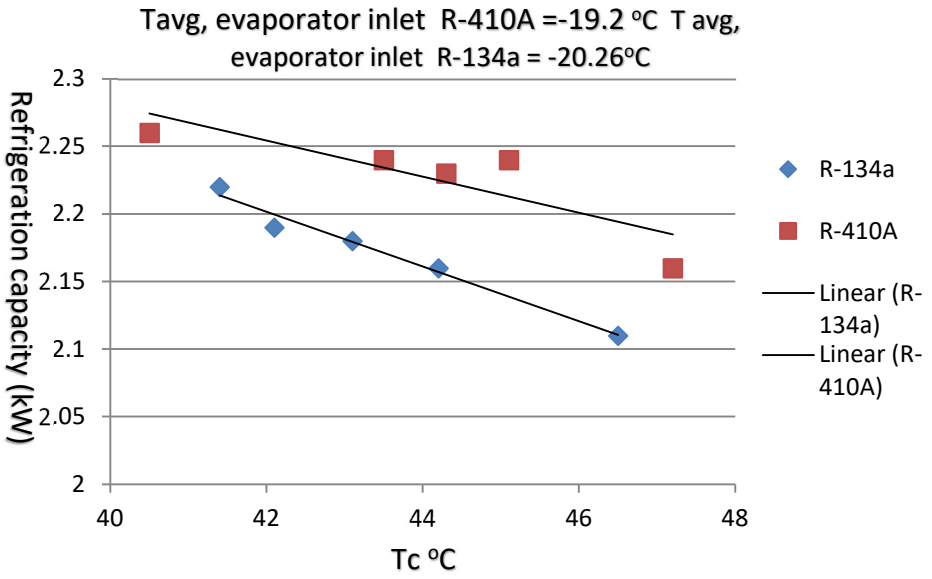

FIGURE. 7. Effect of condenser temperature on refrigeration capacity.

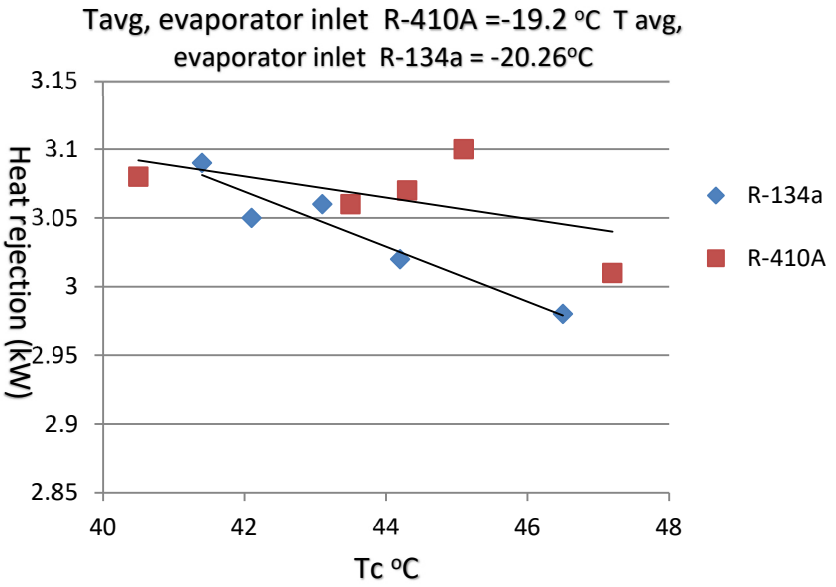

FIGURE. 8. Effect of condenser temperature on heat rejection rate.

The relation between the coefficient of performance, COP, and the condensing temperature is illustrated in Figure. 9. The figure indicates that as the condenser temperature increases, the COP decreases for both refrigerants. This is so since the refrigeration capacity decreases, and the compressor power increases with an increase in the condensing temperature. The COP values are higher for R-410A by about 7% than for R-134a.

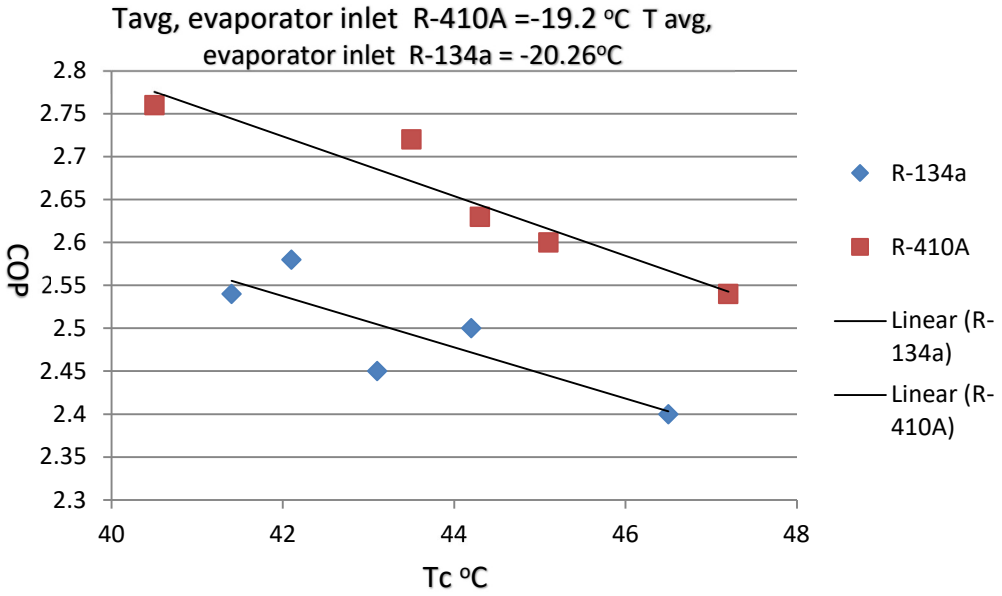

FIGURE. 9. Effect of condenser temperature on coefficient of performance.

The isentropic efficiency of the compressor is slightly higher for R-134a than R410A when the condensing temperature was changed as given in Figure. 10. Both trends of efficiencies are reduced with reduced condenser temperature.

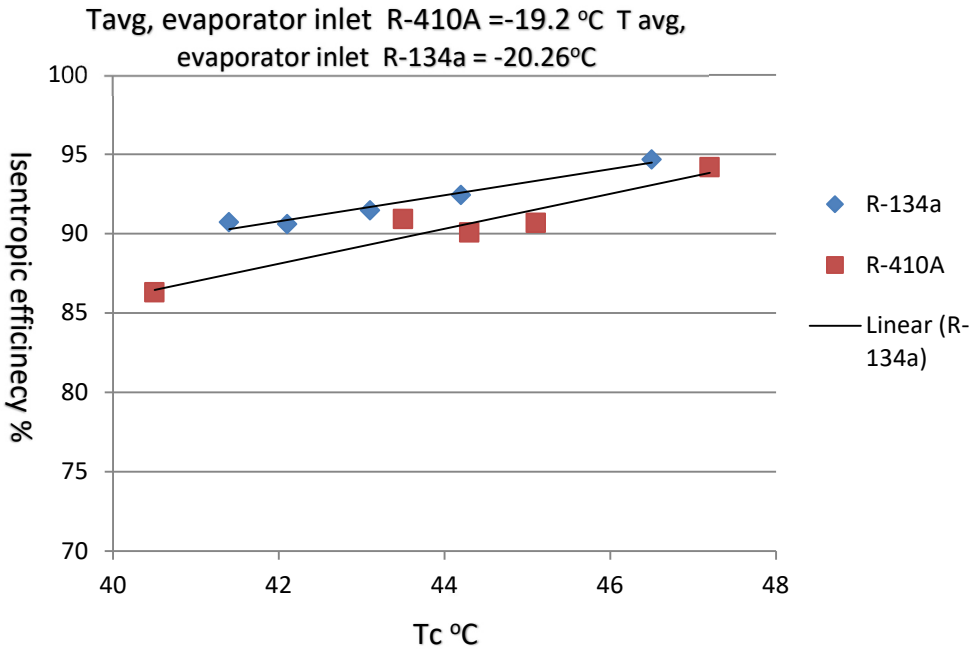

FIGURE. 10. Effect of condenser temperature on compressor isentropic efficiency.

Conclusions. This experimental study was carried on a small refrigerator to study the performance of the refrigerator using each of two refrigerants R-134a and R-410A. The test results have provided the following conclusive remarks:

- The power consumption was slightly lower when R-134a was used when the evaporator temperature was varied. On the other hand, it was the other way round when the condenser temperature was varied.
- The refrigeration capacity was higher by about 23% for R-410A when the evaporator temperature was varied.
- The heat rejection was higher when R-410A was used at both sets of experiments.
- The COP of the refrigerator was higher by about 24% for R-410A when the evaporator temperature was varied.

The isentropic efficiency, however, was generally slightly higher when R-134a was used, not forgetting that the compressor used was an R-134a compressor.

In general, the results indicate the possibility of dropping in refrigerant R-410A in place of refrigerant R-134a with a remarkable improvement in the coefficient of performance.

REFERENCES

[1] Adriansyah, W., Combined AC-HWH System for Indonesian Climate Condition. Bali Indonesia, 2003. FTEC.

[2] Yoon, S.H., et al., Characteristics of evaporative heat transfer and pressure drop of carbon dioxide and correlation development. International Journal of Refrigeration, 2004. 27(2): p. 111-119.

[3] Fatouh, M. and M. El Kafafy, Assessment of propane/commercial butane mixtures as possible alternatives to R134a in domestic refrigerators. Energy Conversion and Management, 2006. 47(15): p. 2644-2658.

[4] Bolaji, B.O., Performance investigation of ozone-friendly R404A and R507 refrigerants as alternatives to R22 in a window air-conditioner. Energy and Buildings, 2011. 43(11): p. 3139-3143.

[5] Kazakov, A., M.O. McLinden, and M. Frenkel, Computational Design of New Refrigerant Fluids Based on Environmental, Safety, and Thermodynamic Characteristics. Industrial & Engineering Chemistry Research, 2012. 51(38): p. 12537-12548.

[6] Barta, R.B., D. Ziviani, and E.A. Groll, Experimental analyses of different control strategies of an R-410A split-system heat pump by employing a turbomachinery expansion recovery device. International Journal of Refrigeration, 2020. 112: p. 189-200.

[7] Kaew-On, J. and S. Wongwises, Experimental investigation of evaporation heat transfer coefficient and pressure drop of R-410A in a multiport mini-channel. International Journal of Refrigeration, 2009. 32(1): p. 124-137.

[8] Markötter, H., et al., Morphology correction technique for tomographic in-situ and operando studies in energy research. Journal of Power Sources, 2019. 414: p. 8-12.

[9] Saraireh, M.A., F.M. Alsaraireh, and S.S. Alrwashdeh, Investigation of heat transfer for staggered and in-line tubes. International Journal of Mechanical Engineering and Technology, 2017. 8(11): p. 476-483.

[10] Román, A., et al., Measurement of the void fraction and maximum dry angle using electrical capacitance tomography applied to a 7 mm tube with R-134a. International Journal of Refrigeration, 2018. 95: p. 122-132.

[11] Pamitran, A.S., et al., Forced convective boiling heat transfer of R-410A in horizontal minichannels. International Journal of Refrigeration, 2007. 30(1): p. 155-165.

[12] Mateu-Royo, C., et al., Comparative analysis of HFO-1234ze(E) and R-515B as low GWP alternatives to HFC-134a in moderately high temperature heat pumps. International Journal of Refrigeration, 2021. 124: p. 197-206.

[13] Göbel, M., et al., Transient limiting current measurements for characterization of gas diffusion layers. Journal of Power Sources, 2018. 402: p. 237-245.

[14] fundamentals, A.S.o.H.R.a.A.C.E.h.o., ASHREA 1993, Atlanta

[15] Jones, W.F.S.a.J.W., Refrigeration and Air Conditioning. 1982: McGraw –Hill, New York.

Jordan Journal of Energy
Volume1, Number 1, 2023

ISSN (Online): 2790-7678
ISSN (Print): 2790-766X

Jordan Journal of Energy (JJE)
Journal Homepage:ttp://dsr.mutah.edu.jo/index.php/jje
JJE an official peer review journal of Mutah University,

Global-Binary Algorithm; New Optimal Phasor Measurement Unit Placement Algorithm

Mohammad M. Al-Momani[1*], Amneh Almbaideen[2], Seba F. Al-Gharaibah[3], Khaled Al-Awasa[4], Allahham Ahmed J.[5]

[1]Department of Electrical Engineering, National Electric Power Company, Amman, Jordan
[1]Emails: monqedmohammad@gmail.com
[2]Department of Electrical Engineering, Mutah University, Karak, Postal Code (61710), Jordan
[2]Emails: a.mbaideen@mutah.edu.jo
[3]Department of Electrical Engineering, Mutah University, Karak, Postal Code (61710), Jordan
[3]Emails: 620180441015@mutah.edu.jo
[4]Department of Electrical and Computer Engineering, Sultan Qaboos University, Muscat, Oman
[4]Emails: k.alawasa@squ.edu.om
[5]Sustainable Energy Technologies Department, University of Oldenburg, , Lower Saxony, Oldenburg, Germany
[5]Email: Ahmed.allahham@uni-oldenburg.de

Received: 4th May, 2022 ; Accepted: 2nd August 6, 2022
*Corresponding Author Email: **monqedmohammad@gmail.com** (M. M. Al-Momani)

ABSTRACT. *This paper proposes a new algorithm for the optimal placement of the phasor measurement unit. The proposed algorithm is based on the concept of finite space solution of any binary problem. This algorithm has considered all possible cases; therefore, the possibility of obtaining a global solution is very high. The large system is divided into several subsystems. The buses (transmission lines) connected between the subsystems are called interconnected buses (lines). The proposed algorithm is implemented through two steps. First step identifies the optimal placement for each subsystem by checking on all possible solutions, the overall optimal placement for the entire system is gathered in the second step. Finally, all possible placements of the phasor measuring units with the optimal numbers are identified to select the best placement based on the user applications. In this work, the Jordanian power system is considered as a case study to validate the proposed algorithm. Four algorithms in the literature are used for the comparison using different IEEE test systems. The algorithm is computed in MATLAB 2020a.*

Keywords: Wide-area monitoring system, Phasor measurement units, Optimal PMU placements, Jordan power system, Global Binary Algorithm, Connectivity matrix algorithm.

1. Introduction.

Wide Area Monitoring Systems (WAMS) can be defined as a collective of information, communication, and measurement technologies to measure, transfer, and manage data of the power system dynamically. Different main applications of WAMS are presented in the literature for various power system aspects [1-5]. Phasor measurement units (PMUs) can provide synchronized phasor measurements of voltages and currents in a wide geographical area based on a standard reference time frame. Considering the financial cost, data transmission and analysis, and technical benefits, the suitable placement of PMUs in power systems becomes critical [6]. The concept of Optimal PMU Placement (OPP) is to install the minimum number of PMUs that can provide full observability [7-8].

Different OPP algorithms are presented in the literature. Artificial intelligence techniques based on the Practical Swarm Optimization (PSO) algorithm are used to improve the result of OPP algorithms in [9]. Other algorithms [10] use the linear optimization technique to solve the binary problem of OPP. Multi-Stage OPP considering substation infrastructure is presented in [10]. An integer linear program (ILP) is a fast and easy-to-implement algorithm, and it is used to solve the OPP problem [11-13]. In [14], a hybrid ILP-based method is proposed to cover all possible solutions to the OPP problem. Some common OPP approaches are the Depth-First Search (DFS), Graph-Theoretic (GTH), and Simulated Annealing (SA) Methods. A more detailed summary of these common methods is in [15]. The Modified Simulated Annealing Method is proposed in [16]. Generally, OPP can be categorized into: Heuristic, Meta-Heuristic, and Deterministic Methods [17], where DFS [18-19] Domination Set [12,20], and Greedy Algorithm [21] are examples of Heuristic Method. GA [22] and PSO [23] are examples of Meta-Heuristic Method, and Integer Programming [24]. Binary Search Method [25-28] are examples of Deterministic Method.

The significant difference among the previous algorithms is the number of PMUs required in a specific system [29-32]. Some algorithms give an acceptable solution for some systems and are not sufficient for others. Therefore, there is a necessity to develop a new algorithm for the OPP problem for any scenario [33-35]. In this paper, the proposed algorithm searches for all optimal PMU placements of any power system.

2. The Problem Definition.

The main application of the WAMS plays a significant role in the selection of the OPP (number of PMU and their locations) in any system; on the other hand, the primary application of WAMS is monitoring. For monitoring application, the system should be fully observable by the PMUs where the definition of the fully visible system is derived from the linear state estimator. The phasor voltage at all buses (substations) can be known by direct measurements or pseudo measurements. The phasor voltage is obtained by direct measurement when a PMU is installed at a bus. The pseudo measurements can be summarized as follow:

- If a PMU is installed at a bus, all adjacent buses are observable using Ohm's law on the interconnected lines.

- If the voltages of two adjacent buses are known, the current in the connection line can be calculated.

In addition to these two straightforward relations, any ideal node (does not have any load or generator), called zero-injection bus (ZIB), has another two concerns:

- If ZIB and all connected buses are observable except one, then the non-observable bus's voltage can be estimated using ohms law.

- If all adjacent buses to a ZIB are observable, then the voltage of the ZIB can be estimated using nodal analysis.

Either the first or the second relation should be used at a ZIB, not both. The selection between these relations gives the problem additional Freedom of Solution (FOS). The merging technique in [7] is applied to implement the ZIB in this algorithm. The OPP problem can be translated into a constrained optimization problem where the objective function (cost) minimizes the total number of PMUs needed to be placed, and the constraint is the observability of each bus in the network. In general, the optimization problem can be written as follow:

$$objective = \min \sum x_i \ , \ \ f_k = \sum_{i=1}^{N} a_{ik} x_i, F \geq I \qquad (1)$$

Where F is the observability vector $[f_1, \dots., f_N]$, $f_k = 1$ if bus k is observable and 0 if not. X is a binary vector that represents the placement of the PMUs $[x_1, \dots. x_N]$, $x_k = 1$ if a PMU is placed at bus k and 0 if not. N is the total number of buses. I is a unit $1 \times n$ vector $[1\ 1\ 1 \dots 1]$. The connectivity matrix A is a square $n \times n$ matrix represents the network topology $[a_{11}, .. a_{ij} .., a_{NN}]$. If bus i and bus k are connected, $a_{ik} = 1$ and zero if not. The elements in the main diagonal of A are always ones.

If the redundancy on measurements is needed, the observability condition ($F \geq I$) shall be changed to ($F \geq B$). The new term (B) represents the order of measurement redundancy. Hence, in the power system, to apply the n-1 criteria, the B vector should be twos. Based on the concept of the connectivity matrix and redundancy vector, equation (1) can be updated to:

$$F = A \times X \quad , \quad F \geq B \qquad (2)$$

3. The Proposed Algorithm.

The proposed algorithm assumes that the local bus does not affect the observability of the remote one. Hence, the vast interconnected power system can be divided into multi areas

(subsystems). The observability of each subsystem is independent of the others. As the space solution of binary problems is finite, it can check all possible solutions without exceptions. The probability of getting a global solution here is 100% because all potential cases are considered. The proposed algorithm has three major stages: split the system into smaller subsystems, obtain the OPP of each subsystem, and gather the OPP for the overall system.

3.1 Splitting Algorithm.

This algorithm provides a new connectivity matrix (modified matrix) to make the global binary method more efficient. The necessity of this algorithm comes from the problem of vital size space solutions for massive systems. At 30-bus system, the size of the space solutions is $(r = 2^{30} - 1)$. The division process must ensure the minimum number of interconnected buses to improve the algorithm's behavoiur and reduce the operation of the second step.

The systematic procedure of the splitting algorithm can be summarized as follow:

1- Select the minimum integer number greater than or equal to (N/30), the number of subsystems, and select the size of each subsystem.

2- Start from the first row and sum all the first subsystem, second, third, … to the end. The summation should not include main diagonals elements.

3- The maximum summation in the k row corresponds to the appropriate group. Then, move the k^{th} row and the k^{th} column to a position in the best group.

4- Carry on until all buses are selected in their best group and make a modified connectivity matrix that is all centralized around the main diagonal. Change the size of any subsystem if it is necessary.

5- Identify the inter-connected buses.

For example, consider a small system with ten buses is used. The connectivity matrix is shown in Figure 1(a). The empty elements refer to zeros. Applying the previous steps as follow:

1. Suppose that the system is divided into three subsystems (3, 3, and 4 buses, respectively). In the connectivity matrix, Figure 1(a), the matrix is colored by yellow, green, and brown to distinguish between subsystems.

2. From the figure, the summation of the elements of the first row is zero in the first area, one in the second, and 2 in the third (Do not consider main diagonal in summation).

3. The first row is classified in the third area, so the appropriate group of the first bus is the

third. The first row should be replaced by bus 7 or 9, classified in the first area. Let us select bus 9; the ninths must replace the first column and row. The new matrix will be as shown in Figure 1 (b).

4. The second iteration shows that bus two is classified in the second zone, while bus six is ranked in the third and bus 7 in the first zones. The final modified matrix is shown in Figure 1 (c).

5. From Figure 1 (c), the interconnected buses are buses 2 and 3.

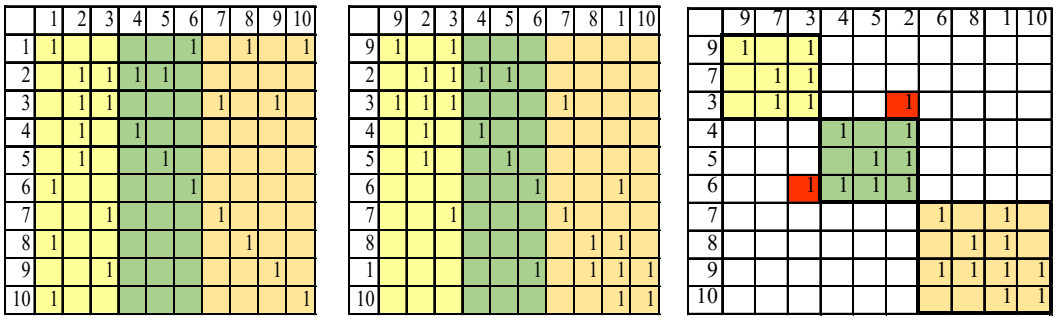

(a) original matrix (b) the first modification (c) the last modification

FIGURE 1. Split Algorithm, Example of 10-bus system.

From Figure 1(c), the density of the ones is around the main diagonal. All subsystem connectivity matrices can be identified by ignoring all ones out of the selected area, Figure 1(c). The connectivity matrix of the first subsystem is the yellow 3 × 3 matrix. The green 3 × 3 matrix represents the second subsystem connectivity matrix. Finally, the third subsystem connectivity matrix is represented by the orange 4 × 4 matrix. Based on this algorithm, any vast system can be divided into any number of smaller subsystems.

3.2 Step one: OPP of each subsystem

In the first step, as shown in Figure 2 (a), the proposed binary global algorithm is applied to each subsystem to obtain sub-space solutions. It uses the concept of limited space solutions for any binary problem. Figure 1 consists of 13 blocks described below:

- The split algorithm, previous section, defines blocks 1,2 and 3. This algorithm is repeated for each subsystem.

- Block 4: select a random number of PMUs (K) around (N/4) where N is the subsystem's size. Set Y=2 for termination condition to stop the algorithm when the OPP is achieved.

- Block 5: generate all possible combinations of K digits on N space, representing the different distribution of K PMUs in the N-Bus system. The total variety of K PMU on the N-bus system is given by equation 3. The set of solutions are saved in matrix X.

$$M = \frac{N!}{K! \times (N-K)!} \quad (3)$$

- Block 6: compute observability condition Equation 2.
- Block 7: check on observability based on required redundancy on measurements.
- Block 8: If K PMUs make the system observable, check on the value of Y. If Y = 1, stop the algorithm, and K is the optimal number. If Y is not equal to one, try to reduce the number of PMUs (K) in block 9, set the Y =0, and go back to block 5.
- Block 10: if K PMUs are not sufficient to obtain the required observability level, check on the value of Y. If Y is zero, then the optimal number of PMU is greater than the current (K) block 12 and generate the location using the observability condition, block 13. If Y is not zero, try to add a PMU to the current number (K), set the y value to 1 and go back to block 5.

Once this step computes the optimal number of PMUs, the space solution of each subsystem (X1, X2, ….) called sub-space solution is identified. A sub-space solution defines all combinations of optimal PMU placements for a specific subsystem. Each subspace solution matrix has many rows (vectors); each vector represents a particular placement of PMUs.

3.2. Step two: Global OPP solution.

The second step, Figure 2 (b), selects the new space solution from the combination of sub-space solutions. By trying to remove PMUs at interconnected buses (which connect one zone to another), the final optimal PMU placements will be defined. All sub-space solutions aggregation should take all possible crossing between vectors in each sub-space matrix, step 1. The second step tries to remove the PMU placed at the interconnected bus and check for system observability, see Figure 2 (b). The flow chart of this step is described below:

- Block one generates a space solution by gathering all subspace solutions from step 1. The space solution should cover all combinations between the subspace vectors. In this block, the stop criterion (y) is initialized, where (m) is the number of interconnected buses.
- Block 2: Identify interconnected buses from the split algorithm and initialize counter (i).
- Block 3: remove the PMU at i^{th} interconnected bus if exist from all space solution matrix.
- Block 4: compute the observability vector (F) from equation 2 using the complete system connectivity matrix.
- Block 5: check on observability. If any space solution makes the system observable, check on stop condition in block 7, return the removed PMU from block 3 and increase the counter (i) by one, block 6.

- Block 7: check the stop conditions.

Two conditions are defined: Y for an external loop and (i) for an internal loop. If the stop criteria are not achieved, and the system is observable, the removed PMU is permanently absent from the space solution to obtain a new space solution with a lower number of PMUs and return to block 2.

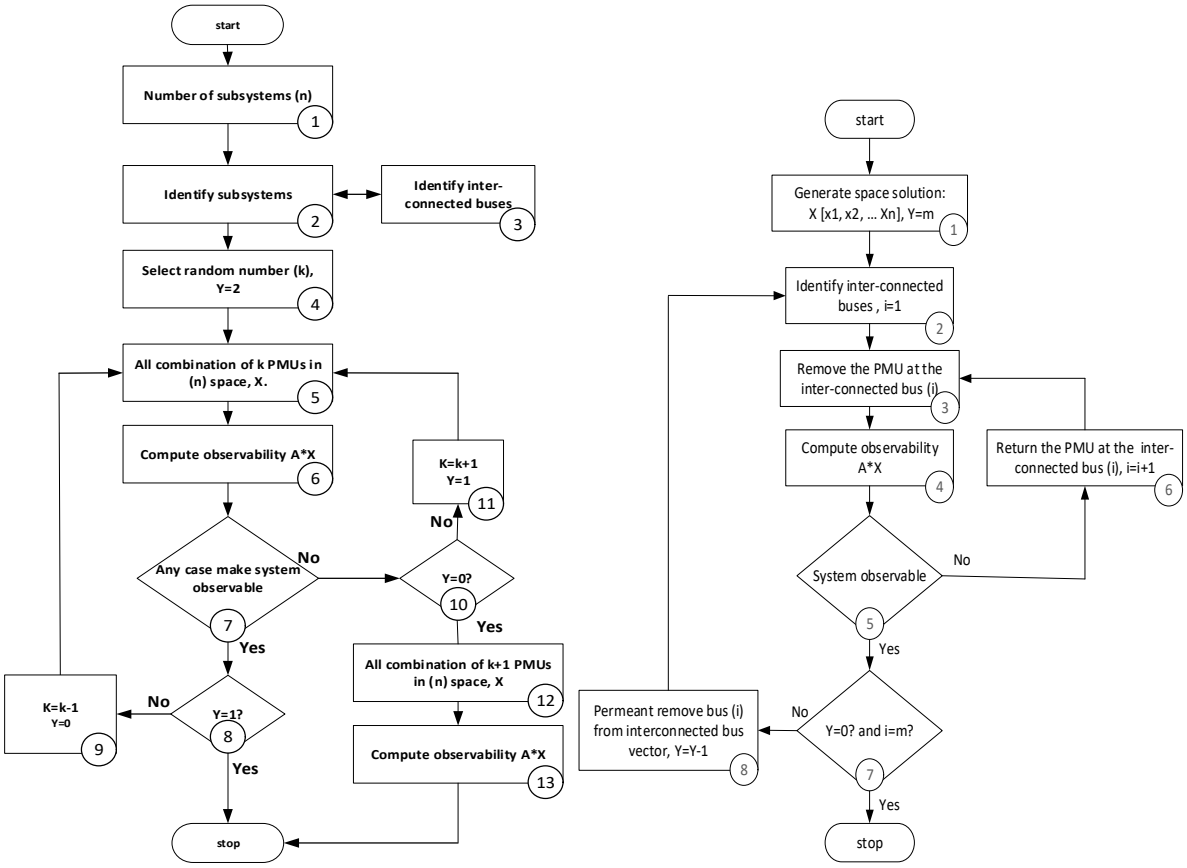

FIGURE 2. Flow chart of the global binary algorithm, (a) step 1, (b) step 2.

Finally, the proposed algorithm generates the final space solution consisting of all possible combinations of PMU placements with the minimum number. Jordanian power network is considered as an example in the next section to illustrate the previous sub-sections.

4. Case Study: Jordanian Power System.

The Jordan transmission power system has 68 substations after considering the ZIBs, Figure 3. The proposed split algorithm divides the system into three subsystems, as shown in Figure 3. The first subsystem, brown color, consists of 22-bus, the second subsystem, green color,

consists of 22-bus, and the third subsystem, black color, consists of 24-bus. The interconnected buses are: 34, 36, 40, 7, 2, 30, 35, 40, 15, 18, 28, 29, 49, 43 and 44.

At each subsystem, the global binary algorithm is applied separately, step one. The optimal numbers of PMUs are 7, 7 and 8, and the size of each subspace solution is 30, 5, and 55, respectively. The total space solution, Figure 2 (b): block 1, consist of (7+7+8=21) PMUs with size (30×5×55=8250).

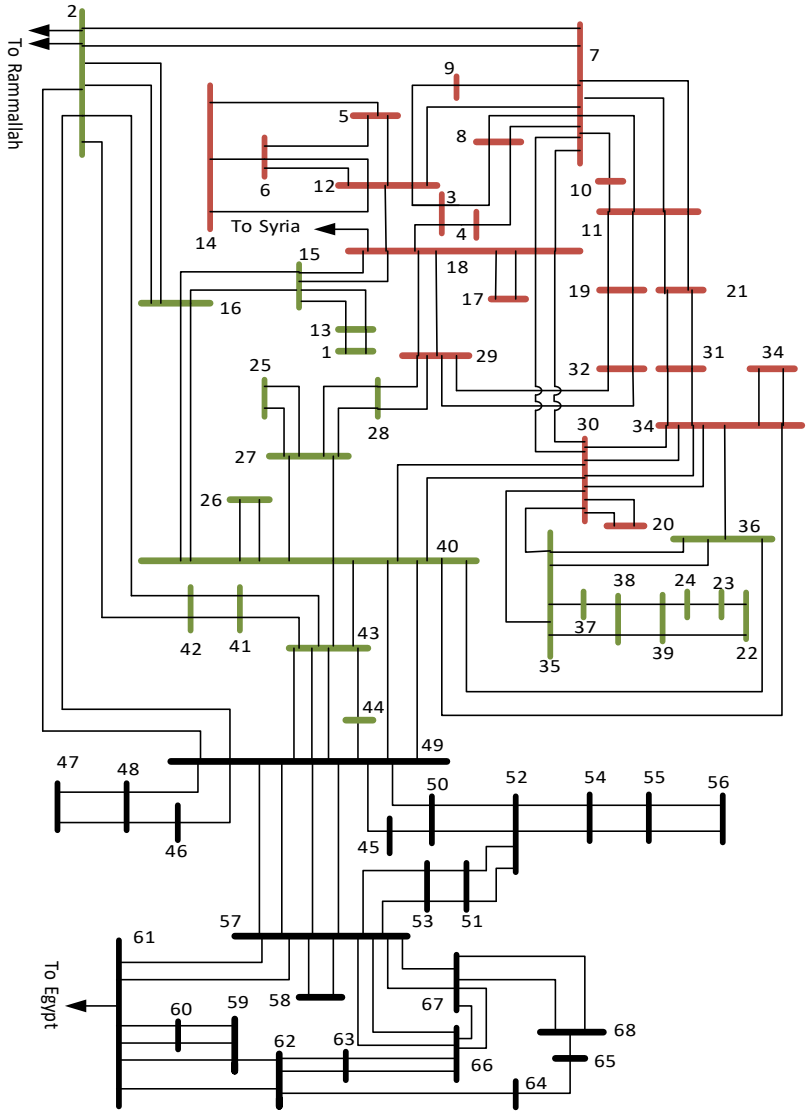

FIGURE 3. Single Line Diagram of Jordanian power system

When applying the second step by removing inter-connected buses, the result shows that 21 PMUs are enough to observe the overall system with 2760 placement options. The second step results show that the PMU at bus 43 or bus 44 (not both) is unnecessary. Based on this result,

2760 placement options are available for the linear state estimation to get full observability. Other criteria could be achieved to select one of these placements like:

- Maximum redundancy: which solution gives the maximum number of redundant buses?
- Oscillation monitoring and analysis: which solution covers the maximum number of generator substations and tie-lines?
- Stability assessments: Which solution consists of the maximum number of critical buses and the maximum number of loge transmission lines?
- Remedial Action Scheme (RAS): the solution's priority can be defined based on special applications like load rejection, reactive power compensation control, HVDC controls, local generation units trip based on transmission line outages, wide-area generation tripping based on extra-high voltage line outages.
- Other applications like black start monitoring, model validation, disturbance analysis, frequency response analysis,

For example, each special function can be given a weight based on the user priority. Then, the optimal placement can be selected based on the maximum wights. Some applications with weights are defined for the Jordanian power system as follow:

1. Monitor the low-frequency oscillations with weight 40%
2. Voltage stability monitoring with weight 24 %
3. Disturbance analysis for some transmission lines (TL43-49, TL 49-40, TL 40-30, TL 30-18, TL 18-7, TL 7-2, TL 2-49, TL 49-57, TL 57-61) with weight 20 %
4. RAS: Wide area generation tripping based on tie-lines outages in addition to some extra-high voltage outages like (TL 57-61 and TL57-49) with weight 10%
5. RAS: Load rejection based with weight 5%.

In addition to these objectives, the maximum location that provides maximum redundancy in the measurements will be preferable. Table 1 shows the implementation of these objectives for each busbar. The cross indicates that the bus affects the goal. The summation of the weights is calculated in the last column to define the bus importance. From the space solution in the proposed algorithm, the maximum weights vectors are the best. Appling these objectives to the 2760 options in the proposed algorithm give us the optimal 18 locations with the maximum weights presented in Table 2.

TABLE 1. Implementation of real application in each substation (busbar)

Bus number	Obj. 1 (40%)	Obj. 2 (25%)	Obj. 3 (20%)	Obj. 4 (10%)	Obj. 5 (5%)	Total (%)
1					X	5
2		X	X	X		55
7	X	X	X	X		95
8					X	5
11	X		X			60
12	X		X		X	65
13					X	5
14		X				25
15					X	5
16					X	5
18	X	X	X	X		95
19					X	5
20	X					40
22	X					40
23					X	5
24					X	5
25					X	5
30	X	X	X			85
33					X	5
34		X			X	30
35		X			X	30
36					X	5
40	X	X	X	X		95
41					X	5
42	X	X	X			85
46					X	5
48					X	5
49	X	X	X	X		95
52	X	X				65
57	X	X	X	X		95
58	X					40
59	X	X				65
60					X	5
61	X	X	X	X		95
62	X	X				65

TABLE 2. optimal 18 PMU locations for Jordan power system considering some real applications

s.n	Optimal 18 locations																				
1	3	11	12	13	18	19	23	27	30	34	38	40	42	48	49	52	54	57	61	62	65
2	3	11	12	13	18	19	23	27	30	34	38	40	42	48	49	52	54	57	61	62	68
3	3	11	12	13	18	19	23	27	30	34	38	40	42	48	49	52	55	57	61	62	65
4	3	11	12	13	18	19	23	27	30	34	38	40	42	48	49	52	55	57	61	62	68
5	3	11	12	13	18	19	23	27	30	34	38	40	42	48	49	52	56	57	61	62	65
6	3	11	12	13	18	19	23	27	30	34	38	40	42	48	49	52	56	57	61	62	68
7	4	11	12	13	18	19	23	27	30	34	38	40	42	48	49	52	54	57	61	62	65
8	4	11	12	13	18	19	23	27	30	34	38	40	42	48	49	52	54	57	61	62	68
9	4	11	12	13	18	19	23	27	30	34	38	40	42	48	49	52	55	57	61	62	65
10	4	11	12	13	18	19	23	27	30	34	38	40	42	48	49	52	55	57	61	62	68
11	4	11	12	13	18	19	23	27	30	34	38	40	42	48	49	52	56	57	61	62	65
12	4	11	12	13	18	19	23	27	30	34	38	40	42	48	49	52	56	57	61	62	68
13	8	11	12	13	18	19	23	27	30	34	38	40	42	48	49	52	54	57	61	62	65
14	8	11	12	13	18	19	23	27	30	34	38	40	42	48	49	52	54	57	61	62	68
15	8	11	12	13	18	19	23	27	30	34	38	40	42	48	49	52	55	57	61	62	65
16	8	11	12	13	18	19	23	27	30	34	38	40	42	48	49	52	55	57	61	62	68
17	8	11	12	13	18	19	23	27	30	34	38	40	42	48	49	52	56	57	61	62	65

Table 2 shows the optimal 18 locations for the Jordanian power system considering the previous applications. The best solution should give the maximum number of redundant buses. The maximum number of redundant buses can be achieved by the first six solutions from the 18 cases, Table 2. For these six sets, 27 buses can be observed by more than one PMU.

Finally, the proposed algorithm is applied to different IEEE test systems with different scenarios. Table 3 shows the comparison of the proposed algorithm with the previous literature. The results of the second step in the proposed algorithm, observability for linear state estimation, are used in the table.

TABLE 3. comparison results with other methods

Test system	Case	Proposed Algorithm		Ref [7]	Ref [26]	Ref [27]	Ref [28]
		Space solution size	No. of PMU				
IEEE-14 Bus	Without ZIB	5	4	4	4	4	N/A
	With ZIB	1	3	3	3	3	3
	n-1 criteria	4	7	7	7	7	7
IEEE 30-bus	Without ZIB	858	10	10	10	10	N/A
	With ZIB	68	7	7	7	7	7
	n-1 criteria	184	15	15	15	17	16
IEEE 118-bus	Without ZIB	1457	31	32	32	32	N/A
	With ZIB	765	28	28	28	28	29
	n-1 criteria	3521	61	62	64	65	62

5. Conclusions.

This paper proposes a new algorithm to obtain a global solution to the OPP problem. This search algorithm considers all possible solutions without any exceptions. In this algorithm, the probability of getting the global solution for any system is 100 % because all space solutions are checked. Jordan Power system, which contains 68 buses, is taken as an actual system for validation purposes. Different WAMS applications are selected as examples to obtain the optimal placements that can achieve the maximum benefits for specific applications. Different IEEE test systems are used to validate the algorithm and compare it with others.

Acknowledgement

This paper is based upon project No. Ene/2/9/2016 supported by the Scientific Research and Innovation Support Fund (SRISF) / Ministry of Higher Education and Scientific Research/ Jordan.

REFERENCES

[1] M. M. Almomani, A. Odienat, S. F. Al-Gharaibeh and K. Alawasa, "The Impact of Wind Generation on Low Frequency Oscillation in Power Systems," 2021 IEEE PES/IAS PowerAfrica, 2021, pp. 1-5, doi: 10.1109/PowerAfrica52236.2021.9543283.

[2] Mohammad M. Almomani and Seba F. Algharaibeh, "Modelling and Testing of a Numerical Pilot Distance Relay for Compensated Transmission Lines", International Journal of Scientific Research and Engineering Development, vol. 3, no. 6, pp. 776-786, 2020.

[3] M.M. Al-Momani, A.S.M. Hatmi and S.F. Al-Gharaibeh, "Performance analysis of the distance relay characteristics in a compensated transmission line", European Journal of Electrical Engineering, vol. 23, no. 3, pp. 197-205, 2021. https://doi.org/10.18280/ejee.230304

[4] Tauseef Gulrez, Abdullah Al-Odienat, "A New Perspective on Principal Component Analysis using Inverse Covariance", International Arab Journal of Information Technology (IAJIT), Vol. 12, Issue 1, 2015.

[5] K. M. Alawasa and A. I. Al-Odienat, Power quality characteristics of residential grid-connected inverter of photovoltaic solar system, 2017 IEEE 6th International Conference on Renewable Energy Research and Applications (ICRERA), 2017, pp. 1097-1101.

[6] Odienat, M. M. Al Momani, K. Alawasa and S. F. Gharaibeh, "Low Frequency Oscillation Analysis for Dynamic Performance of Power Systems," 2021 12th International Renewable Engineering Conference (IREC), 2021, pp. 1-6, doi: 10.1109/IREC51415.2021.9427818.

[7] I. Al-Odienat, K. Al-Awasa, M. Al-Momani and S. Al-Gharaibah, "Connectivity Matrix Algorithm: A New Optimal Phasor Measurement Unit Placement Algorithm", IOP Conference Series: Earth and Environmental Science, vol. 551, no. 1, pp. 012008, August 2020. Doi. 10.1088/1755-1315/551/1/012008

[8] A. I. Al-Odienat, B. Malahmeh and A. R. Tarawneh, The Optimal PMU Placement in the Power Systems for the Enhancement of State Estimation, 2020 International Conference on Electrical, Communication, and Computer Engineering (ICECCE), 2020, pp. 1-6, doi: 10.1109/ICECCE49384.2020.9179214.

[9] B. Gou, Generalized integer linear programming formulation for optimal PMU placement, IEEE transactions on Power Systems, vol. 23, no. 3, 2008, pp. 1099–1104.

[10] S. Almasabi and J. Mitra, Multi-stage optimal PMU placement including substation infrastructure, in 2017 IEEE Industry Applications Society Annual Meeting, 2017, pp. 1–8.

[11] R. Manam and S. R. Rayapudi, Sensitive Constrained Optimal PMU Allocation with Complete Observability for State Estimation Solution, Eng. Technol. Appl. Sci. Res., vol. 7, no. 6, pp. 2240–2250, Dec. 2017.

[12] Almomani Mohammad, Ali S. Al-Dmour and Seba Algharaibeh, "Application of Artificial Intelligence Techniques for Modeling and Simulation of Photovoltaic Arrays", Jordan Journal of Electrical Engineering, vol. 6, no. 4, pp. 296-314, 2020.

[13] X. Chen, L. Sun, T. Chen, Y. Sun, K. J. Tseng, K. V. Ling, W. K. Ho, G. A. Amaratunga et al., Full coverage of optimal phasor measurement unit placement solutions in distribution systems using integer linear programming, Journal Energies, vol. 12, no. 8, 2019.

[14] N. M. Manousakis, G. N. Korres, and P. S. Georgilakis, Taxonomy of PMU placement methodologies, IEEE Transactions on Power Systems, vol. 27, no. 2, 2012, pp. 1070–1077.

[15] P. Xu, Power system observability and optimal phasor measurement unit placement, Master thesis, University of Minnesota - Twin Cities December 2015.

[16] N. Manousakis, G. Korres, and P. Georgilakis, Optimal placement of phasor measurement units: A literature review, 2011 16th International Conference on Intelligent System Applications to Power Systems IEEE, 2011, pp. 1–6.

[17] M. Farsadi, H. Golahmadi and H. Shojaei, Phasor Measurement Unit (PMU) allocation in power system with different algorithms, 2009 International Conference on Electrical and Electronics Engineering - ELECO 2009, Bursa, Turkey, 2009, pp. I-396-I-400.

[18] T. Cai and Q. Ai, Research of PMU optimal placement in power systems, International conference on system theory and scientific computation, 2005, pp. 38–43.

[19] T. W. Haynes, S. M. Hedetniemi, S. T. Hedetniemi, and M. A. Henning, Domination in graphs applied to electric power networks, SIAM Journal on Discrete Mathematics, vol. 15, no. 4, 2002, pp. 519–529.

[20] X. A. Yuan, A linear algorithm for minimum phasor measurement units placement, 2010 Innovative Smart Grid Technologies (ISGT). IEEE, 2010, pp. 1–3.

[21] M. Zhou, V. A. Centeno, A. G. Phadke, Y. Hu, D. Novosel, and H. A. Volskis, A preprocessing method for effective PMU placement studies, 2008 Third International Conference on Electric Utility Deregulation and Restructuring and Power Technologies, IEEE, 2008, pp. 2862– 2867.

[22] F. Marin, F. Garcia-Lagos, G. Joya, and F. Sandoval, Genetic algorithms for optimal placement of phasor measurement units in electrical networks, Electronics Letters, vol. 39, no. 19, 2003, pp. 1403–1405.

[23] J. Kennedy and R. Eberhart, Particle swarm optimization (PSO), Proc. IEEE International Conference on Neural Networks, Perth, Australia, 1995, pp. 1942–1948.

[24] F. Aminifar, A. Khodaei, M. Fotuhi-Firuzabad, and M. Shahidehpour, Contingency-constrained PMU placement in power networks, IEEE Transactions on Power Systems, vol. 25, no. 1, 2009, pp. 516–523.

[25] S. Chakrabarti and E. Kyriakides, Optimal placement of phasor measurement units for power system observability, IEEE Transactions on power systems, vol. 23, no. 3, 2008, pp. 1433–1440.

[26] Xu, Bei, and Ali Abur, Optimal placement of phasor measurement units for state estimation, Final Project Report, Power Systems Engineering Research Center (2005): 05-58.

[27] Roy, BK Saha, A. K. Sinha, and A. K. Pradhan, An optimal PMU placement technique for power system observability, International Journal of Electrical Power & Energy Systems, 42.1 (2012): 71-77.

[28] C. Lu, Z. Wang, M. Ma, R. Shen and Y. Yu, An Optimal PMU Placement With Reliable Zero Injection Observation, IEEE Access, vol. 6, pp. 54417-54426, 2018, DOI: 10.1109/ACCESS.2018.2865513.

[29] Abdullah Al-Odienat, Power System Blackouts: Analysis and Simulation of August 9, 2004, Blackout in Jordan Power System, Information Technology Journal, Vol. 5, 2006. pp. 1078-1082.

[30] M. M. Al-Momani, A. Odienate, S. F. Algharaibeh, K. Awasa and O. Radaideh, "Modified Connectivity Matrix Algorithm," 2022 Advances in Science and Engineering Technology International Conferences (ASET), 2022, pp. 1-6, doi: 10.1109/ASET53988.2022.9735116.

[31] K. Al-Maitah, A. Al-Odienat, The Improvement of Weighted Least Square State Estimation Accuracy Using Optimal PMU Placement, WSEAS TRANSACTIONS ON POWER SYSTEMS, Vol. 15, 2020, pp. 1-7.

[32] Abdullah I. Al-Odienat & Khaled Al-Maitah, A New Wide Area Protection Scheme Based on the Phase Angles of the Sequence Components, Electric Power Components and Systems, 2021, DOI: 10.1080/15325008.2021.1971335

[33] K. Al-Maitah, A. Al-Odienat, Wide Area Protection Scheme for Active Distribution Network Aided µPMU, 7th Annual IEEE PES/IAS PowerAfrica Conference (PAC 2020), August 25-28, 2020, pp. 1-5.

[34] Al-Momani, Mohammad M., and Seba F. Al-Gharaibeh. "Prediction of Transient Stability Using Wide Area Measurements Based on ANN." International Journal of Emerging Trends in Engineering

Research 9.11 (2021).doi:10.30534/ijeter/2021/029112021

[35] M. M. Al-Momani, A. Odienate, S. F. Algharaibeh, K. Awasa and I. Reda, "Ringdown analysis for Low-Frequency Oscillation Identification," 2022 Advances in Science and Engineering Technology International Conferences (ASET), 2022, pp. 1-6, doi: 10.1109/ASET53988.2022.9735122.